STUDIES ON SOL-GEL SYNTHESIS AND PROPERTIES OF GOLD MICROCRYSTAL-DOPED OXIDE FILMS

JUN MATSUOKA

1998

Contents

General Introduction

Nano-composite materials, in which one material phase with nanometer order dimension is surrounded by another material phase, are interesting because of their unique electronic, dielectric, optical, and chemical properties. This uniqueness is considered to be derived from the following three origins.

One origin is the quantum size effect. As a sold becomes small in size, its electronic band changes from continuous to discrete. When the separation of energy levels in the discrete electronic band is larger than the thermal energy k_BT, the assembly of energy levels can not be regard as a single energy band. This is the quantum size effect. In addition, the finite size of the solid forbids the electrons to take the excitation state with their half wavelength longer than the solid size. This is also called the quantum size effect and is a particular case of the effect described above. The quantum size effect affects not only the energy level but also the transition probability of electronic transitions.

The second origin of the uniqueness is the dielectric confinement effect. When one material phase with high dielectric constant is surrounded by another material phase with low dielectric constant, the applied electrostatic field is concentrated at the high dielectric phase. This effect is important because it enhances the apparent (or macroscopic) oscillator strength.

The third origin is the large surface (or interface) effect. When the volume fraction of one phase in a composite is fixed, the total surface area of the phase is inversely proportional to the size of the phase. Therefore,

the assembly of nano-particles has a very large surface area, and then the surface feature becomes important.

In the nano-composite materials, these three effects appear at the same time, giving various many functions to the materials. One of the most important properties of nano-composites is the photonic one. The optical properties of metal and semiconductor nano-particles are of interest to materials scientists, electronic engineers, photonics engineers, and physicists [1,2]. This photonic feature of nano-composites results from the difference between photon and electron. Nanometer size is considered very small in the optics area, but not in the electronic area. For example, a photon with 1 eV energy (near-IR region) has its wavelength of 1.24μm from the relation $E=hc/\lambda_1$. On the other hand, an electron with 1 eV energy has its wavelength of 0.613 nm when one assumes an electron in 1-d box and adopts the relation $\lambda_e=h/(8\cdot m_e\cdot E)^{1/2}$. This wavelength is about the same order as the size of nano-structures. This means that electrons are sensitive to the nano-sized structure. Therefore, in nano-composites, photons can not scatter diffusely but electrons can.

Among various metal microcrystal-dispersed nano-composites, gold microcrystal-doped inorganic glasses[3-5] with the microcrystal radius of 10 to 100 Å have been extensively studied because of their high optical nonlinearity, femtosecond order fast response time, convenient operating wavelength near the second harmonic of Nd:YAG laser, and thermal and photochemical stability of the matrix.

In order to use the gold-doped glasses as photonic devices, they should be made as a form of thin film waveguide. There are several thin film preparation processes such as ion implantation, sputtering and sol-gel methods. Fukumi et al.[6,7] used the ion implantation method and obtained

a gold microcrystal-doped silica glass with the Au/Si atomic ratio of 0.22 and the third order nonlinear optical susceptibility $\chi^{(3)}$ of 1.0×10^{-7} esu. Wakabayashi et al.[8] used the r.f. sputtering method and obtained a Au-doped glass with the Au/Si atomic ratio of 0.03 and $\chi^{(3)}$ of 2.8×10^{-8} esu.

As for the sol-gel synthesis of transparent oxide materials in which gold microcrystals are embedded, it can be classified into two types. In the first type, Au-containing compound is added to the gelling solution and subsequently decomposed thermally to form Au microcrystals. An example of this type is the Au microcrystal-doped silica glasses prepared by using $HAuCl_4\cdot4H_2O$ [9,10] as the starting material of Au. In the other type, Au microcrystals are prepared in aqueous or organic solutions, and then, they are added to porous oxide gels or alkoxide solutions to be gelled [9,11-14]. Since the former method has an advantage of incorporating a larger amount of Au microcrystals into the gel than the latter type, it is attracting much attention at the present time.

There are, however, several problems needed to be solved when the sol-gel method is used to make Au microcrystal-doped oxide films. As a source of gold microcrystals, tetrachloroauric acid or sodium tetrachloroaurate can be used, but the amount of resulting microcrystals depends on the kind of oxide matrix as well as the kind of gold compound used. In order to achieve a suitable Au microcrystal-doped films for photonic use, the decomposition process of $AuCl_4^-$ ions in the gel to form Au-microcrystals has to be clarified.

Another important matter is the optical nonlinearity of the films made by the sol-gel method. Since the optical nonlinearity is considered to increase with increasing volume fraction of microcrystals, the sol-gel derived oxide films, in which a higher amount of gold microcrystals can be

incorporated [10,11,15], should give a better characteristics than the melt-derived one. However, it is necessary to confirm that the behavior of optical nonlinearity or the third order susceptibility of the Au microcrystal-doped films made by the sol-gel method is similar to that of the melt-derived one.

The origin of optical nonlinearity in the metal microcrystal-doped glasses is considered to be plasmon resonance caused by the cooperative motion of free electrons by photon absorption in microcrystals. The wavelength of this resonance depends not only the metal itself but also the dielectric constant of the matrix in which metal microcrystals are embedded. Therefore, in order to make metal microcrystal-doped oxide films having a desired refractive index and operating wavelength for the practical use, the independent control of refractive index of matrix and wavelength of plasmon resonance is required. Although the alloying of metals in microcrystals is expected to change the plasmon resonance or optical nonlinearity, there has been no papers on the formation of metal alloy microcrystal-doped films except for the formation of Ag-Cu alloy [16,17]. Alloying of metal microcrystal has been also interested in their use as catalyst.

The optical nonlinearity of metal microcrystal-doped oxide films depends also on the refractive index of matrix oxides and consequently on the kind of oxides used. Also, the stability of gold microcrystals in oxide matrix depends on the matrix composition and co-existing chemical spices. However, it is still unclear what determines the stability of Au microcrystals as well as the maximum amount of Au microcrystals attainable in the sol-gel derived oxide films.

One disadvantage of the sol-gel method of making the film is the limited lifetime of dip-coating solutions against gelation, which makes precious gold wasteful in the solutions. Therefore, for the practical application, it is desired to develop a new method for the preparation of gold microcrystal-doped oxide films through sol-gel dip-coating process, in which the gold materials in the process are used effectively.

In this thesis, nano-composites of gold microcrystal-doped oxide films are studied from the viewpoint of materials chemistry and electronic state of solids in order to clarify the above described matters, which are rather basic problems but important to prepare a new nonlinear optical material.

In Chapter 1, Au microcrystal-doped silica glass film is synthesized through the sol-gel process using $NaAuCl_4 \cdot 2H_2O$ as a starting dopant material. Its microstructure is investigated by TEM, and the effect of preparation condition on the optical property is examined.

In Chapter 2, the role of metal cations in the sol-solution on the stability of Au/SiO_2 nano-composite at its sol-gel preparation process is examined. A guideline to prepare highly Au-contained metal/oxide composites is proposed.

In Chapter 3, the third-order optical nonlinearity of Au/SiO_2 nano-composites is measured. Electronic nonlinearity and optothermal nonlinearity are separated using a picosecond-duration laser. The relation between optical nonlinearity and the structure of composite is discussed.

In Chapter 4, Au-Pd co-doped metal/SiO_2 composites are prepared. The microstructure of the composites is investigated, and the evolution of microstructure caused by heat-treatment is discussed in terms of the stability of Au-Cl and Pd-Cl bonds.

In Chapter 5, Au microcrystal-doped titania, zirconia and alumina films are synthesized through the sol-gel process. The stability of these nano-composites at the formation process is discussed in terms of the surface

character of oxides.

In Chapter 6, a new process for the preparation of Au microcrystal-doped oxide films, in which the diffusion of $AuCl_4^-$ ions into oxide gel films is utilized, is developed. The applicability of this process for several oxides is investigated and discussed in terms of the surface character of oxides.

In Summary, the whole results and discussions in Capters 1 to 6 are summarized.

References

[1] Uwe Kreibig and Michael Vollmer: "Optical Properties of Metal Clusters (Springer Series in Materials Science 25)", Springer-Verlag, 1995

[2] Ulrike Woggon: "Optical Properties of Semiconductor Quantum Dots (Springer Tracts in Modern Physics 136)", Springer-Verlag, 1996

[3] D. Ricard, Ph.Roussignol and Chr. Flytzanis, Opt. Lett., **10**, 511-13 (1985)

[4] F. Hache, D. Ricard, C. Flytzanis and K. Kreibig, Appl. Phys., **A47**, 347-57 (1988)

[5] T. Dutton, B. VanWonterghem, S. Saltiel, N. V. Chestnoy, P. M. Rentzepis, T. P. Shen and D. Rogovin, J. Phys. Chem., **94**, 1100-05 (1990)

[6] K. Fukumi, A. Chyayahara, K. Kadono, T. Sakaguchi, Y. Horino, M. Miya, J. Hayakawa and M. Satou, Jpn. J. Appl. Phys., **30**, L742-44 (1991)

[7] idem, "Science and Technology of new Glasses, Proceedings of the International Conference on Science and Technology of New Glasses", ed. by S. Sakka and N. Soga, (1991) pp.353-58.

[8] H. Wakabayashi, H. Yamanaka, K. Kadono, T. Sakaguchi and M. Miya, ibid, pp.412-17

[9] J. M. Fernández-Navarro and M. Angeles Villegas, Glastech. Ber. 65, 32 (1992)

[10] H. Kozuka and S. Sakka, Chem. Mater 5, 222 (1993)

[11] L. Spanhel, M. Menning and H. Schmidt, in Proc. XVIIth Internat. Cong. Glass, (Sociedad Espanola de Ceramica y Vidrio, Madrid, 1992), Vol.7 p.9

[12] T. Gacoin, F. Chaput, J. P. Boilot and G. Jaskierowicz, Chem. Mater. 5, 1150 (1993)

[13] M. Ohtaki, Y. Ohshima, K. Eguchi and H. Arai, Chem. Lett. 1992, 2201

[14] T. Yazawa, K. Kadono, H. Tanaka, T. Sakaguchi, S. Tsubota, K. Kuraoka, M. Miya and Wang De-Xian, J. Non-Cryst. Solids 170, 105 (1994)

[15] J. Y. Tseng, C.-Y. Li, T. Takada, C. Lechner and J. D. Mackenzie, in Proc. SPIE : Sol-Gel Optics II, Vol. 1758, p. 612 (1992)

[16] R. H. Magruder III, J. E. Wittig and R. A. Zuhr, J. Non-Cryst. Solids, 163, 162-168 (1993)

[17] G. De, M. Gusso, L. Tapfer, M. Catalano, F. Gonella, G. Mattei, P. Mazzoldi and G. Battaglin, J. Appl. Phys., 80, 6734-6739 (1996)

Chapter 1

Sol-Gel Synthesis of Au Microcrystal-Doped SiO_2 Glass Films from $NaAuCl_4 \cdot 2H_2O$ and TEOS

1. Introduction

As described in the general introduction, the sol-gel method using dip-coating is one of the effective methods for the preparation of glass films on substrate. So, in this chapter, the preparation of Au microcrystal-embedded SiO_2 films with high Au content by the sol-gel method is attempted. Then the microstructure of the glass films obtained is investigated by transmitting electron microscopy, and the formation process of gold microcrystals is discussed on the bases of the distribution of crystal radius. Furthermore, the effect of the concentration of $NaAuCl_4$ in the precursor silica solution on the glass film formation was investigated.

2. Experimental

Au-doped silica glass films were prepared on silica glass plates by dip-coating method. Starting solutions were prepared from tetraethyl orthosilicate ($Si(OC_2H_5)_4$, TEOS), sodium tetrachloroaurate ($NaAuCl_4 \cdot 2H_2O$), ethanol, water and HCl. Molar ratio of TEOS : $NaAuCl_4$: EtOH : H_2O : HCl was 1 : x : 6 : 6 : 0.03, where x corresponds with the Au/Si atomic ratio and varied in the range from 0.01 to 0.06. Most of the experiments were carried out for x=0.01 which

corresponds to 0.37 vol% of Au in the resultant Au/SiO_2 composite film. The withdrawal velocity of the silica substrate was fixed at 0.15 mm/sec, resulting in a glass film with about 0.05 μm thickness after heat treatment. Heat treatment was carried out in air for 15 min at different temperatures ranging from 100 to 600° C. This dipping / heat treatment procedure was repeated several times to obtain films with sufficient thickness for optical measurements. The coated-films heat-treated once at 400° C were further heat-treated at temperatures ranging from 600° to 1000° C for 15 min to 170 hr to explore the effect of post heat-treatment on the optical property.

Optical absorption spectra were measured from 200 to 800 nm at room temperature. By assuming that the microcrystals are spherical and the size distribution is not so diffuse, the average crystal radius of Au microcrystals was calculated from the spectra according to Eq.1.[1]

$$r = v_F/\Delta\omega_{1/2} \qquad (1)$$

where r is the crystal radius, v_F the Fermi velocity of electron and 1.39×10^8 cm/s for Au, and $\Delta\omega_{1/2}$ the full width at half maximum of the absorption peak in wavenumber.

Crystal radius and its distribution were also measured directly by using a Hitachi H-800 transmission electron microscope. For the TEM observation, the Au-doped gel film was dip-coated on a platinum foil and heat treated at 400° C for 15 min, and then the glass film was scraped out from the foil.

3. Results

The coated films remained colorless and had rough surfaces up to

200° C. On the other hand, when heated above 300° C, they turned to be let colored, clear and transparent.

Fig.1 shows the absorption spectra of gold-doped silica glass films with Au/Si=0.01 which were heat-treated at different temperatures for 15 min. As is seen, the films heat-treated at 100° and 200° C showed a strong absorption peak at 311 nm. It is known that $NaAuCl_4$ aqueous solution has a strong absorption shoulder around 293 nm although its exact wavelength is difficult to determine due to the overlapping with the absorption of H_2O. Therefore, as the absorption peak position of the film is close to the position of absorption shoulder in $NaAuCl_4$ aqueous solution, the absorption peak at 311 nm is attributed to the absorption by tetrachloroaurate anions.

An absorption peak emerged at 543 nm in the films when heat-treated above 300° C. This 543 nm peak has been attributed to Au microcrystals [1] formed between 200° and 300° C. The film heated at 300° C shows also a small absorption around 311 nm, indicating that a small amount of tetrachloroaurate anion remained in the film. Longer heat-treatment at this temperature range caused no significant change in the absorption spectra, except the decrease of absorption around 311 nm in 300° C-heated sample.

Fig.2 shows the TEM photograph of a Au-doped glass heat-treated at 400°C. Two kinds of particles with different sizes were observed. One has the average radius less than 10Å and the other has radius more than 20Å. Both of the particles should be metallic Au, because these particles were not seen in pure silica glass prepared by the similar method, and because the temperature of heat treatment was much higher than the decomposition temperature of $NaAuCl_4$ to Au. The

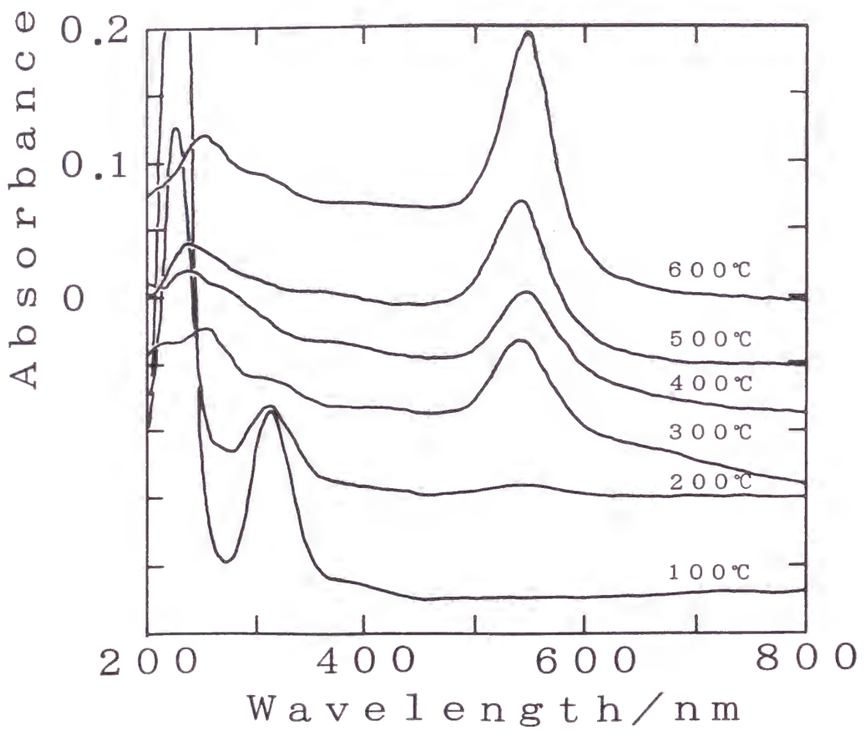

Fig.1 Absorption spectra of five-times coated Au-doped glass films with the Au/Si atomic ratio of 0.01 heat treated at different temperatures ranging from 100° to 600°C. A silica glass was used as a reference sample.

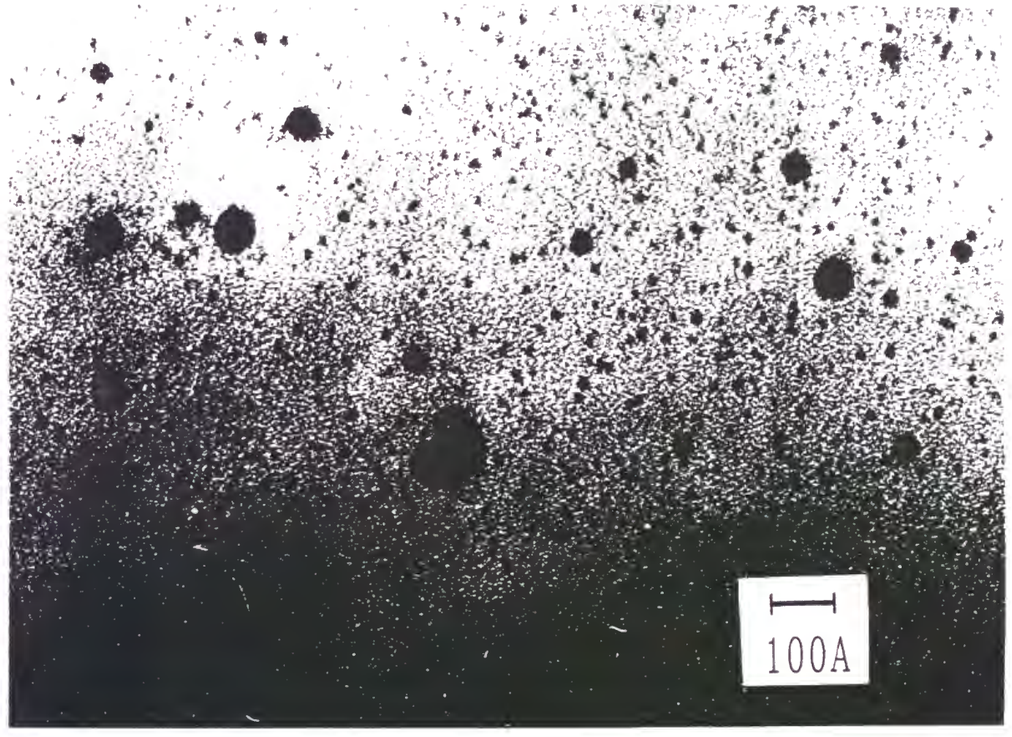

Fig.2 TEM photograph of Au-doped glass with the Au/Si atomic ratio of 0.01 heat-treated at 400°C.

number and volume distributions of the particles are indicated in Fig.3. More than 300 particles were accounted for obtaining the distribution. Although there is only one peak around 7 Å in the number distribution of particle radius, two peaks, around 7 Å and around 30 Å, are seen in the volume distribution of the radius. As the optical absorption coefficient is related to the volume fraction of particles [2], the volume distribution of particles is important to understand the optical property of the sample.

Post heat treatment at 900° or 1000° C changed the absorption spectra of the Au-doped glass, and changed the color from purple to wine red. Fig.4a and 4b show the absorption spectra of Au/Si=0.01 samples once heated at 400° C and then (a): heat-treated at 900° or at 1000° C up to 4 hr, and (b): heat-treated at 1000° C up to 170 hr. These post heat-treatments shifted the absorption peak to the short wavelength side and increased the peak width in a short time less than 1 hr. Further heating did not change the peak position but slowly made the peak width narrower, which may be caused by the increase in crystal radius [1]. The changes in position and FWHM of the peak as a function of heat treatment time are shown in Fig.5a and 5b. The apparent mean crystal radius calculated from FWHM using Eq.1 is 39 Å for FWHM = 55 nm, 36 Å for 59 nm, and 42 Å for 52 nm. As shown in Fig.6, similar changes are also observed when the post heat-treatment temperature is higher than 700° C.

Fig.7 shows the absorption spectra of samples with different Au contents. The Au microcrystal-doped glasses with Au/Si ratio up to 0.04 were successfully prepared. The absorption spectra of the samples with Au/Si atomic ratio from 0.01 to 0.04 represent similar

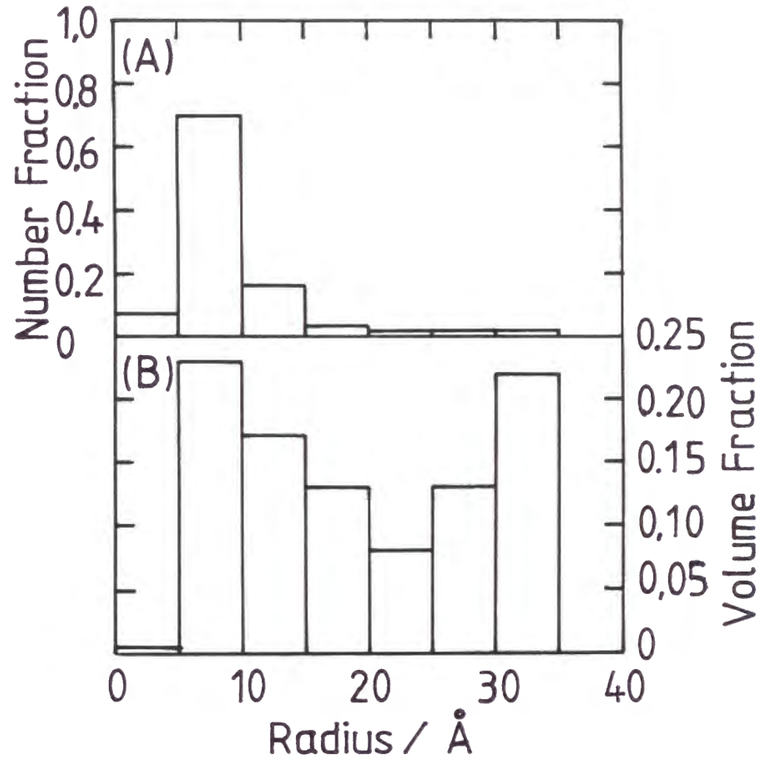

Fig.3 Number (A) and volume (B) distributions of Au microcrystal in the glass shown in Fig.2.

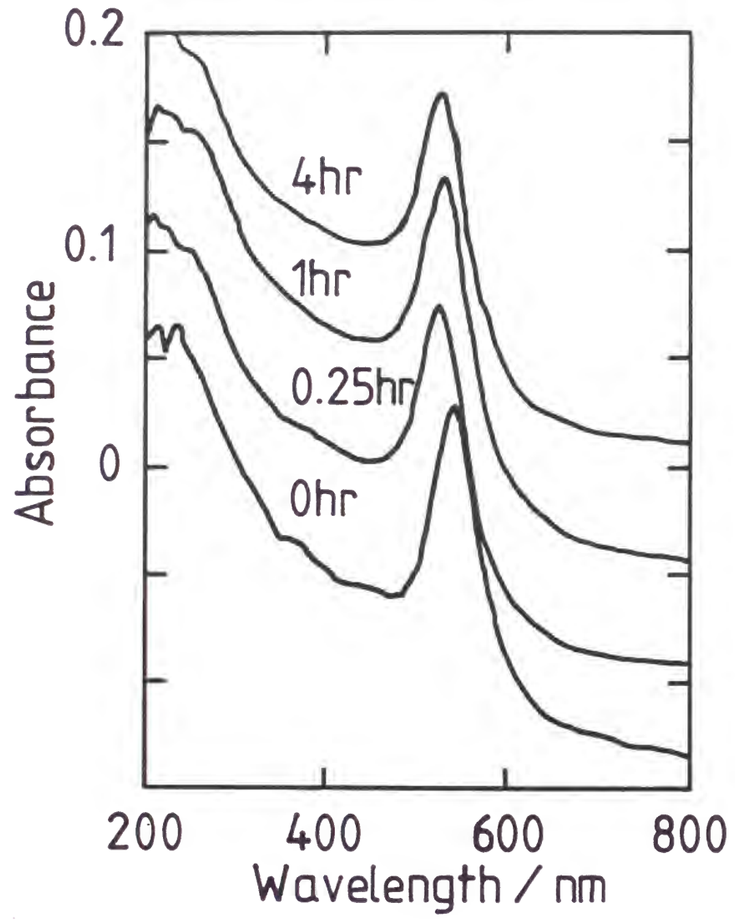

Fig.4(a) Absorption spectra of ten-times coated Au-doped glass films with the Au/Si ratio of 0.01 once heat treated at 400° C and subsequently post heat-treated at 900° or 1000° C for 0.25 to 4 hours.

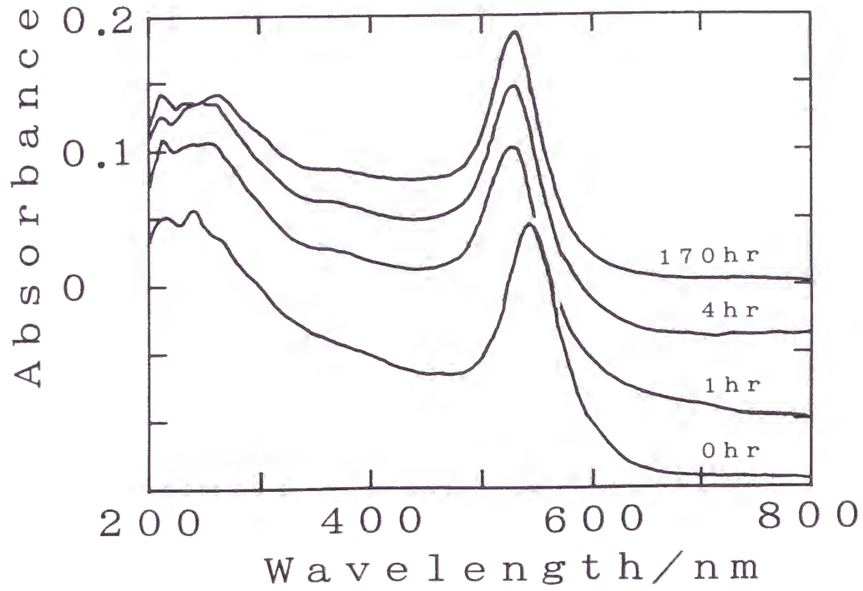

Fig.4(b) Absorption spectra of ten-times coated Au-doped glass films with the Au/Si ratio of 0.01 once heat treated at 400° C and subsequently post heat-treated at 1000° C for 1 to 170 hours.

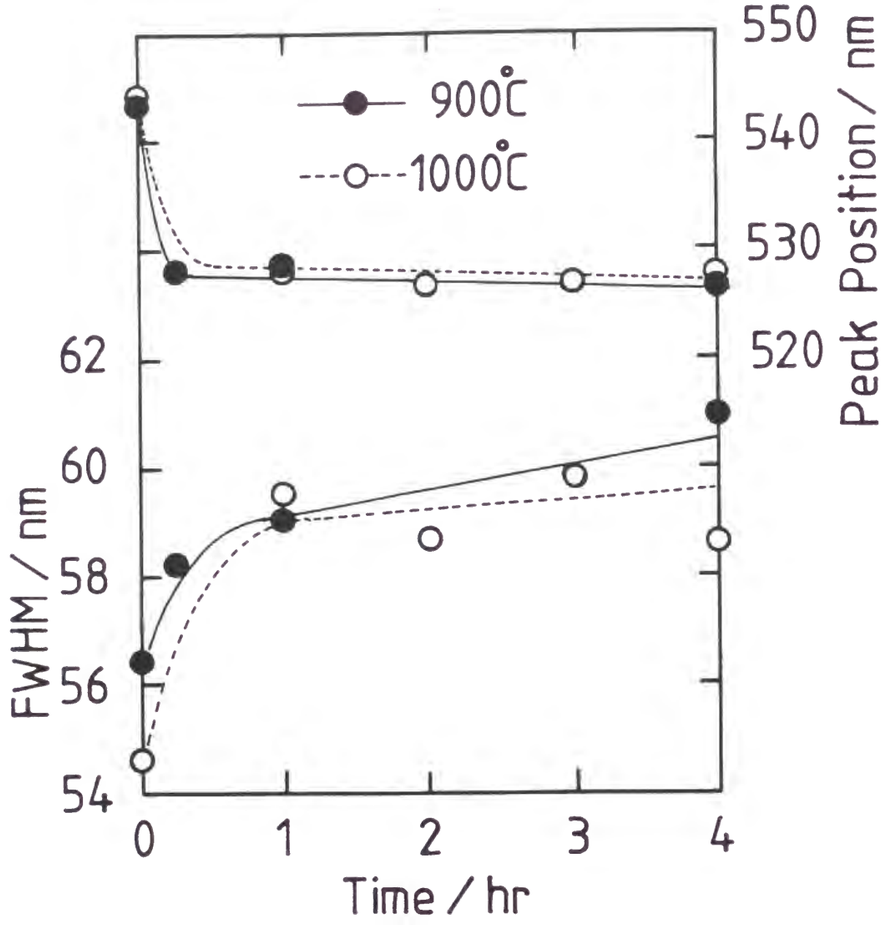

Fig.5(a) Post heat-treatment induced changes in absorption peak position and peak width of 400° C-heated Au-doped glass with the Au/Si ratio of 0.01 as a function of post heat-treatment time at 900° or 1000° C up to 4 hr.

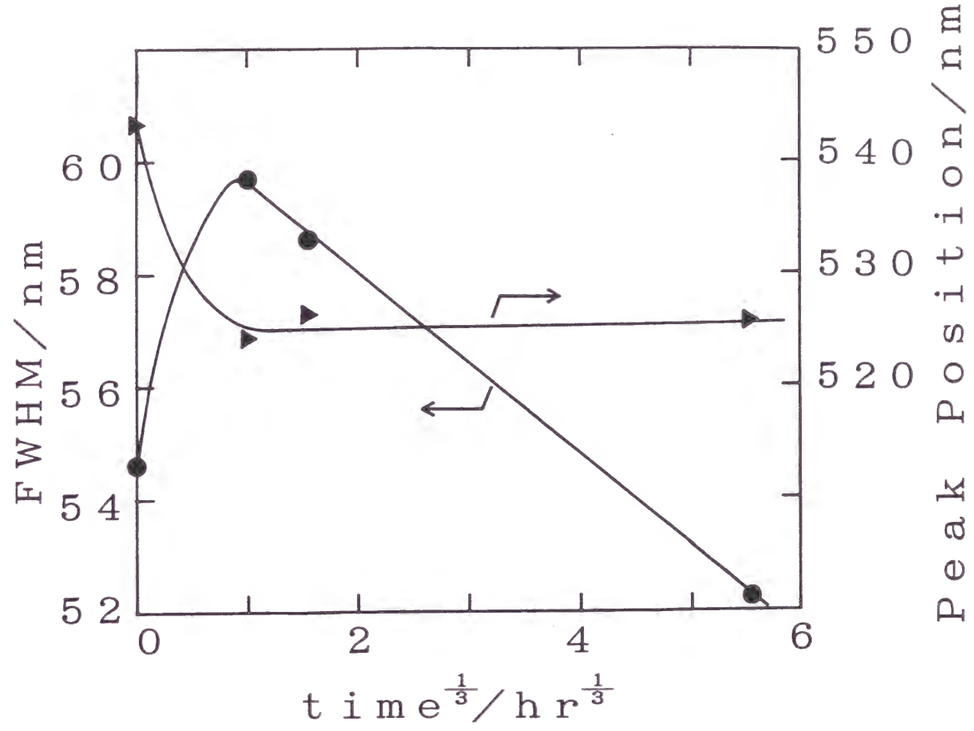

Fig.5(b) Post heat-treatment induced changes in absorption peak position and peak width of 400° C-heated Au-doped glass with the Au/Si ratio of 0.01 as a function of post heat-treatment time at 1000° C up to 216 hr.

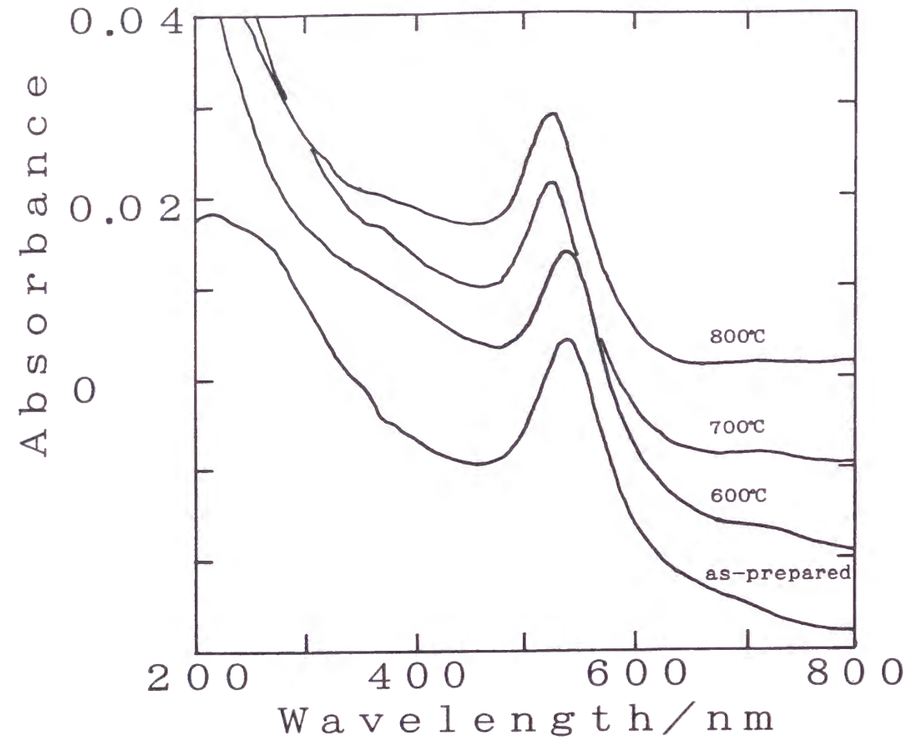

Fig.6 Absorption spectra of Au-doped glass films with the Au/Si ratio of 0.01 once heat treated at 400° C and subsequently post heat-treated at different temperatures ranging from 600° to 800° C for 1 hour.

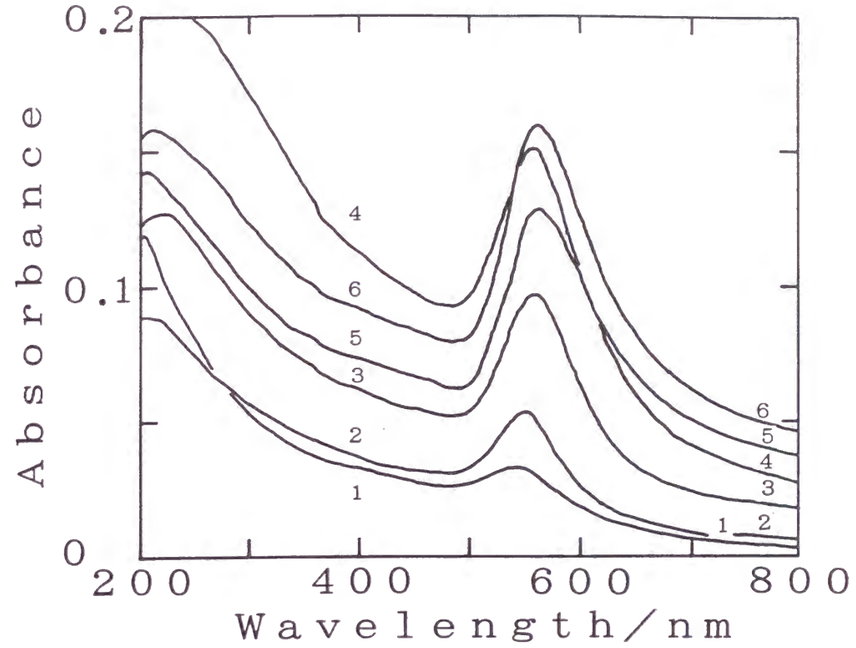

Fig.7 Absorption spectra of two-times coated Au-doped glass films with different Au/Si atomic ratios which were heat treated at 400° C. After the two-times coating and heating, the samples were wiped with tissue paper before the absorption measurement. The numerals in the figure are the Au/Si atomic ratios in the coating solutions multiplied by 100.

shape around the absorption peak in spite of the change in intensity. The color of these films was purple in both transmission and reflection. When Au/Si ratio was increased to 0.05 or more, the obtained film became rough surfaced and was seen by naked eyes as mat gold-colored in reflection. In this case, very small gold-colored powders were formed on the surface and they were able to be wiped out easily. Similar behavior was found by Kozuka and Sakka[3] using $HAuCl_4 \cdot 4H_2O$ as a starting material. The absorption spectra shown in Fig.7 are those after wiped, and the peak intensity of these samples was similar to that of Au/Si=0.04.

4. Discussion

The decomposition of $AuCl_4^-$ anions and the formation of Au microcrystals occurred between 200° and 300°C in the film. This temperature is somewhat higher than the decomposition temperature of pure $NaAuCl_4 \cdot 2H_2O$ to form metallic Au in air. As the $AuCl_4^-$ anion is surrounded by silica network in the gel film and thus the equilibrium of the decomposition reaction, $2AuCl_4^- \Leftrightarrow 2Au + 3Cl_2 + 2Cl^-$, may shift to the left hand side because of the accumulation of Cl_2 in the film due to low diffusion of Cl_2 through the gel network.

The Au atoms produced by the decomposition of $AuCl_4^-$ should tend to aggregate to form a microcrystal. The distribution of crystal radius shows that the fraction of microcrystal with the radius of about 7 Å is very high. When we assume that the structure of the microcrystals is the same as that of bulk crystal, that is fcc, and that the atomic radius of Au in the microcrystal is nearly the same as that in the bulk, then the crystal radius of 7 Å corresponds to

the cluster of Au_{85} (crystal radius of 6 Å corresponds to Au_{54} and that of 8 Å corresponds to Au_{127}). It is known that a stable Au_{55} cluster with ligands at the surface can be synthesized by chemical process [4], and its structure is based on the fcc lattice like in the bulk crystal or constructed by 8 (= 2^3) unit cells without cornered eight atoms [5], which is illustrated in Fig. 8. Considering that the crystal radius determined by TEM has a tendency toward overestimating because of the incompleteness of focussing, the microcrystal with the radius of about 7 Å in the present SiO_2 glass film is considered to be the same as the above mentioned Au_{55} cluster or similar to it, which may be written as $Au_{55+\alpha}$. It is considered stable as a form of bare cluster, being coordinated by silica network, like that of a chemically synthesized ligand-covered cluster. In addition to A_{55} cluster, A_{13} cluster is known to be stable when surrounded by some ligands [6]. However, the existence of clusters of this type in this glass film cannot be confirmed at this moment, because its cluster size is much smaller than the TEM resolution limit.

The clusters having radius larger than 10 Å may be formed by aggregation or by growth of the 7 Å clusters. As shown in Fig. 1, however, the evolution of 545 nm peak and dissipation of 310 nm peak took place in a short time less than 15 min on heating the gel film at a temperature lower than 600 °C and longer heat-treatment has no further effect, it is considered that the formation and growth of Au microcrystals occur at the gel state or during the gel to glass conversion process, but not once a rigid and dense glass network is formed.

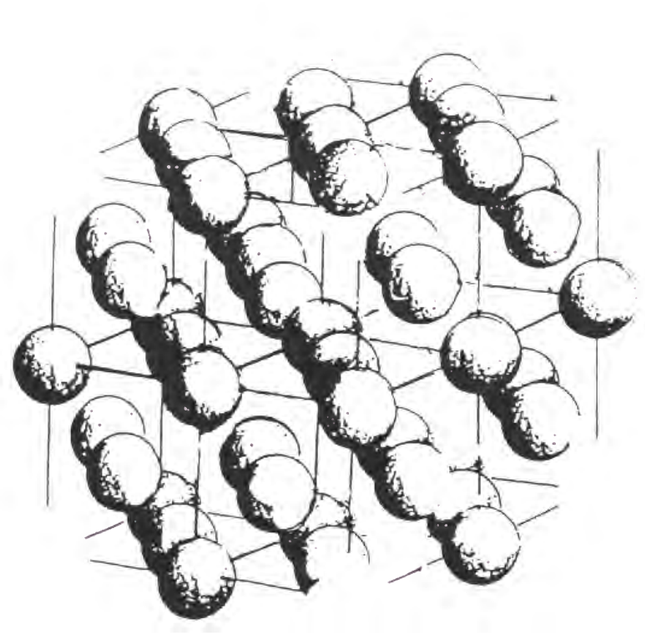

Fig.8 Structure of Au_{55} cluster. Ligands are not indicated.

The volume fraction profile of microcrystals has two peaks around 30 Å and around 7 Å as shown in Fig. 3. The former size corresponds fairly well to the radius calculated from the FWHM of the optical absorption peak. Although the absorption by 7 Å-radius microcrystals is known to occur at a similar wavelength to Au_{55} cluster, that is at about 520 nm [4], its very low absorption coefficient and extremely broad peak width makes its peak indistinguishable when it is overlapped with a strong and sharp peak caused by the 30 Å-centered microcrystals. Thus, the crystal radius obtained from FWHM represents the average crystal radius of microcrystals involving only the larger radius group in the volume distribution histogram shown in Fig. 3. Consequently, the difference in average crystal radius calculated from FWHM and that observed by TEM is considered to be originated from the simple assumption that the size distribution is not so diffuse.

The post-heat treatment above 700° C of the Au-precipitated films changes their absorption spectra. It is clear from Fig. 5 that there are two steps in this change. At the first step, the peak position shifts to shorter wavelength and the FWHM increases rapidly. This process is rapid and occurs at a temperature as low as 700° C, so that it is considered to be a diffusion-free process. It should be noted that the formation of Au microcrystals by the heat-treatment of gel films is very rapid and so the shape of the as-precipitated microcrystals may be irregular even though the spherical shape is thermodynamically stable. It is known that the peak position of Au microcrystals with non-spherical shape, such as spheroidal, is at a longer wavelength than that of spherical microcrystals [7]. There-

fore, the change in peak position observed in the first step should be due to the structure reform of microcrystals from a non-spherical to the spherical shape, which does not require the diffusion of Au atoms in SiO_2 glass matrix.

At the second process, the peak position does not change and only the FWHM becomes large. This means that the crystal radius becomes large without changing the crystal shape. In addition, the speed of the spectral change in this step is very slow compared with that in the first step. Therefore, the change is considered due to the Ostwald ripening of microcrystals which requires the diffusion of Au atoms in SiO_2 matrix, and thus the speed is not so fast.

The atomic ratio of Au/Si can be increased to 0.04 from 0.01. A further addition of $NaAuCl_4 \cdot 2H_2O$ to the coating solution was not effective to increase the Au content in the film. The absorption peak height measured after wiping the surface of Au/Si=0.05 and 0.06 glass films was similar to that of Au/Si=0.04 glass, implying that the excess Au is depleted from the glass film. Since the absorption spectra of the glass with Au/Si=0.04 is similar to that of Au/Si=0.01 glass except for the amplitude, it is considered that the microstructure and the size of Au microcrystals in these glasses are the same. So, the nonlinear susceptibility of about 3×10^{-8} esu would be expected by multiplying the $\chi^{(3)}$ of Au/Si=0.01 glass by the increment of the content of Au, i.e. four. This will be dealt with in Chapter 4.

5. Conclusion

An attempt was made to prepare Au microcrystal-doped glass films with different Au/Si atomic ratios from 0.01 to 0.06 by sol-gel

method with dip-coating using $NaAuCl_4 \cdot 2H_2O$ and TEOS as the starting materials. The glass films with the Au/Si atomic ratio up to 0.04 were successfully obtained by heating the gel film at a temperature ranging from 300° to 600°C. The detailed TEM observations revealed that microcrystals with the radius of about 7 Å and of about 30 Å coexist in the glass film with the Au/Si atomic ratio of 0.01. The latter radius was comparable to the average radius calculated from the FWHM of the optical absorption peak. The structure of the small sized one is considered similar to that of stable Au_{55} clusters, which have an extremely broad peak with low absorption coefficient, resulting in little effect on the FWHM of the experimentally observed absorption spectra. The subsequent heat treatment of these glass films at 900°or 1000° C shifted the absorption peak from 545 nm to 528 nm, caused by the change in microcrystal shape from irregular to spherical one. A longer treatment made the width of this peak narrower due to an increase in spherical crystal size. The atomic ratio of Au/Si can be increased to 0.04.

References

[1] G. W. Arnold, J. Appl. Phys., **46**, 4466-73 (1975)

[2] F. Hache, D. Ricard, C. Flytzanis and K. Kreibig, Appl. Phys., **A47**, 347-57 (1988)

[3] H. Kozuka and S. Sakka, Chemistry of Materials, 5, 222-28 (1993)

[4] G. Schmid, R. Pfeil, R. Boese, F. Bandermann, S. Meyer, G. H. M. Calis and J. A. M. van der Verden, Chem. Ber., **144**, 3634-42 (1981)

[5] M. A. Marcus, M. P. Andrews, J. Zegenhagen, A. S. Bommannavar and P. Montano, Phys. Rev., **B42**, 3312-16 (1990)

[6] C. E. Briant, B. R. C. Theobald, J. W. White, L. K. Bell, D. M. P. Mingos and A. J. Welch, J. Chem. Soc., Chem. Commun., **1981**, 201-02

[7] H. Kozuka, Proc. SPIE: Sol-Gel Optics IV, **3136**, 304-14 (1997)

Chapter 2

Sol-Gel Synthesis of Au Microcrystal-Doped SiO_2 Glass Films from $HAuCl_4 \cdot 4H_2O$, $M(NO_3)_3$ and TEOS

1. Introduction

In the previous chapter, gold microcrystal-doped silica glass films are prepared by heating the dip-coated silica gel films from sodium tetrachloroaurate ($NaAuCl_4 \cdot 2H_2O$) and tetraethyl orthosilicate (TEOS) under weak acidic condition (HCl/TEOS=0.03). The maximum amount of gold microcrystals which can be incorporated in the silica matrix is Au/SiO_2=0.04 in molar ratio [1]. When the concentration of sodium tetrachloroaurate in the coating solution exceeds this limit, aggregated gold crystals are exhausted to the film surface at the heat treatment of the gel film. On the other hand, when tetrachloroauric acid ($HAuCl_4 \cdot 4H_2O$) is used as a source of gold in the weak acidic dip-coating solution, the amount of gold which can be incorporated in the silica film is as small as Au/SiO_2=0.01. Incorporation of gold microcrystals in silica matrix is possible only at the case of highly acidic condition (HCl/TEOS>1.0) when tetrachloroauric acid is used [2]. Therefore, it is obvious that the amount of gold microcrystals which can be incorporated in silica gel matrix depends on the coexisting chemical species in dip-coating solutions. In this chapter, the effect of coexisting cations in the dip-coating solutions on the formation of gold microcrystal-doped silica films through sol-gel process is examined using tetraethyl orthosilicate and tetrachloroauric acid as starting materials.

2. Experimental

Gold microcrystal-doped glass films were prepared by the sol-gel dip-coating method in a similar manner as described in Chapter 1. The composition of the dip-coating solutions are listed in Table 1. Tetraethyl orthosilicate was used as a source of silica matrix, and tetrachloroauric acid was used as a source of gold microcrystals. Nitrates of sodium, calcium and lanthanum were added to the dip-coating solutions to investigate the effect of additive ions on the amount of Au microcrystals. These three elements have different valency but similar electronegativity (0.9 - 1.1 in Pauling's definition) and similar ionic radius (0.100 - 0.106 nm). The molar ratio of $HAuCl_4 \cdot 4H_2O$ / TEOS was changed in the range from 0 to 0.08 with a step of 0.01.

The gel films were dip-coated on silica glass substrates with the withdrawal velocity of 0.15 mm/sec. The resultant film thickness after heat treatment was about $5x10^2$ nm. Heat treatments of the gel films were carried out at 600°C for 10min, which is enough for the decomposition of tetrachloroauric acid to form metallic gold and for the condensation of silica gel matrix [1,3]. This dip-coating / heat treatment procedure was repeated five times to obtain the films with sufficient thickness for optical measurements.

The optical absorption spectra of the films were measured from 200 to 1200 nm. It is known that when the concentration of $AuCl_4^-$ ion in the dip-coating solution exceeds a critical value which depends on the solution composition, the heat treatment of gel film causes the depletion of the excess amount of Au microcrystals to the film surface, and the optical absorption intensity of such films is known to be decreased by wiping the film surface [2,4]. On the other hand, if all of the gold microcrystals stay in the film, wiping does not affect the optical absorption spectra. Therefore,

Table 1 Composition series of dip-coating solutions in molar ratio.

series	TEOS	H_2O	C_2H_5OH	HCl	$NaNO_3$	$Ca(NO_3)_2$	$La(NO_3)_3$	$HAuCl_4 \cdot 4H_2O$
F0	1.0	6.0	6.0	0.03				0 - 0.08
S1	1.0	6.0	6.0	0.03	0.01			0 - 0.08
S2	1.0	6.0	6.0	0.03	0.02			0 - 0.08
S4	1.0	6.0	6.0	0.03	0.04			0 - 0.08
S6	1.0	6.0	6.0	0.03	0.06			0 - 0.08
C1	1.0	6.0	6.0	0.03		0.01		0 - 0.08
L1	1.0	6.0	6.0	0.03			0.01	0 - 0.08

the absorption spectra were measured on both of the as-prepared and surface-wiped films, and the results were compared to determine the maximum amount of Au which can be incorporated in the film as microcrystals.

3. Results

Figure 1 shows the absorption spectra of the as-prepared and surface-wiped films prepared from the additive-free (a) and $NaNO_3$-added (b, c) dip-coating solutions. All of the spectra except for Au/Si=0.00 have an absorption peak around 550nm which is due to the plasmon resonance of gold microcrystals. In the absorption spectra of the additive-free films, wiping of the film surface decreases the peak height even though the concentration ratio of $HAuCl_4 \cdot 4H_2O$ / TEOS in the dip-coating solution is as small as 0.02. Therefore, the maximum amount of gold microcrystals in the film free from additives is Au/SiO_2=0.01.

On the other hand, it can be seen from Fig's 1(b) and (c) that the addition of $NaNO_3$ to the dip-coating solution is effective to increase the amount of gold microcrystals which can be incorporated in the SiO_2 film. The maximum amount of gold microcrystals in the film as a function of the $NaNO_3$ concentration in the dip-coating solutions is summarized in Fig. 2. An increase in $NaNO_3$ concentration is found to cause the monotonous increase of the maximum amount of gold in the film in the experimental range.

Figure 3 shows the as-prepared and surface-wiped films prepared from the $Ca(NO_3)_2$-added (a) and $La(NO_3)_3$-added (b) dip-coating solutions. The maximum amount of gold incorporated in these films are also increased from the case of additive-free one similar to the case of $NaNO_3$. The maximum amount of gold microcrystals in the film as a function of the valence of additive cations is shown in Fig. 4. It is clear that an increase in valence

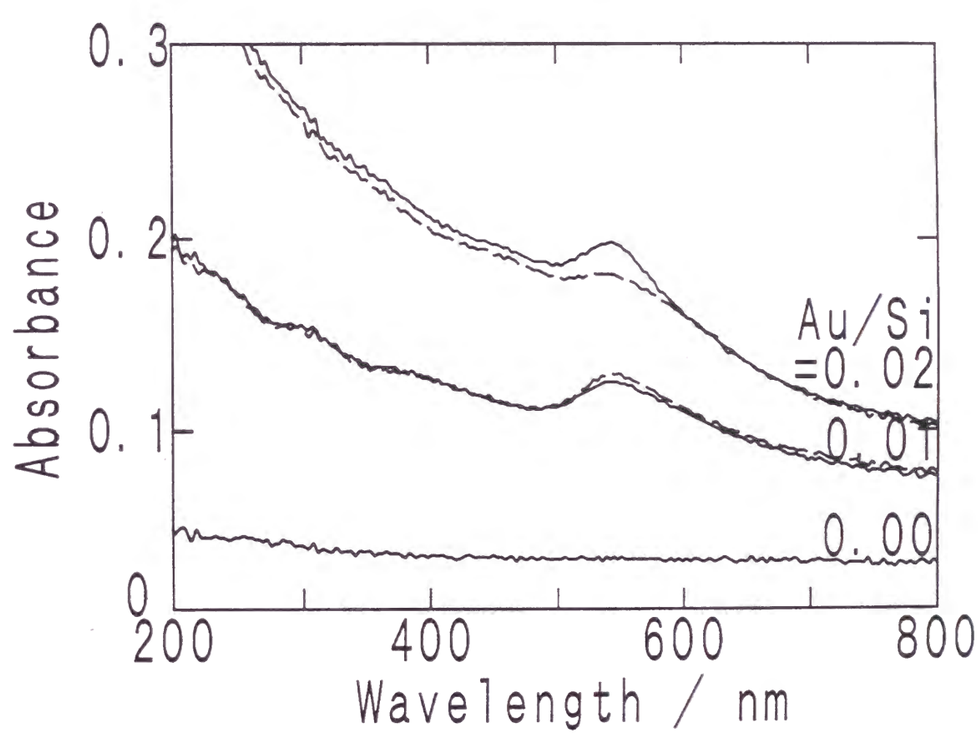

Fig.1(a) Optical absorption spectra of as-prepared (solid line) and surface wiped (dashed line) films with different Au/Si molar ratio and additive-free.

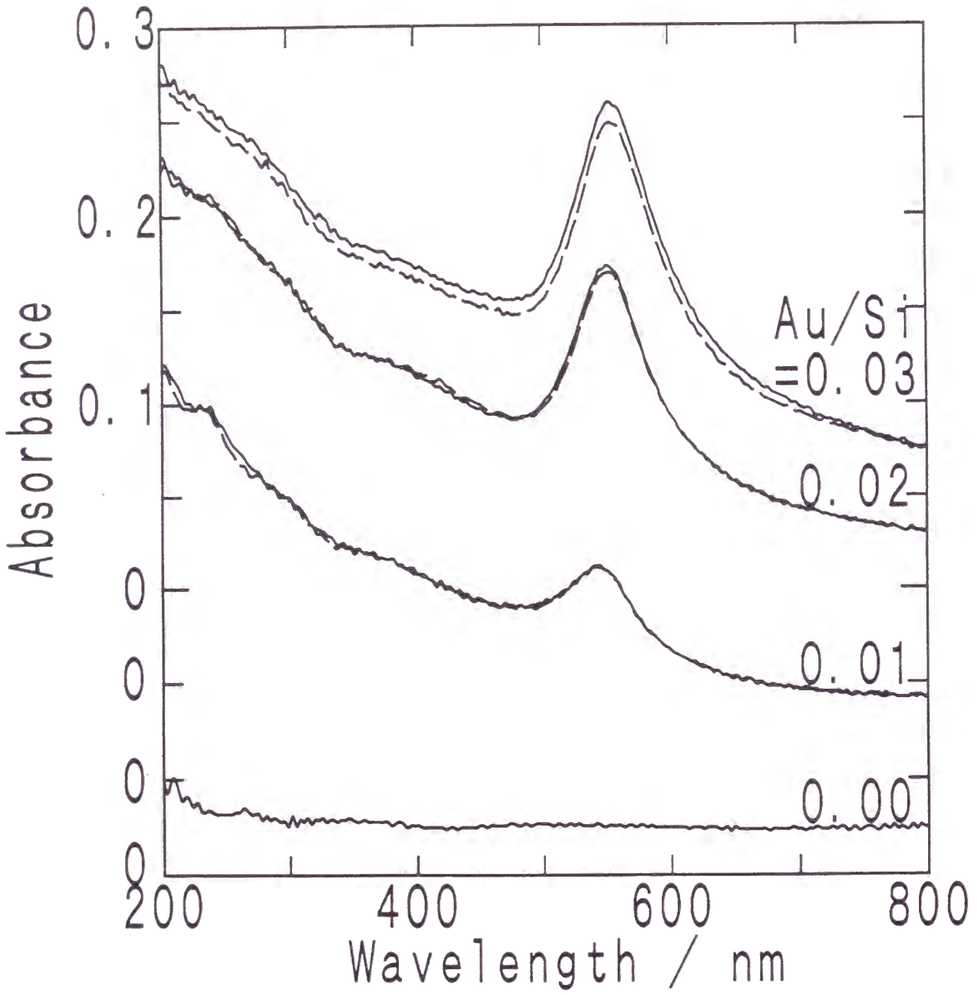

Fig.1(b) Optical absorption spectra of as-prepared (solid line) and surface wiped (dashed line) films with different Au/Si molar ratio and $NaNO_3$/TEOS = 0.01.

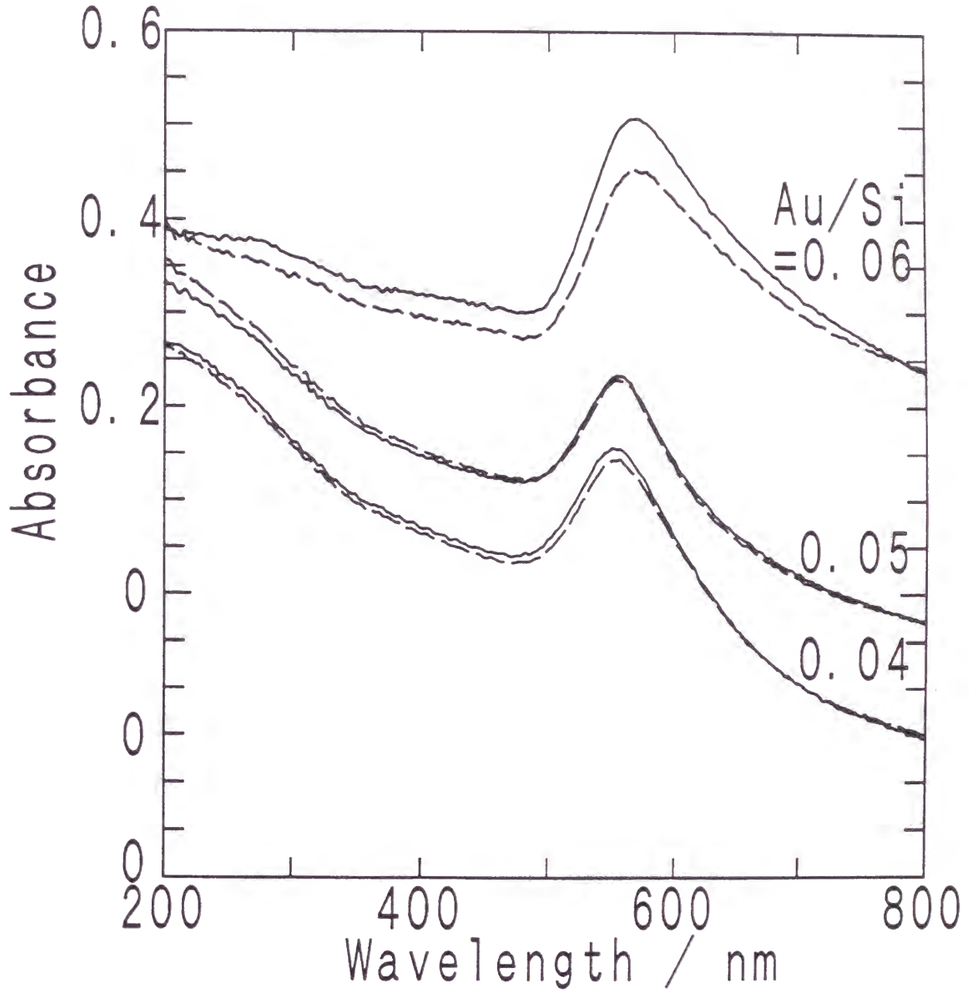

Fig.1(c) Optical absorption spectra of as-prepared (solid line) and surface wiped (dashed line) films with different Au/Si molar ratio and $NaNO_3$/TEOS = 0.06.

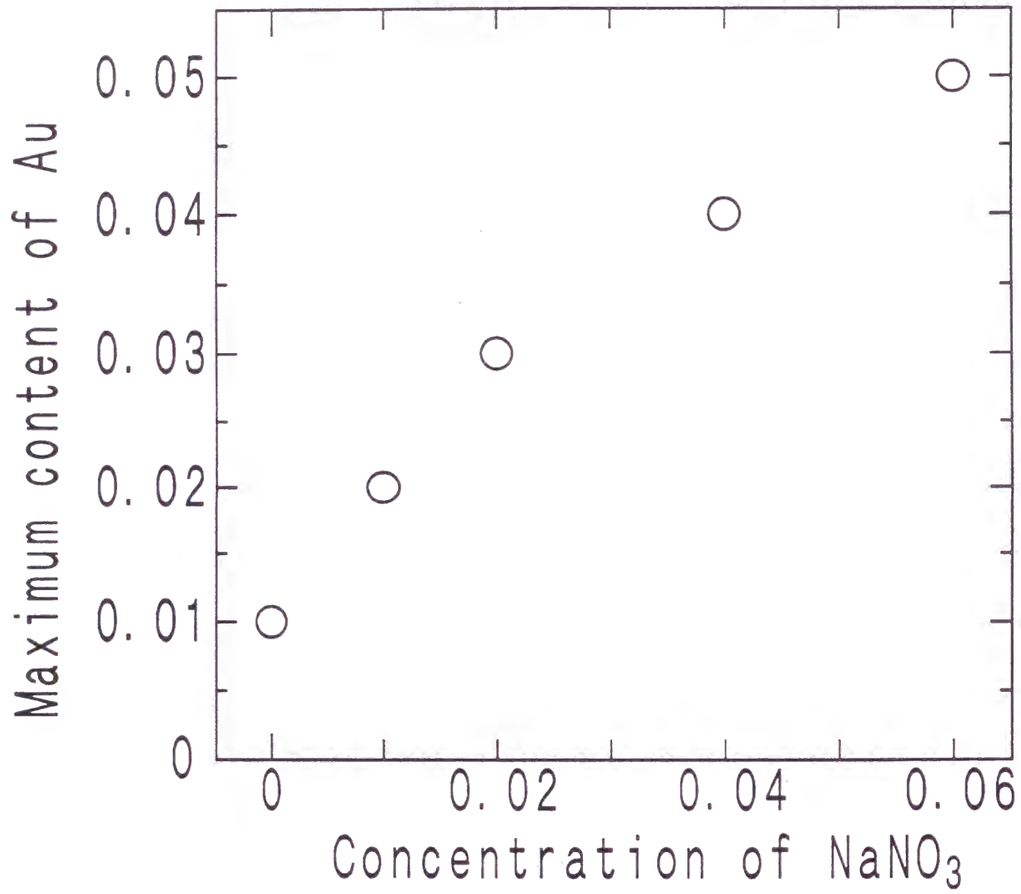

Fig.2 Dependence of the maximum amount of gold microcrystals incorporated in the films on the concentration of $NaNO_3$ in dip-coating solutions.

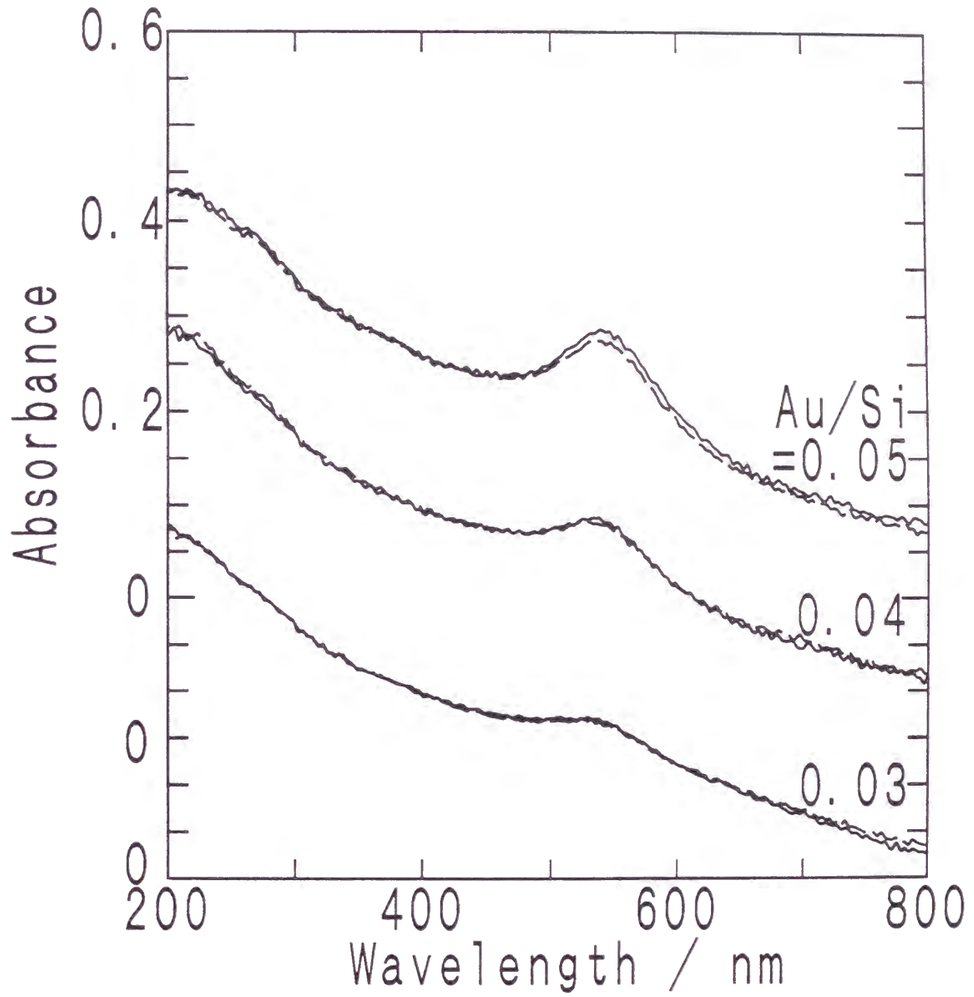

Fig.3(a) Optical absorption spectra of as-prepared (solid line) and surface wiped (dashed line) films with different Au/Si molar ratio and $Ca(NO_3)_2$/TEOS=0.01.

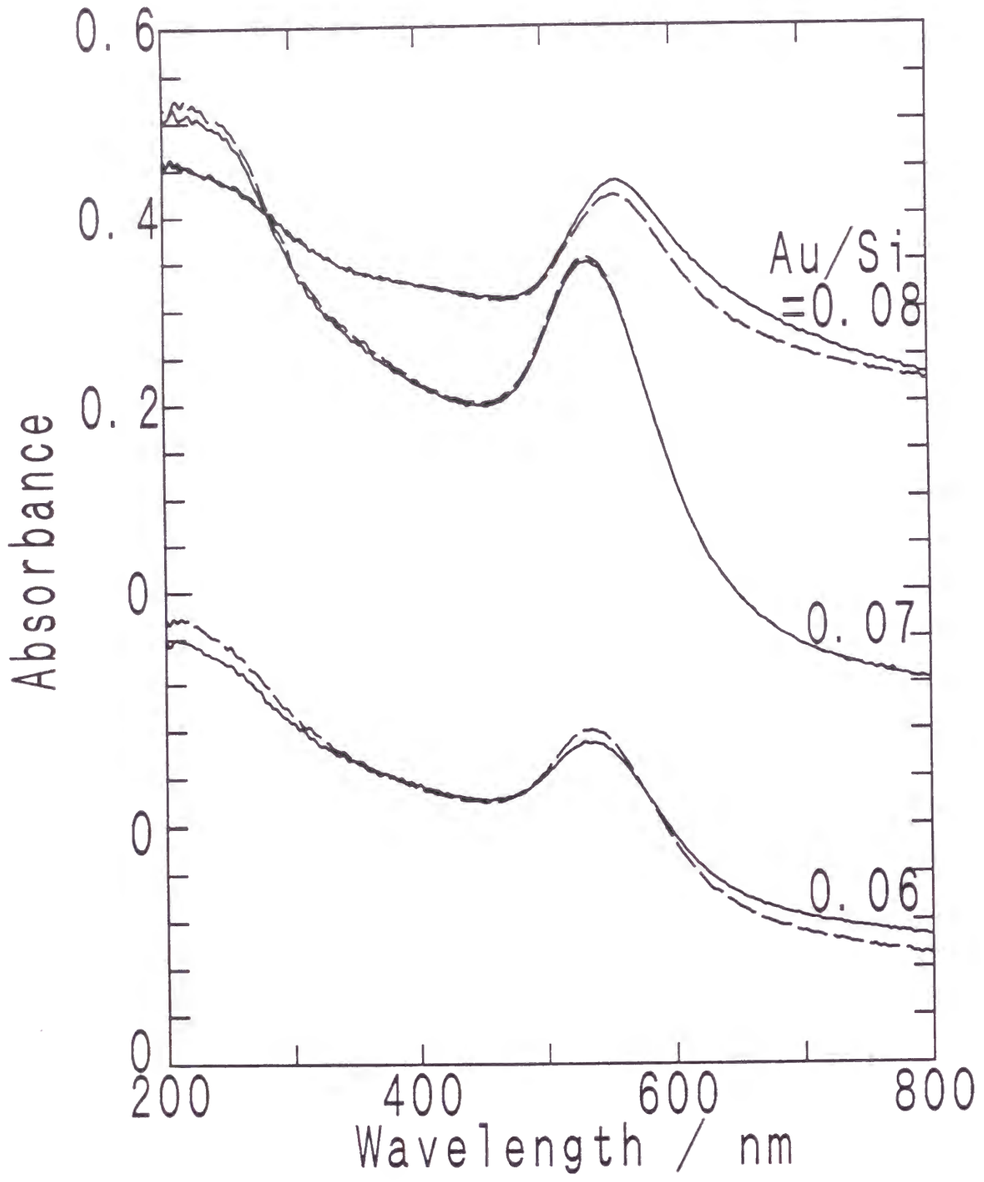

Fig.3(b) Optical absorption spectra of as-prepared (solid line) and surface wiped (dashed line) films with different Au/Si molar ratio and $La(NO_3)_3$/TEOS=0.01.

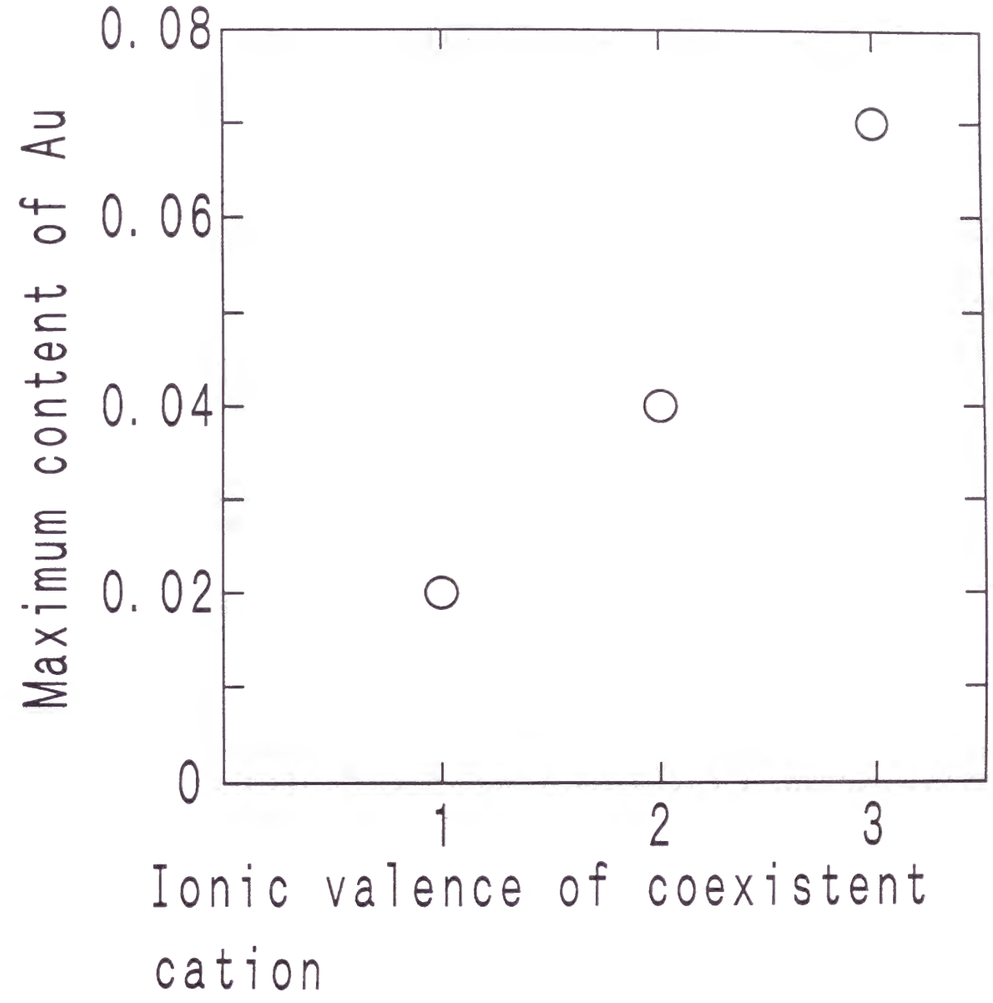

Fig.4 The maximum amount of gold microcrystals incorporated in the films prepared from dip-coating solutions containing $M(NO_3)_n$ (M=Na, Ca, and La) with the molar concentration of $M(NO_3)_n$/TEOS = 0.01.

of the additive cation increases the maximum amount of gold microcrystals in the SiO_2 film though the concentration of the additives is kept constant, i.e., $M(NO_3)_n$/TEOS = 0.01. The maximum amount of gold in the case of $Ca(NO_3)_2$-addition is Au/TEOS = 0.04, and that in the case of $La(NO_3)_3$-addition is Au/TEOS = 0.07.

The absorption spectra of the films prepared from $La(NO_3)_3$/TEOS = 0.01 and $HAuCl_4 \cdot 4H_2O$/TEOS = 0.08 solutions, in which the excess amount of gold microcrystals are depleted to the film surface, have the absorption peak position about 20nm longer than those of the films prepared from $HAuCl_4 \cdot 4H_2O$/TEOS = 0.06 and = 0.07 solutions with the same $La(NO_3)$ content. In addition, the absorption peak of the former is broad and has a long wavelength-side tail compared with the peak of the latter.

4. Discussion

The maximum amount of gold microcrystals in the SiO_2 film prepared from the additive-free TEOS and $HAuCl_4 \cdot 4H_2O$ solution is Au/SiO_2 = 0.01. As will be described in chapter 5, the study on gold microcrystal-doped oxide films of $AlO_{1.5}$, TiO_2 and ZrO_2 using metal alkoxides and $HAuCl_4 \cdot 4H_2O$ show that the maximum amount of gold microcrystals decreases with decreasing the point of zero charge, pH_0, of the gel matrix. As pH_0 of SiO_2 is very low, i.e. 1.9, it is considered that only a very small amount of gold can be incorporated in the SiO_2 film [5]. This should be due to the fact that SiO_2 gel has low pH_0 and hence its surface tends to be charged negative, thus the Coulomb's repulsive force would exist between $AuCl_4^-$ ions and SiO_2 gel matrix. In this case, most of the $AuCl_4^-$ ions should be depleted from gel matrix and this is why the maximum amount of gold becomes as small as Au/SiO_2 = 0.01 for SiO_2 gel.

The increase of the amount of gold which can be incorporated in SiO_2 matrix was achieved by the addition of $NaNO_3$ to the dip-coating solution, i.e., addition of Na^+ and NO_3^- to the solution. It must be noted that, as $NaNO_3$ is a strong salt and thus the addition of $NaNO_3$ to the coating solution should not change its pH, this change of the maximum amount of gold can not be attributed to the change in degree of condensation of silica sol in the dip-coating solutions. As given in Chapter 1, the use of $NaAuCl_4 \cdot 2H_2O$ instead of $HAuCl_4 \cdot 4H_2O$ enables the formation of gold microcrystal-doped SiO_2 film with $Au/SiO_2 = Na^+/SiO_2$ = 0.04 [1]. This value agrees with the result shown in Fig.2 that the maximum amount of gold for the case of $NaNO_3/SiO_2$=0.04 is Au/SiO_2=0.04 and that the molar ratio of the maximum amount of Au to $NaNO_3$ decreases to less than one when the concentration of $NaNO_3$ exceeds the value of $NaNO_3/SiO_2$=0.04.

From these results, the increase of the maximum amount of gold which can be incorporated in the SiO_2 matrix is considered to be due to the coexistence of Na^+ ions in the coating solution, but not due to that of NO_3^- ions. It is known that the addition of ions to sol solution usually changes the surface charge of sol particles by the compression of the thickness of electric double layer and by the adsorption of ions on the sol surface which tend to neutralize the surface charge [6,7]. Therefore, the increase of the maximum amount of gold in silica films by addition of $NaNO_3$ to the dip-coating solution should be due to the change in Coulomb's repulsive force between the negatively charged inner surface of silica gel films and the $AuCl_4^-$ ions in gel films, which is illustrated in Fig.5 (a) and (b). In the case of additive-free dip-coating solution (a), Coulomb's repulsive force exists between gel matrix and $AuCl_4^-$ ions, and then the $AuCl_4^-$ ions move toward the film surface together with the solvent during the shrinkage and

sintering of gel films by heat treatment. On the other hand, when Na^+ ions are present in the dip-coating solution (b), they should be adsorbed on the inner surface of silica gel films and then Coulomb's repulsive force between gel matrix and $AuCl_4^-$ ions becomes low. In the case of high Na^+ concentration, the attractive force between gel surface and $AuCl_4^-$ ions through Na^+ ions may occur. Thus, the addition of $NaNO_3$ to dip-coating solutions is effective to increase the maximum amount of gold in SiO_2 films.

The addition of $Ca(NO_3)_2$ and $La(NO_3)_3$ was also found to increase the maximum amount of gold in the films. They are considered to give the same effect as in the case of $NaNO_3$. Furthermore, it can be seen from Fig.4 that the maximum amount of gold in the film increases with increasing the valence of cations at the same concentration of M^{n+}/TEOS=0.01. This is related to the fact that polyvalent ions are more effective to neutralize the surface charge of colloid surface [6,7]. The addition of Ca^{2+} and La^{3+} may also has a possibility to change the pH of dip-coating solutions by the reaction $[M(OH_2)_m]^{n+} <=> [M(OH_2)_{m-1}(OH)]^{(n-1)+} + H^+$. However, the dissociation constant of $[Ca(OH_2)_m]^{2+}$ in an aqueous solution is $10^{-11.6}$ [8] and that of $[La(OH_2)_m]^{3+}$ is also very small. Furthermore, as these values become smaller in TEOS-H_2O-C_2H_5OH solution, the amount of H^+ ions formed by this reaction must be negligible compared with the concentration of HCl in the dip-coating solution, i.e. HCl/TEOS=0.03.

Figure 2 indicates that the maximum amount of gold in the case of $NaNO_3$/TEOS=0.03 must be in the range from Au/TEOS=0.03 to 0.04. This amount is about half of that in the case of $La(NO_3)_3$/TEOS=0.01 in Fig.4, although the concentration of NO_3^- ions in the two dip-coationg solutions is the same. This also supports the above conclusion that the factors dominating the maximum amount of gold in the film are the species and concentra

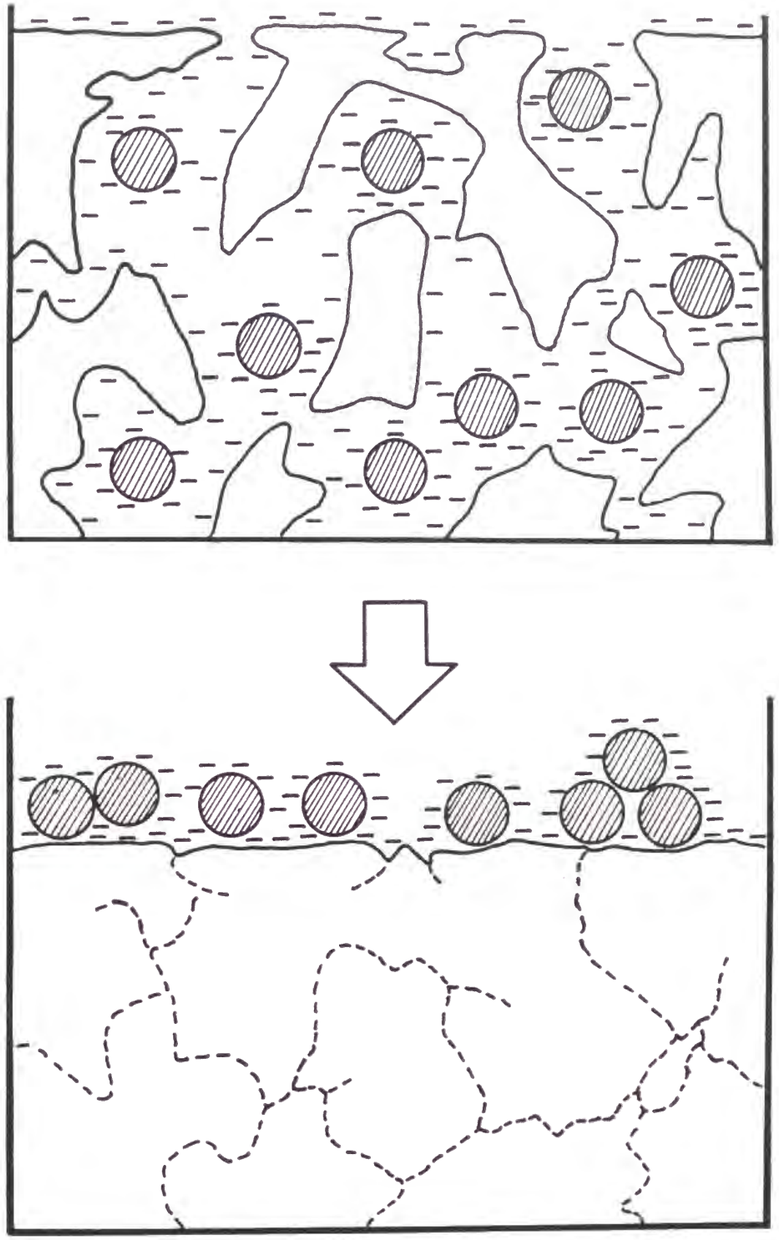

Fig.5(a) Schematic diagram of the sintering process of $AuCl_4^-$-contained SiO_2 gel films free from additive ions. Shadowed circles are $AuCl_4^-$ ions, and small circles.

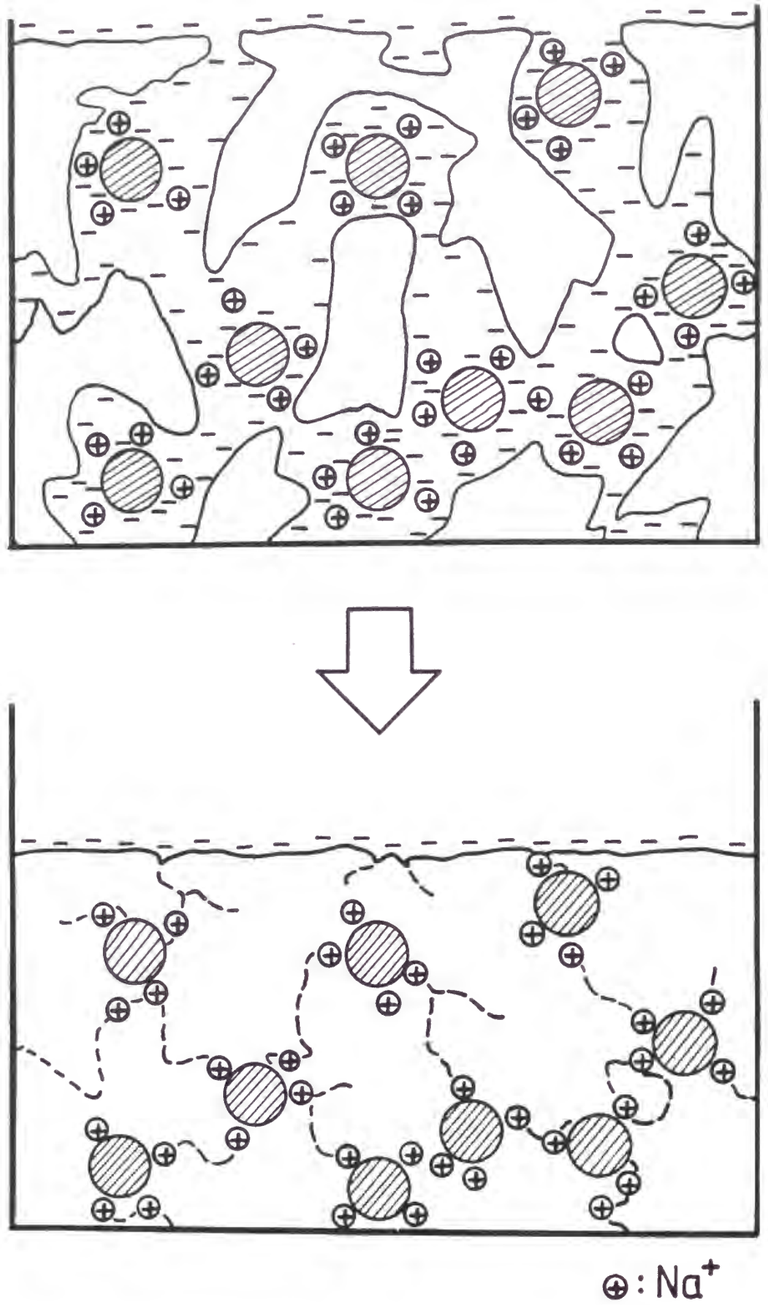

Fig.5(b) Schematic diagram of the sintering process of $AuCl_4^-$-contained SiO_2 gel films containing Na^+ ions. Shadowed circles are $AuCl_4^-$ ions, and small circles are Na^+ ions.

tion of coexisting cations but not those of anions.

The absorption spectra of the films, in which the excess amount of gold microcrystals is depleted to the film surface, have their absorption peaks positioned at the longer wavelength side than those of the films in which all the Au microcrystals stay inside, together with the broadening of the peaks. Similar phenomena are observed in the aggregated Au microcrystals in SiO_2 matrix [9] and also in highly Au microcrystal-doped Al_2O_3 films in which microcrystals may be aggregated [4]. An increase in size of Au microcrystals and the elongation of the microcrystals from spherical shape are also known to cause these spectral changes [10]. Therefore, the spectral change observed in this study is attributed to the aggregation and/or size increase of Au microcrystals both of which might be caused by the decrease of the attractive force between $AuCl_4^-$ ions and gel surface with decreasing of M^{n+}/Au ratio (M=Ca, La) through the aggregation of $AuCl_4^-$ ions in gel micropores.

5. Conclusion

In order to increase the amount of gold microcrystals which can be incorporated in the sol-gel derived silica film made from TEOS and $HAuCl_4 \cdot 4H_2O$, an attempt was made to add $NaNO_3$, $Ca(NO_3)_2$, or $La(NO_3)_3$ to the dip-coating solutions. It was found that the amount of gold microcrystals monotonously increased with increasing the concentration of additive salts. Also the maximum amount of gold microcrystals depended on the valence of added cations; the higher the valency, the larger the maximum amount. These results are explained by the decrease of the Coulomb's repulsive force between silica gel surface and $AuCl_4^-$ ions by the adsorption of cations on the gel surface.

6. References

[1] J. Matsuoka, R. Mizutani, S. Kaneko, H. Nasu, K. Kamiya, K. Kadono, T. Sakaguchi and M. Miya, J. Ceram. Soc. Jpn. 101 (1993) 53

[2] H. Kozuka and S. Sakka, Chem. Mater. 5 (1993) 222

[3] J. Matsuoka, R. Mizutani, H. Nasu and K. Kamiya, J. Ceram. Soc. Jpn. 100 (1992) 599

[4] J. Matsuoka, H. Yoshida, H. Nasu and K. Kamiya, J. Sol-Gel Sci. Tech. 9 (1997) 145

[5] J. Matsuoka, R. Naruse, H. Nasu and K. Kamiya, J. Non-Cryst. Solids 218 (1997) 151

[6] A. Kitahara and K. Furusawa, Saisin-Koroido-Kagaku (Latest Colloid Chemistry) (Koudansha, Tokyo, 1990), pp.121-126 [in Japanese].

[7]>N. de Rooy, P.L. Bruyn and J.Th.G. Overbeek, J. Colloid Interface Sci., 75 (1980) 542

[8] Kagaku-Binran (Kisohen) (Databook of Chemistry (Pure Chemistry)), 2nd ed., ed. by Chem. Soc. Jpn., (Maruzen, Tokyo, 1975), p.994 [in Japanese]

[9] J.M. Fernández Navarro and M. Angeles Vilegas, Glastech. Ber., 65 (1992) 32

[10] H. Kozuka, Proc. SPIE: Sol-Gel Optics IV 3136 (1997) 304

Chapter 3

Optical Nonlinearity of Au Microcrystal-Doped SiO_2 Glass Films Prepared by Sol-Gel Method

1.Introduction

In this chapter, the third order nonlinear susceptibility, $\chi^{(3)}$, of gold microcrystal-doped silica films prepared by sol-gel process is studied. The effects of the preparation condition and subsequent heat treatment on $\chi^{(3)}$ are discussed from the viewpoint of microstructure. In addition, $\chi^{(3)}$ values measured with a nanosecond-pulse laser and a picosecond-pulse laser are compared for the same sample. Most of the previously reported values of optical nonlinearity have been measured using lasers with a nanosecond-order pulse duration time. In this case, the nonlinear optical response includes not only a response due to the electronic excitation in Au microcrystals but also the photo-thermal response due to the change of refractive index by the temperature increase caused by absorbing light. The response time for the former phenomenon is in the order of picosecond or shorter, and that for the latter response is in the order of nanosecond. This means that the measurement using a laser with picosec.-order pulse width is necessary to estimate the electronic optical nonlinearity and evaluate its applicability to all-optical high-speed switching device. Therefore, in addition to the nanosec.-measurements, both nanosec.- and picosec.-optical nonlinearity are measured using the same samples and the same measurement system for some samples in the present study.

2.Experimental

Au microcrystal-doped silica glass films used in this study were prepared by the same sol-gel method as that in Chapter 1, using $NaAuCl_4 \cdot 2H_2O$ and TEOS as starting materials. The Au/SiO_2 molar ratio in the samples was is 0.01 for nanosec.-measurements and 0.04 for picosec.-measurements. In the picosec.-measurement samples, the film was deposited only on one side of the substrate to prevent the optical interference effect of DFWM signals generated from two coated-films on both sides of the substrate. The one-side coating was achieved by covering the other side with adhesive polymer tape while dip-coating. After removal of the polymer tape, the coated-film was heat-treated at 200° or 400° C for 15 min.

The third order optical nonlinearity of the films was measured using a second harmonic of Q-switched Nd:YAG laser (532nm) as a light source. The measurement system is illustrated in Fig. 1. The laser was operated with a pulse duration time of 7ns and a pulse energy of $5MW \cdot cm^{-2}$ in the nanosecond measurements, and with a pulse duration of 30ps and a pulse energy of $10MW \cdot cm^{-2}$ in the picosecond ones. The third order nonlinear optical susceptibility $\chi^{(3)}$ was calculated using the equation

$$\chi^{(3)} = C \cdot \frac{n^2}{L} \cdot \frac{R^{1/2}}{(I_f I_b)^{1/2}} \cdot \frac{\ln(1/T)}{T^{1/2}(1-T)}$$

where n, L, T and R are the refractive index, thickness, transmittance and phase conjugated reflectivity of the sample, I_f and I_b are the forward and backward pump beam intensity, and C is a constant independent of sample. $\chi^{(3)}$ of the sample was evaluated by referring to that of the standard sample CS_2. $\chi^{(3)}$ of CS_2 was taken as 1.7×10^{-12} esu for the nanosecond measurement and as 2.9×10^{-12} esu for the picosecond measurement. The set-up of DFWM equipment and derivation of $\chi^{(3)}$ from the experimental data

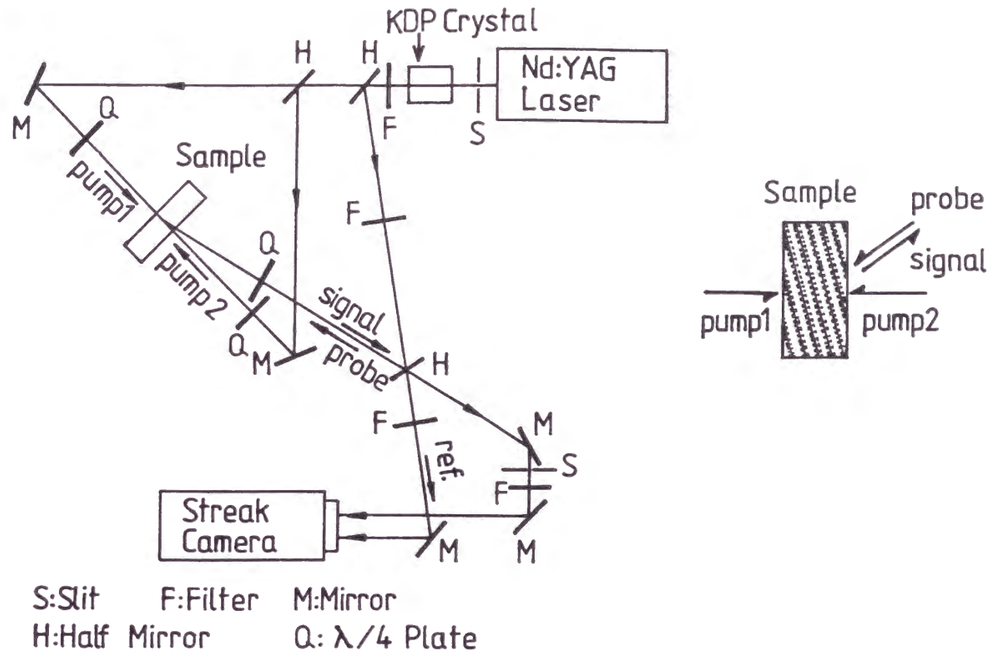

Fig.1 Illustration of the set-up of DFWM measurement system used in this study.

are the same as those described in Ref.[1].

3.Results

The values of third order nonlinear susceptibility determined by nanosec. DFWM method are listed in Table.1 for Au/Si=0.01 samples subjected to different thermal history. The absorption coefficient at 450 nm, which is a linear function of the total amount of Au microcrystals as revealed for those with the radius larger than 5 Å [2], is also listed in the table. The third order nonlinear susceptibility $\chi^{(3)}$ of the sample heat-treated at 400° C was 7.2×10^{-9} esu. The $\chi^{(3)}$ of the sample heat treated at 600° C was similar to that prepared at 400° C, being consistent with the similarity in absorption spectra of these two samples. On the other hand, the sample once heated at 400° C and then post heat-treated at 1000° C showed a lower $\chi^{(3)}$ value, although the peak position in absorption spectra was very close to the wavelength of pump and probe light in this sample.

In order to clarify the origin of the heat-treatment effect on $\chi^{(3)}$, nanosec.- and picosec.-measurements were performed on four samples with different thermal history and different optical absorption spectra. Figure 2 shows the optical absorption spectra of the Au/SiO_2=0.04 samples prepared under the conditions listed in Table 2. In a rough sense, the samples 4a, 4b and 2b show nearly the same optical density around 450nm where the absorption coefficient is proportional to the total volume of Au microcrystals in the sample [2]. Consequently, these three samples are considered to contain nearly the same amount of Au as metal microcrystals. On the other hand, the absorption of sample 2a at 450nm is weak. This indicates that a considerable amount of gold still remains as $AuCl_4^-$ anions in this sample.

Fig. 3a and 3b show the examples of the intensity profile of the signal

Table 1 Optical nonlinearity of sol-gel derived Au microcrystal-doped silica glass measured by DFWM method at 532 nm.

Preparation Condition (esu)	Absorption Peak Position (nm)	Abs. Coeff. at 450nm(μm^{-1})	$\chi^{(3)}$
400° C	547	0.32	7.2×10^{-9}
400° C and 1000° C, 1hr	528	0.30	3.4×10^{-9}
600° C	544	0.30	7.7×10^{-9}

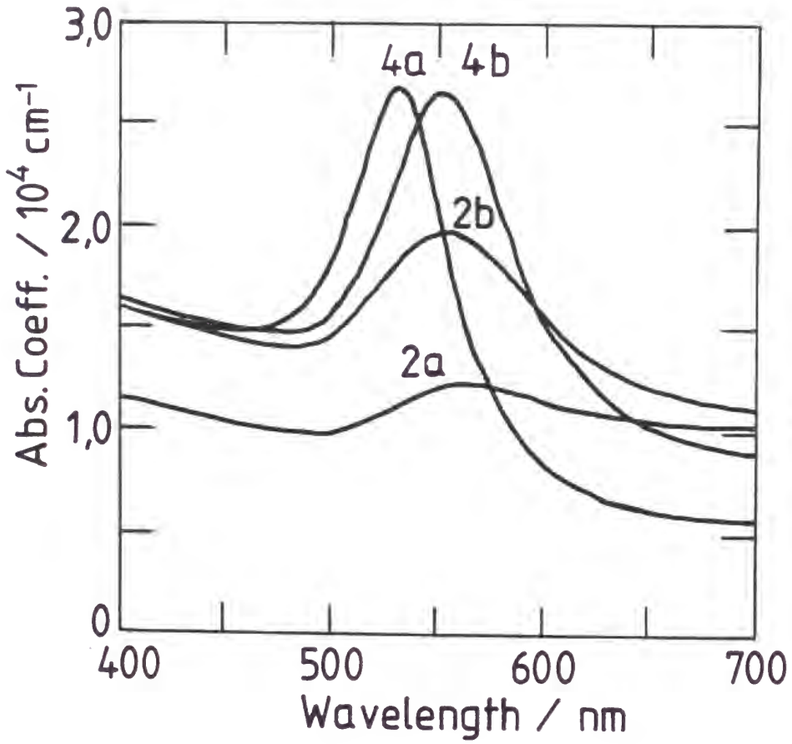

Fig.2 Optical absorption spectra of Au microcrystal-doped silica glass films (0.15μm in thickness) coated on silica substrate. Preparation condition of the films are listed on Table 1.

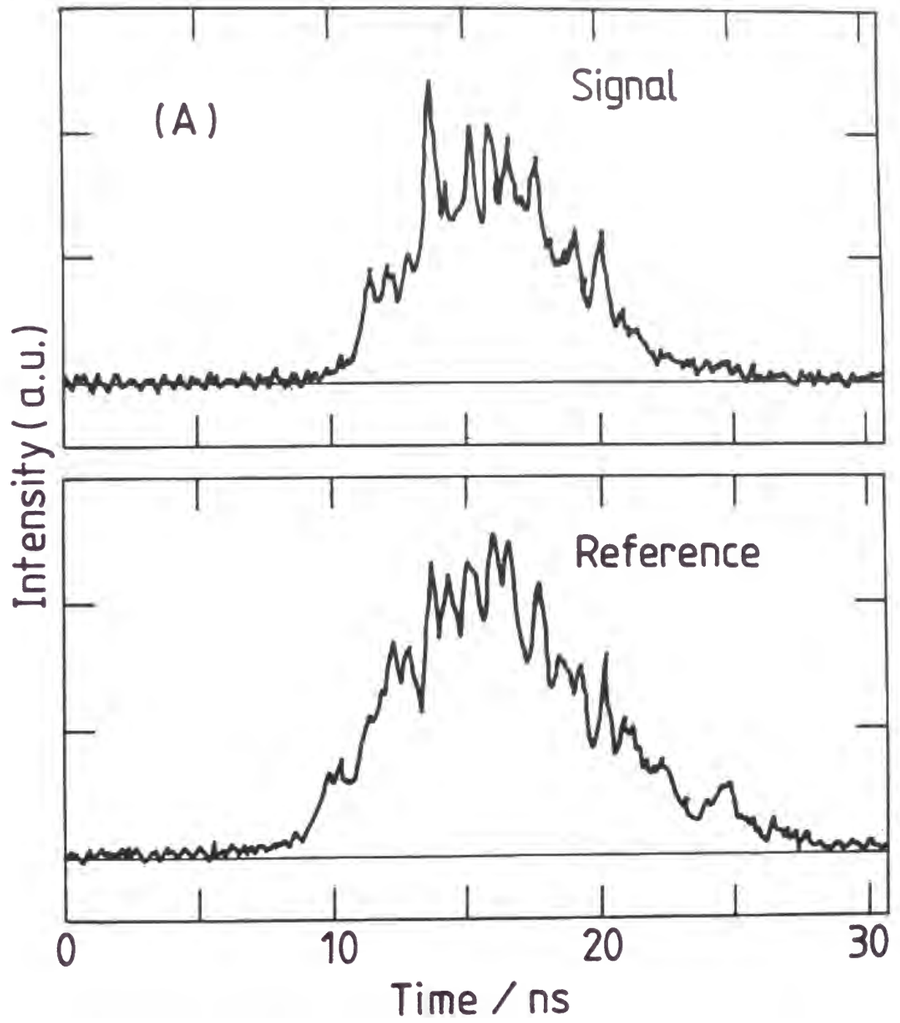

Fig.3(a) Example of the beam profiles of signal and reference light as a function of time in DFWM measurements. (nanosecond-measurements of sample 4a)

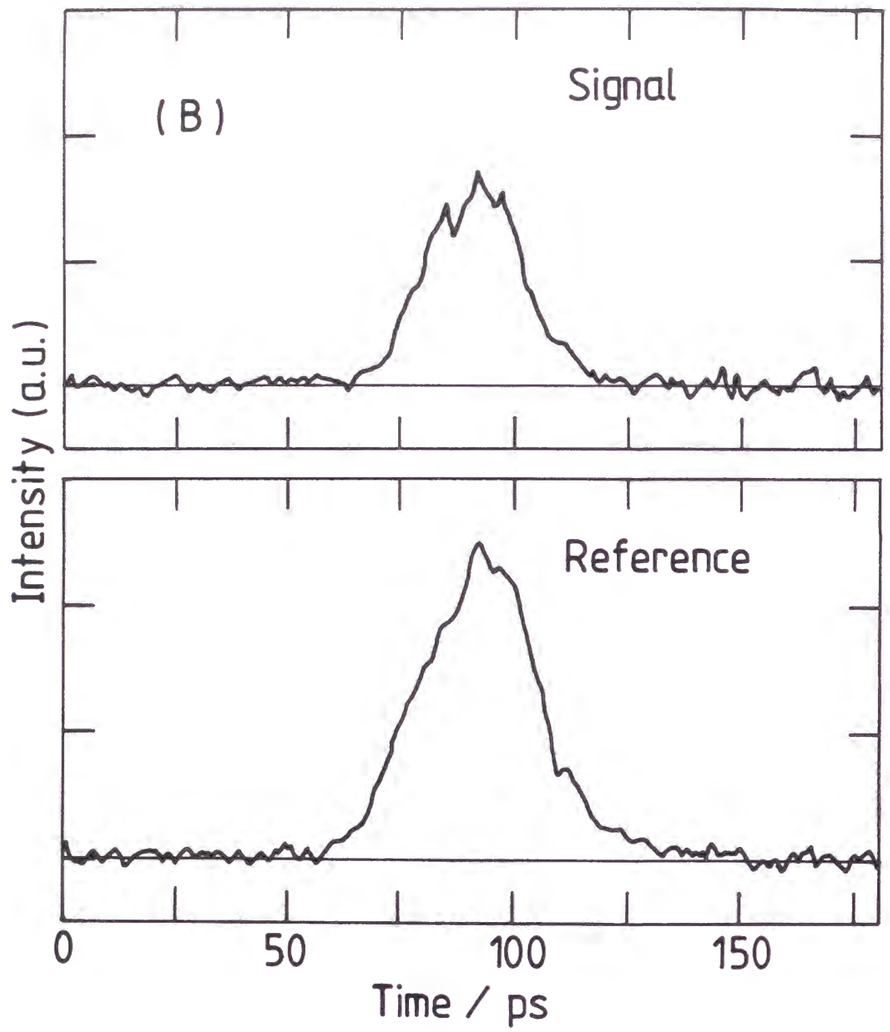

Fig.3(b) Example of the beam profiles of signal and reference light as a function of time in DFWM measurements.
(picosecond-measurements of sample 4a)

Table 2 Preparation condition, nanosecond- and picosecond-measured third order nonlinear optical susceptibility, and absorption coefficient at 532nm of Au microcrystal-doped glass films.

Sample	Heating Temp. / ° C	Post Heat Treatment Condition	$\chi^{(3)}_{nano}$ /10^{-8} esu	$\chi^{(3)}_{pico}$ 10^{-8} esu	Abs. Coeff. (532 nm) /10^{4} cm^{-1}
4a	400	--------	1.38	0.584	2.67
4b	400	1000° C, 1hr	1.68	0.644	2.28
2a	200	--------	0.247	0.100	1.08
2b	200	200° C,23hr	1.34	0.258	1.83

obtained in both the nanosecond (a) and picosecond (b) DFWM measurements, along with the profile of the reference light or the excitation laser pulse profile. In the both measurements, the width of the signal from the sample is narrower than that of the excitation pulse. In the nanosecond measurement, the width of the signal at a quarter of the maximum intensity was 6.8ns while that of the reference was 9.6ns. Similarly, in the picosecond measurement, the width of the signal was 33ps while that of the reference was 43ps. Thus the signal is not due to the scattering at the sample surface as linear response but truly due to the nonlinear optical response.

The third order optical nonlinearity $\chi^{(3)}$ obtained in DFWM measurements are listed in Table 2 for both the nanosecond and picosecond measurements. The ratio of $\chi^{(3)}$ obtained using picosecond pulse to that obtained using nanosecond pulse is about 0.4 for the samples 4a, 4b, 2a, and about 0.2 for the sample 2b.

4.Discussion

The nanosec.-measured third order nonlinear optical susceptibility $\chi^{(3)}$ was 7.2×10^{-9} esu for the 400° C heat-treated Au-doped glass, and 7.7×10^{-9} esu for the 600° C heat-treated one. The nonlinear susceptibility of Au microcrystals themselves in the film, $\chi_m^{(3)}$, can be calculated by using the following relations [3]

$$f_1(\omega) = \frac{3\varepsilon_d}{\varepsilon_m(\omega) + 2\varepsilon_d} \qquad (3)$$

$$\chi(3) = p\, f_1^{\,2}\, |f_1|^2\, \chi_m^{(3)} \qquad (4)$$

where $\varepsilon_m(\omega) = \varepsilon_m' + \varepsilon_m''$ is the frequency dependent complex dielectric constant of Au particle, ε_d is the real part of that of the glass matrix

(imaginary part is negligible at this wavelength), and p is the volume fraction of Au particles. By using the complex refractive index of bulk gold [4] for calculating $\varepsilon_m(\omega)$ and putting $\varepsilon_d = 1.461^2$, which is the square of the refractive index of silica glass at 532nm, the $\chi_m^{(3)}$ in these two glasses was estimated as 1.0×10^{-7} esu. This value is similar to that in a glass prepared by ion implantation, that is 8×10^{-8} esu [5] and is also similar to the value in a sputter-derived glass calculated from the $\chi^{(3)}$ data in Ref. [6]. It is, however, about two times larger than that observed in Au-doped glasses prepared by melting and subsequent heat treatment [3].

The nanosec.-measured nonlinear susceptibility of the glass film decreased rapidly to about a half when the sample was post heat-treated at 1000° C. In Chapter 1, it was pointed out that the post heat-treatment caused the relaxation of the shape of microcrystals. Therefore, it can be said that the unrelaxed and non-spherical microcrystals have higher $\chi^{(3)}$ than that of structure-relaxed and spherical microcrystals.

The nanosec.-measured nonlinear optical susceptibility of the Au microcrystals themselves in the films, $\chi_m^{(3)}$, after the heat treatment at 1000° C is estimated as 6×10^{-8} esu. This value is comparable to that in the glasses prepared by melting and subsequent heat treatment, in which the microcrystals with thermodynamically stable structure may have been formed. As both ion implantation and sputtering are the high energy processes so that the glasses obtained are highly supersaturated by Au atoms, the microcrystals precipitated during subsequent heat treatment may be different from the stable structure one and have a high $\chi_m^{(3)}$ value. Furthermore, the Au-supersaturated nature of the glass network may prevent the relaxation of microstructure to achieve the low $\chi_m^{(3)}$ form.

In Fig.2, the sample 4a shows an absorption peak at 531nm and has

no absorption tail to the long wavelength side. This feature indicates that Au microcrystals are spherical and free from aggregation. Using the equation $r_B = v_F / \Delta\omega_{1/2}$ (v_F is the Fermi velocity of a free electron and $1.39\times10^6 m\cdot s^{-1}$ for Au, and $\Delta\omega_{1/2}$ is the full width at half maximum of the absorption peak [4]), the average crystal radius was estimated to be 250Å for this sample. The absorption peak of samples 4b and 2b is positioned at the longer wavelength side than that of sample 4a, and has a tail toward 700nm, suggesting that the microcrystals are not spherical but spheroidal or have more deformed shape with lower symmetry, or more probably the microcrystals are aggregated. Although the non-spherical nature of microcrystals in the samples 2b and 4b make the precise estimation of microcrystal size impossible, the microcrystal size in the sample 2b is considered to be smaller than that in the sample 4b since the full width at half maximum of the peak of sample 2b is larger than that of sample 4b.

The ratio of $\chi^{(3)}_{pico}$ to $\chi^{(3)}_{nano}$ is in the range from 0.2 to 0.4. This means that 80 to 60 % of the nanosec.-measured $\chi^{(3)}$ is attributable to the optical absorption-induced thermal expansion effect. The contribution of the change in the refractive index by temperature rise to the nonlinear susceptibility, when it is normalized by the absorption coefficient, can be estimated by using the parameter $(\chi^{(3)}_{nano} - \chi^{(3)}_{pico})/\alpha_{532nm}$. The estimated values of samples 4b and 2b were higher than that of sample 4a. This difference is attributed to the aggregation of Au microcrystals in the samples 4b and 2b in which the diffusion of heat from microcrystal to matrix is slower and thus the temperature of Au microcrystals increases higher. The above mentioned value of sample 2a is much smaller than the other three samples. This is ascribable to the small fraction of microcrystals in this sample.

The third order nonlinear optical susceptibility measured using picosec.- pulse is relatively higher for the 400° C heat-treated samples 4a and 4b than that for the 200° C heat-treated samples 2a and 2b. This agrees with the previously reported result stating that the susceptibility increases with increasing microcrystal radius [7]. Furthermore, when the normalized susceptibility in which $\chi^{(3)}$ is divided by the optical absorption coefficient is compared, the values of the former two samples were also larger than those of the latter two. The picosecond susceptibility of the post heat-treated sample 4b was about 10% larger than the as-prepared sample 4a, and also for the normalized susceptibility, the former was about 30% larger than the latter. This is probably related with the change in electronic structure of microcrystals by the aggregation in sample 4b.

5.Conclusion

Au microcrystal-doped SiO_2 films with Au/SiO_2=0.01 prepared by sol-gel method was found to have the nonlinear susceptibility $\chi^{(3)}$ of 7.7×10^{-9} esu in nanosec.-DFWM measurement. The subsequent heat treatment of the glass film at 1000° C decreased $\chi^{(3)}$ of the film by a factor of two. The nonlinear susceptibility of Au microcrystal itself, $\chi^{(3)}_m$, in the as-prepared film was 1.0×10^{-7} esu, which is nearly the same as that reported for the glasses prepared by ion implantation or sputtering. The $\chi^{(3)}_m$ of the 1000° C-heat-treated film was about the half of this value and is the same as that observed in the Au-doped glasses prepared by melting and subsequent heat treatment.

The picosec.-measured third order nonlinear optical susceptibility is in the range of 20 to 40% of the nanosec.-measured one, depending on the sample. The films with larger microcrystals have higher susceptibility than

those with smaller ones in both the nanosec.- and picosec.-measurements. The aggregation of microcrystals is considered to increase both nanosec.- and picosec.-susceptibility.

5.References

[1] K. Kadono, T. Sakaguchi, M. Miya, J. Matsuoka, T. Fukumi and H. Tanaka, J. Mater. Sci. : Mater. Electron., **4** (1993) 59

[2] R. H. Doremus, J. Chem. Phys., **40**, (1964) 2389

[3] F. Hache, D. Ricard, C. Flytzanis and K.Kreibig, Appl. Phys., **A47** (1988) 347

[4] D. W. Lynch and W. R. Hunter, "Handbook of Optical Constants of Solids", Ed. by E. D. Palik, Academic Press, Orland (1985) pp.286-95

[5] H. Kozuka and S. Sakka, Chem. Mater., 5 (1993) 222

[6] H. Wakabayashi, K. Kadono, T. Sakaguchi and M. Miya, in Proc. Inter. Conf. Sci. Tech. New Glasses, ed. by S. Sakka and N. Soga, p. 412 (1991)

[7] M. J. Bloemer, J. W. Haus and P. R. Ashley, J. Opt. Soc. Am. B, 7 (1990) 790

Chapter 4

Sol-Gel Synthesis of Au-Pd Alloy Microcrystal-Doped SiO_2 Glass Films

1.Introduction

In metal microcrystals, plasmon resonance caused by the cooperative motion of free electrons by photon absorption in microcrystals is considered as the origin of optical nonlinearity. The wavelength of this resonance depends not only the metal itself but also the dielectric constant of the matrix in which metal microcrystals are embedded. However, most of the previous studies on the optical nonlinearity of metal microcrystals have been carried out only for gold or copper microcrystals with nearly the same character of plasmon resonance (or resonance wavelength). There has been no papers on the formation of metal alloy microcrystal-doped glasses except for the formation of Ag-Cu alloy [1,2]. In an aqueous sol, Toshima et al.[3] reported the formation of Au-Pd alloy microcrystals. This suggests that the formation of Au-Pd alloy microcrystals may be possible in oxide matrix when the matrix is porous. So, in this chapter, the preparation of Au-Pd co-doped silica glass films by the sol-gel dip-coating method is attempted. For this purpose, silica gel films which contain both $AuCl_4^-$ and $PdCl_4^{2-}$ were prepared, and then the metal microcrystal formation through thermal decomposition was examined on the basis of various spectroscopic techniques. The Au-doped film without Pd and the Pd-doped film without Au are also prepared for comparison.

2.Experimental

$NaAuCl_4 \cdot 2H_2O$, Na_2PdCl_4 and tetraethyl orthosilicate (TEOS) were used as the starting materials and HCl was used as a catalyst for hydrolyzing TEOS. In this study, the molar ratio of $(Au+Pd)/SiO_2$ was fixed to 0.02, and the solution composition of TEOS : H_2O : EtOH : HCl was also fixed to 1 : 6 : 6 : 0.03 in molar ratio.

Figure 1 shows the procedure of the film preparation. First, TEOS and a half of the prescribed amount of EtOH were mixed into a solution, and the rest of the EtOH, H_2O, HCl_{aq} and the starting materials of Au and/or Pd were mixed into another solution. Then, the latter solution was titrated slowly to the former solution to make the coating solution. Color of the coating solution was yellow for the $NaAuCl_4$-containing solution, brown for the Na_2PdCl_4-containing solution, and for the solutions containing both $NaAuCl_4$ and Na_2PdCl_4, the color changed from yellow to brown depending on the composition.

The gel films were coated on both sides of a silica glass substrate by dip-coating method. The withdrawal rate of the substrate was 0.15 mm/s and the thickness of the film obtained after vitrification by heat treatment was about 0.05μm. The gel films obtained were heat treated at different temperatures ranging from 200° to 700° C for 15 min in air. This procedure was repeated for five times to obtain a sufficient thickness for optical absorption and XRD measurements.

Optical absorption spectra was measured with Shimadu UV-3100 UV-VIS-NIR spectrophotometer from 200 to 800 nm using an uncoated silica glass as a reference. As the films were coated on both sides of a substrate, the optical path length of Au/Pd-doped layers was about 0.5μm. X-ray diffraction analysis from 2θ = 36° to 43° using Cu K_α radiation was carried out with

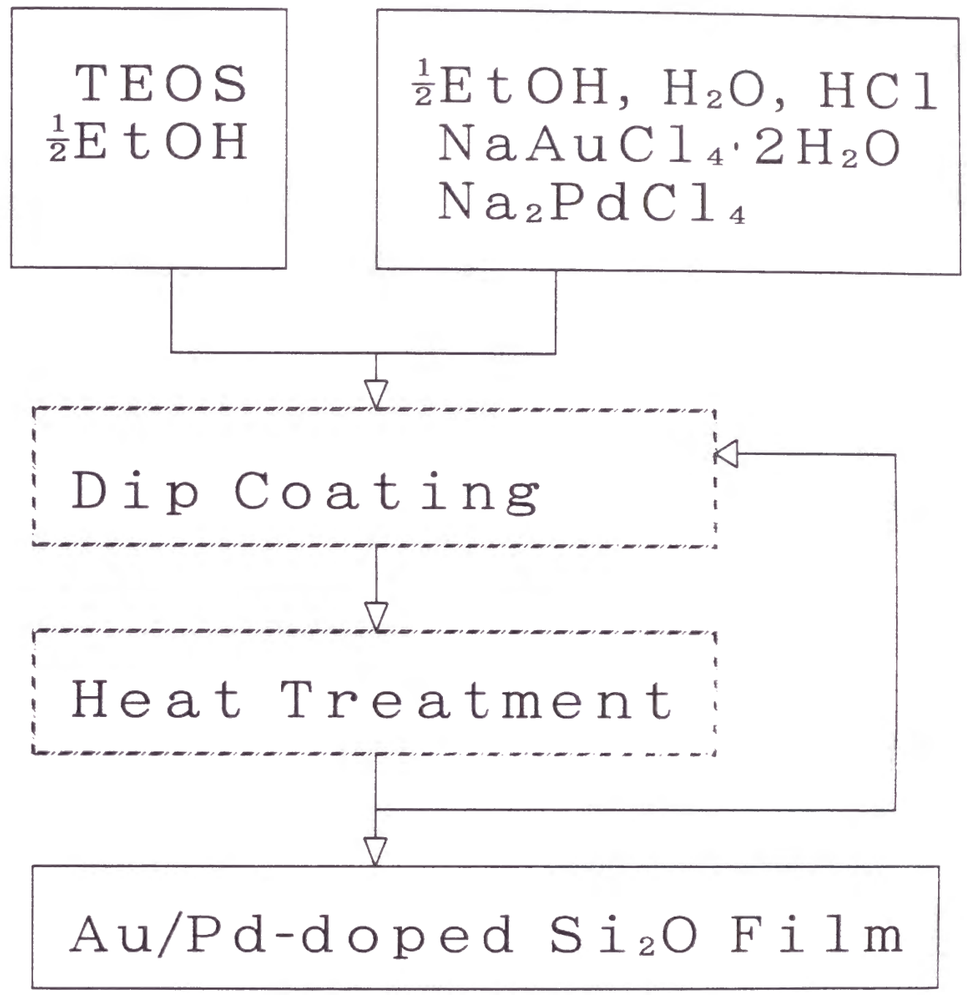

Fig.1 Flow chat for the preparation of Au-Pd co-doped SiO_2 thin film by sol-gel method.

a X-ray diffractometer, Shimadu XD-610, to follow the formation of the microcrystals of metallic Au, Pd, or their alloy and to measure the crystal size of microcrystals. X-ray photoelectron spectra were also measured with Shimadu ESCA 750 to examine the composition of films and the valence states of Au and Pd species.

3.Results

Figure 2 shows the optical absorption spectra of the films with different Au/Pd ratio heat treated at 600° C. The Au-doped film exhibits a strong absorption peak due to plasmon resonance around 560 nm, while the Pd-doped film shows no obvious structure in the spectra except for the increase of absorbance with decreasing wavelength. The Au-Pd co-doped films with Au/(Au+Pd) ≥ 0.5 have an absorption peak close to that of the Au-doped film, intensity of which decreases with decreasing the fraction of Au. The X-ray diffraction patterns of these films are shown in Fig. 3. A strong diffraction peak was observed in The Au-doped film with its position nearby (111) line of bulk Au. A partial substitution of Au by Pd decreases the peak intensity, accompanying a very small shift of the peak position toward Pd(111). No peak was observed around the (111) line position of bulk Pd in both Pd-doped and Au-Pd co-doped films.

Figures 4a-4c show the optical absorption spectra of Au/Pd-doped coating films heat-treated at different temperatures ranging from 200° to 700° C for Au : Pd = 0.02 : 0 (a), = 0.01 : 0.01 (b) and = 0 : 0.02 (c). In the Au-doped film (a) heat-treated at 200° C, the strong absorption peaks around 225 nm and around 310 nm due to $AuCl_4^-$ ions remain and the absorption peak around 550 nm due to plasmon resonance of Au microcrystals is small. When the heat-treatment temperature is raised to 300° C or higher, the peaks due

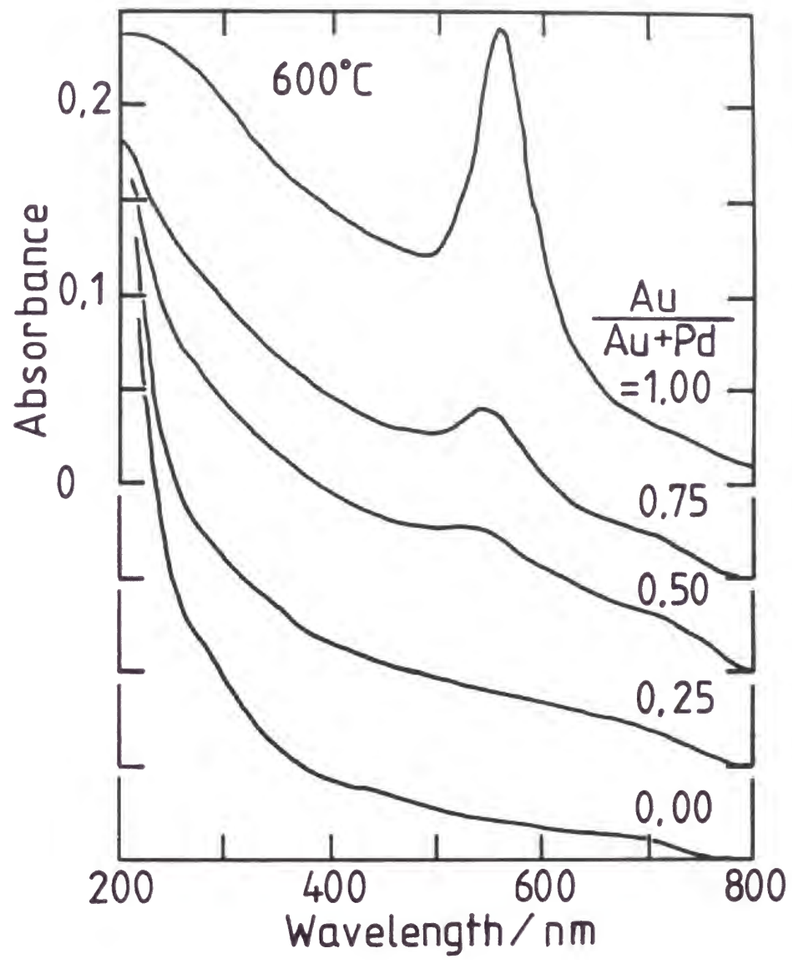

Fig.2 Optical absorption spectra of films with several Au/(Au+Pd) atomic fraction heat treated at 600°C.

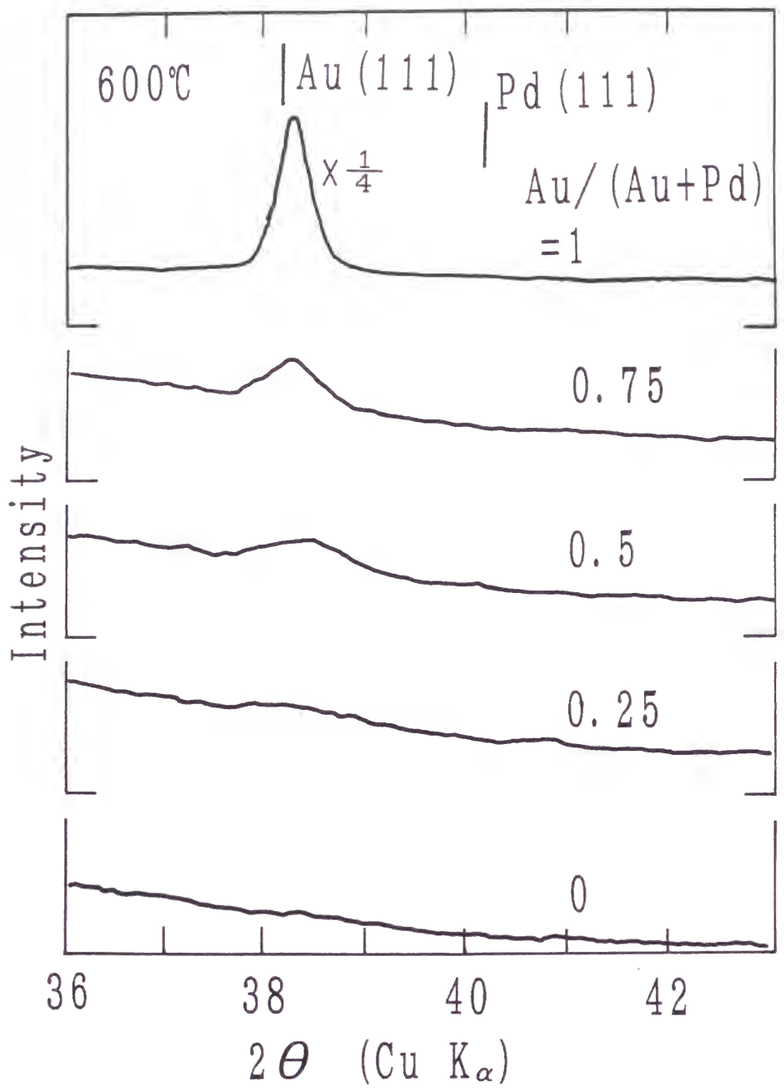

Fig.3 X-ray diffraction patterns of films with several Au/(Au+Pd) atomic fraction heat treated at 600° C around the Au(111) and Pd(111) peak positions.

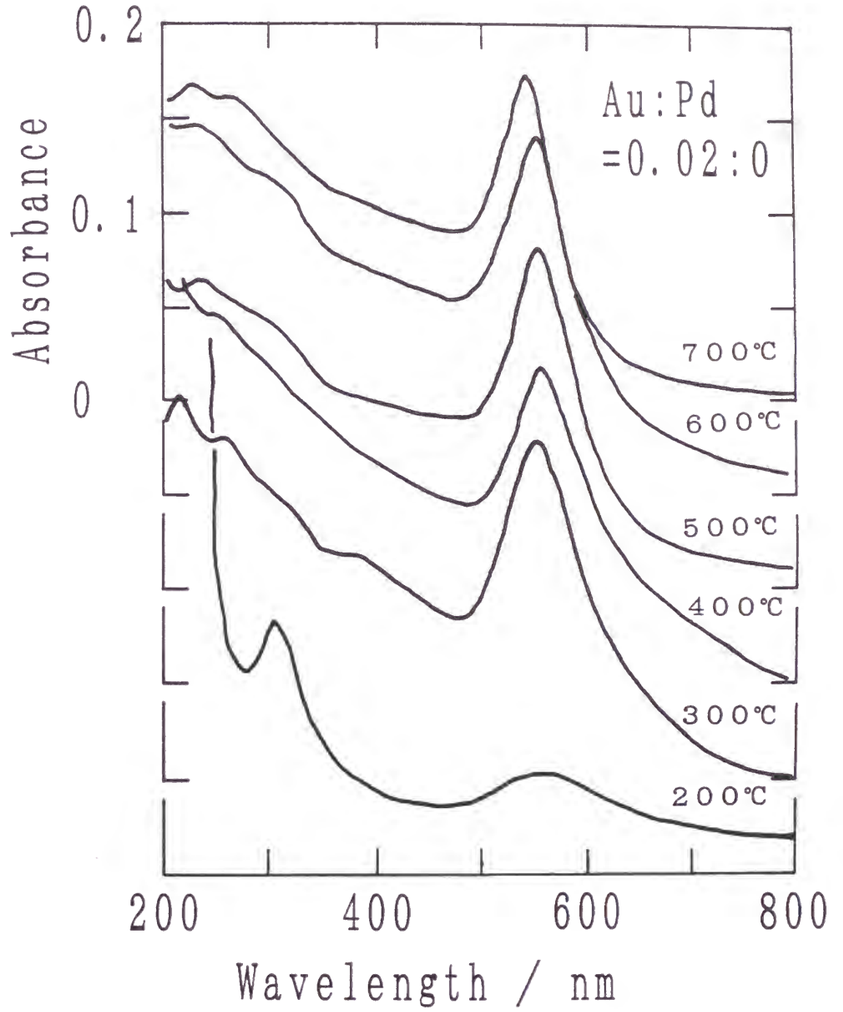

Fig.4(a) Optical absorption spectra of Au-doped films heat treated at a temperature from 200° to 700° C.

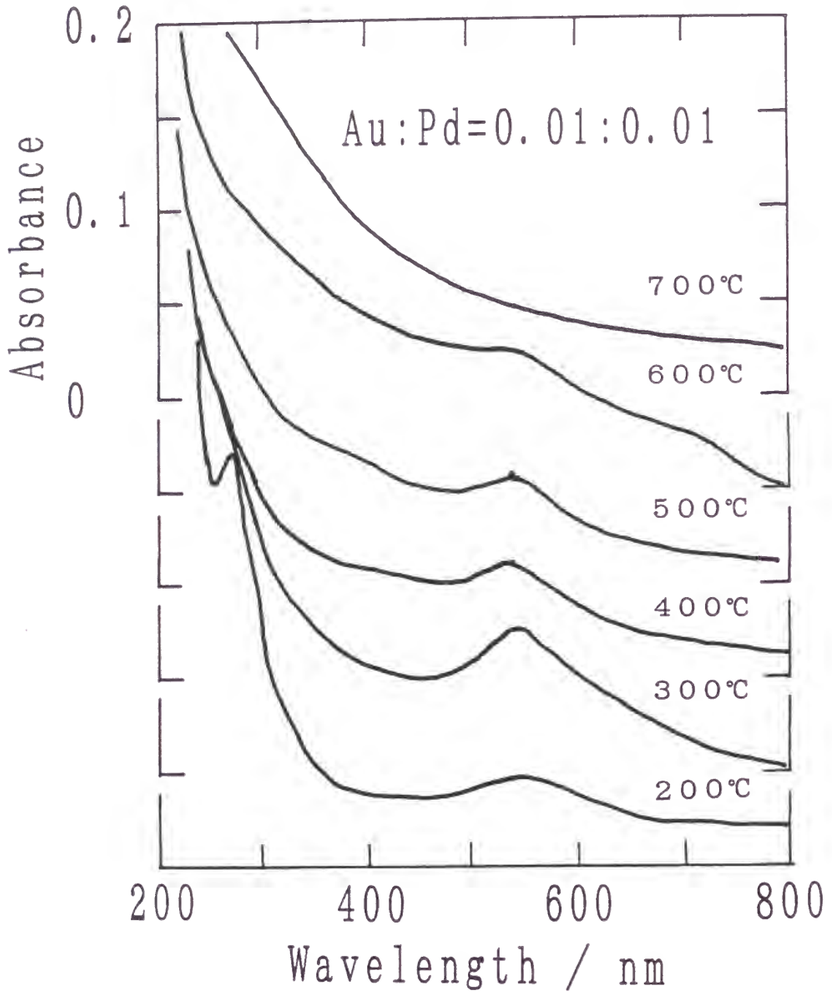

Fig.4(b) Optical absorption spectra of Au-Pd co-doped films heat treated at a temperature from 200° to 700° C.

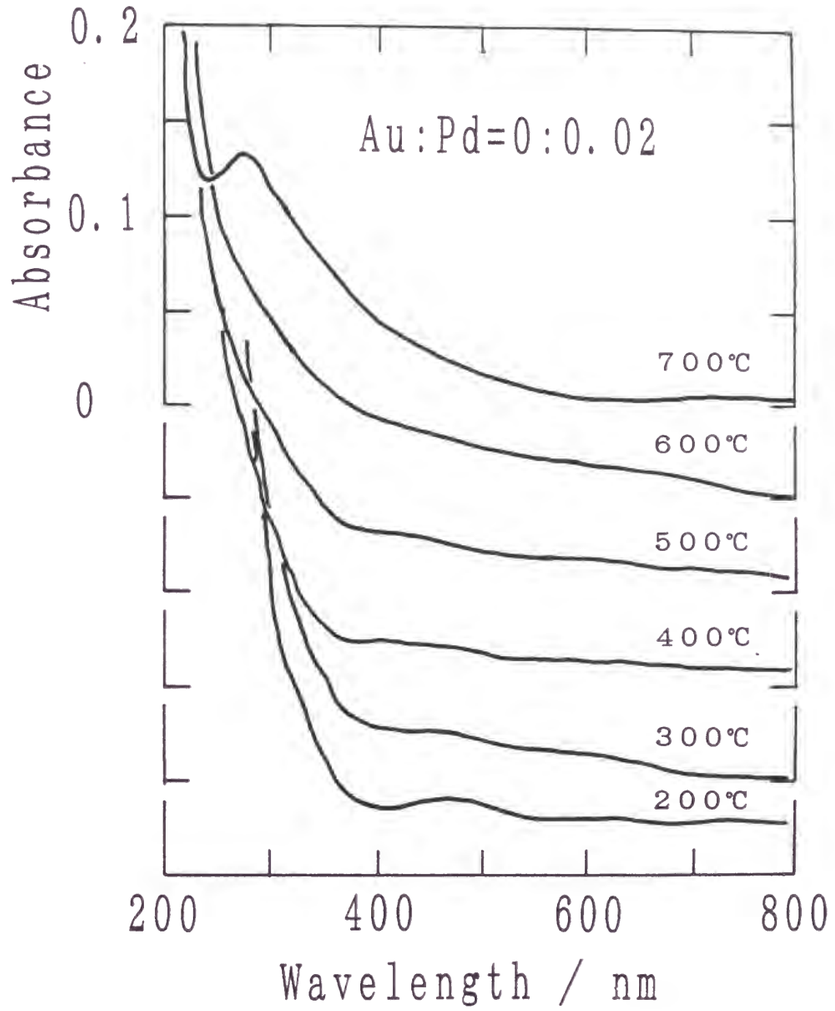

Fig.4(c) Optical absorption spectra of Pd-doped(c) films heat treated at a temperature from 200° to 700° C.

to $AuCl_4^-$ ions disappear and the peak intensity of plasmon resonance is increased. These results agrees with those described in Chapter 1.

In the Pd-doped films (Fig 4(c)), the absorption edge of about 390 nm with a shoulder around 310 nm and a broad and weak absorption band around 480 nm was observed in the film heat-treated at 200° C. This feature is similar to that of Na_2PdCl_4 aqueous solution which has the absorption edge at 360 nm with a shoulder around 310 nm and also has a broad-band absorption peak at 420 nm, indicating that the optical absorption of the film is due to $PdCl_4^-$ ion. The similar absorption spectra are observed for the films heat-treated up to 600° C. When the film was heat-treated at 700° C, an absorption peak around 290 nm appeared with a broad shoulder on the long wavelength side.

As shown in Fig. 4(b), Au-Pd co-doped glass films show a more complicated change of absorption spectra with the heat treatment temperatures. An absorption peak located at the same position as that in Au-doped film is seen in the 200° C-treated film, and the similar peak is also observed for the films heat-treated at 300° to 600° C. The intensity of this peak is strongest in the 300° C-treated film, and decreases with increasing heat-treatment temperature, while no obvious change in the absorption peak intensity is seen in the spectra of Au-doped films above 300° C. Furthermore, these Au-Pd co-doped films also show the increscent absorption with decreasing wavelength as the Pd-doped films. When the Au-Pd co-doped film is heat-treated at 700°C, the plasmon resonance peak around 550 nm completely disappears and also the peak around 390 nm seen in the Pd-doped film is not observed. Only a monotonous increase in absorption with decreasing wavelength is seen.

Figures 5a-5c show the X-ray diffraction patterns of the above mentioned films. In the Au-doped films (a), a strong diffraction peak corresponding to Au is observed irrespective of heat-treatment temperature. The Au peak of the film heat-treated at 200° C is relatively sharp, and the peak width for the other films heat-treated at 300° to 700° C is about 2 times larger than the 200° C-treated film. As shown in Fig. 5(c), no peak corresponding to Pd metal is observed in any of the Pd-doped films heat-treated at a temperature from 200° to 700° C.

In the Au-Pd co-doped films heat-treated at 200° C (Fig.5(b)), a diffraction peak is observed at the position of Au(111). The increase of heat-treatment temperature to 400° C causes its broadening and intensity decrease without changing the peak position. Further increase of heat treatment temperature, causes more broadening of the diffraction peak, accompanied by the shift of the peak position from that of Au(111) to that of Pd(111). At 700° C, the peak shifts more toward the Pd(111) line and is split into two broad peaks, one near Au(111) and the other around the midpoint of Au(111) and Pd(111) line. The shift of the diffraction peak of Au to higher 2θ side seems to indicate the formation of Au-Pd alloy.

Figures 6a-6c show the wide range X-ray photoelectron spectra of the Au-, Au-Pd-, and Pd-doped films heat-treated at 200°, 300°, 500°, and 700° C. In the Au-doped film, a strong peak of Cl-2p is observed in the 200° C-heated film, but its intensity becomes small in the 300° C-heated one and the peak disappears in the 500° C-heated film. On the other hand, Cl remains up to 500° C in the Pd-doped film as well as in the Au-Pd co-doped film. Other features are almost the same for all of the films.

In order to estimate the chemical states of Au and Pd, Au-4f and Pd-3d photoelectron spectra were measured. The results are shown in Fig. 7a and 7b. In the Au-4f spectra, the $4f_{5/2}$ binding energy (BE) peak is

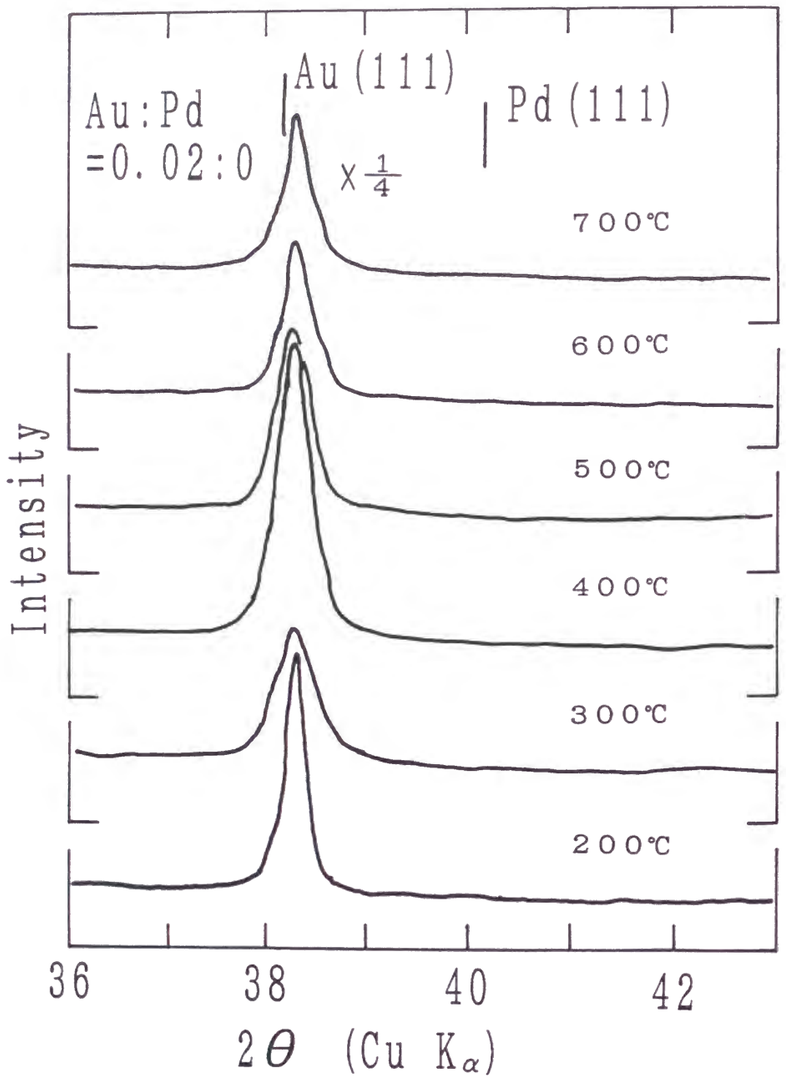

Fig.5(a) X-ray diffraction patterns of Au-doped films heat-treated at a temperature from 200° to 700° C around the Au(111) and Pd(111) peak positions.

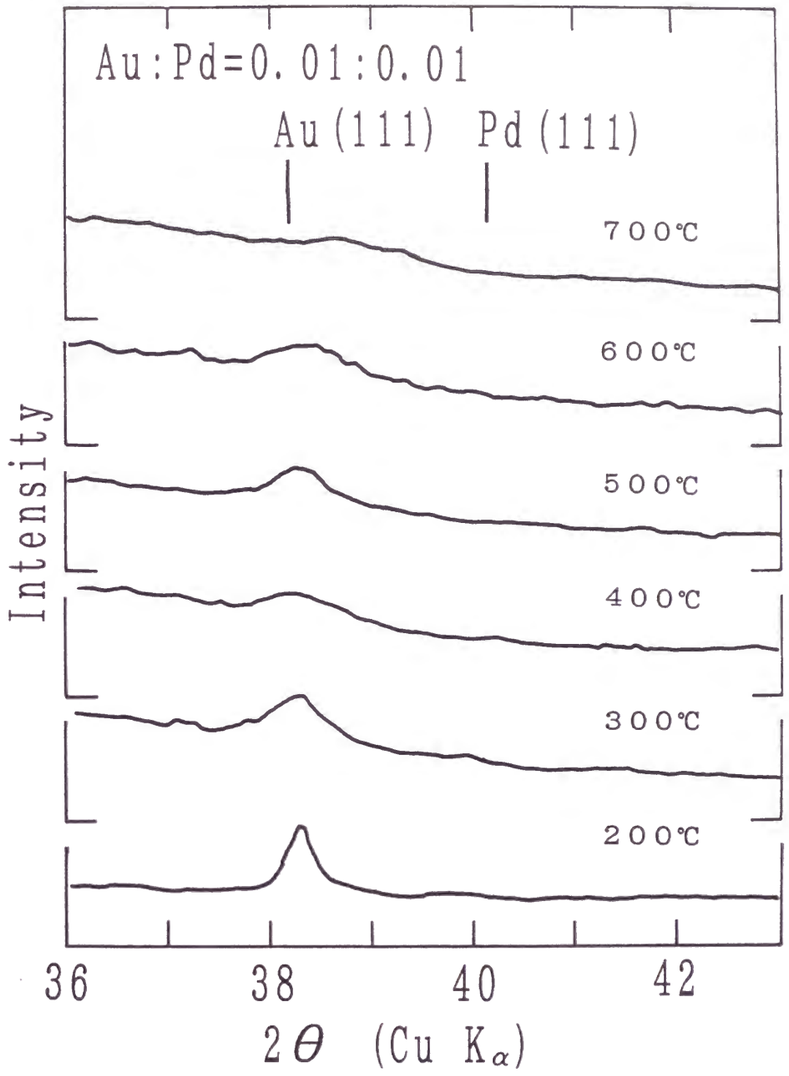

Fig.5(b) X-ray diffraction patterns of Au-Pd co-doped films heat-treated at a temperature from 200° to 700° C around the Au(111) and Pd(111) peak positions.

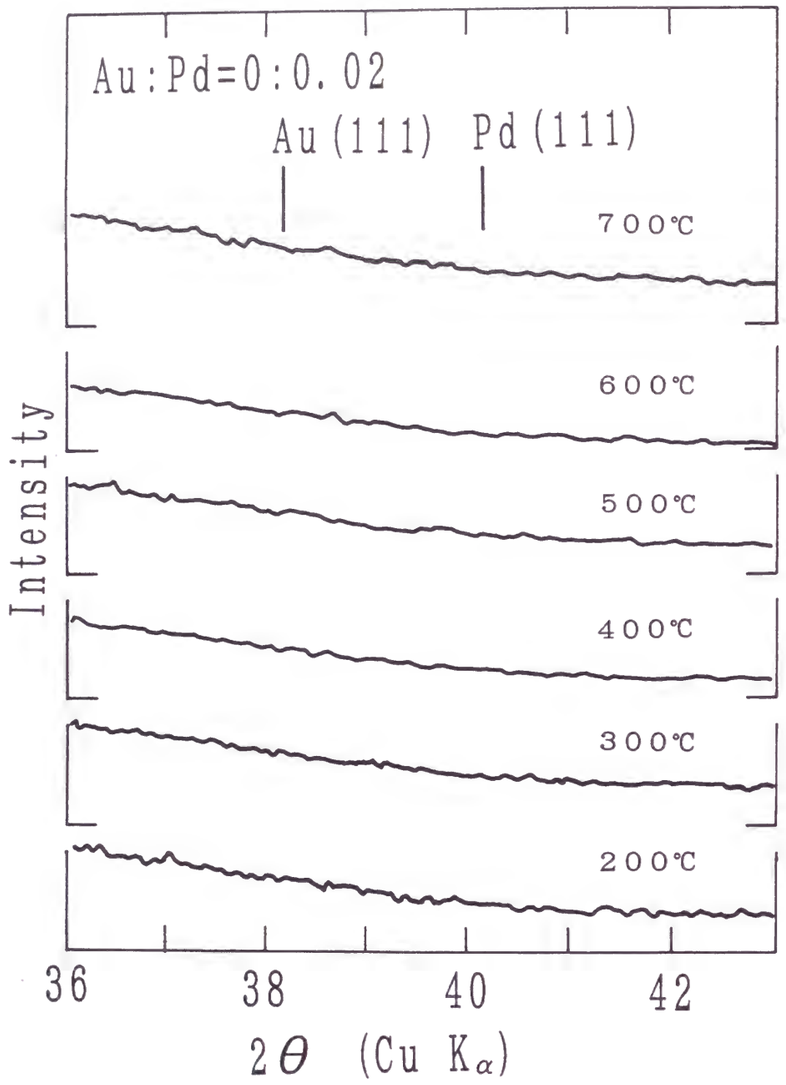

Fig.5(c) X-ray diffraction patterns of Pd-doped(c) films heat-treated at a temperature from 200° to 700° C around the Au(111) and Pd(111) peak positions.

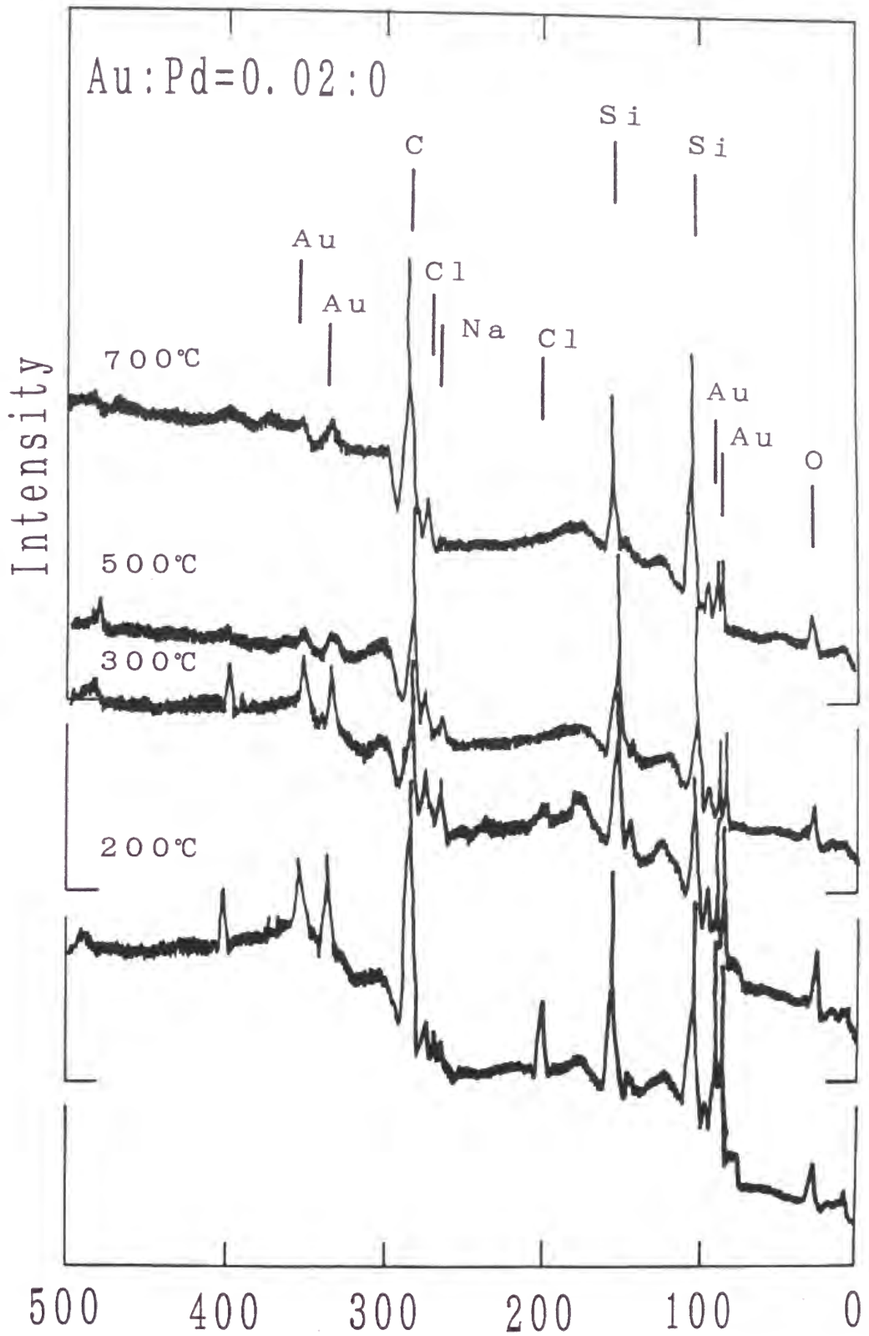

Fig.6(a) Wide range X-ray photoelectron spectra of Au-doped films heat-treated at a temperature from 200° to 700° C.

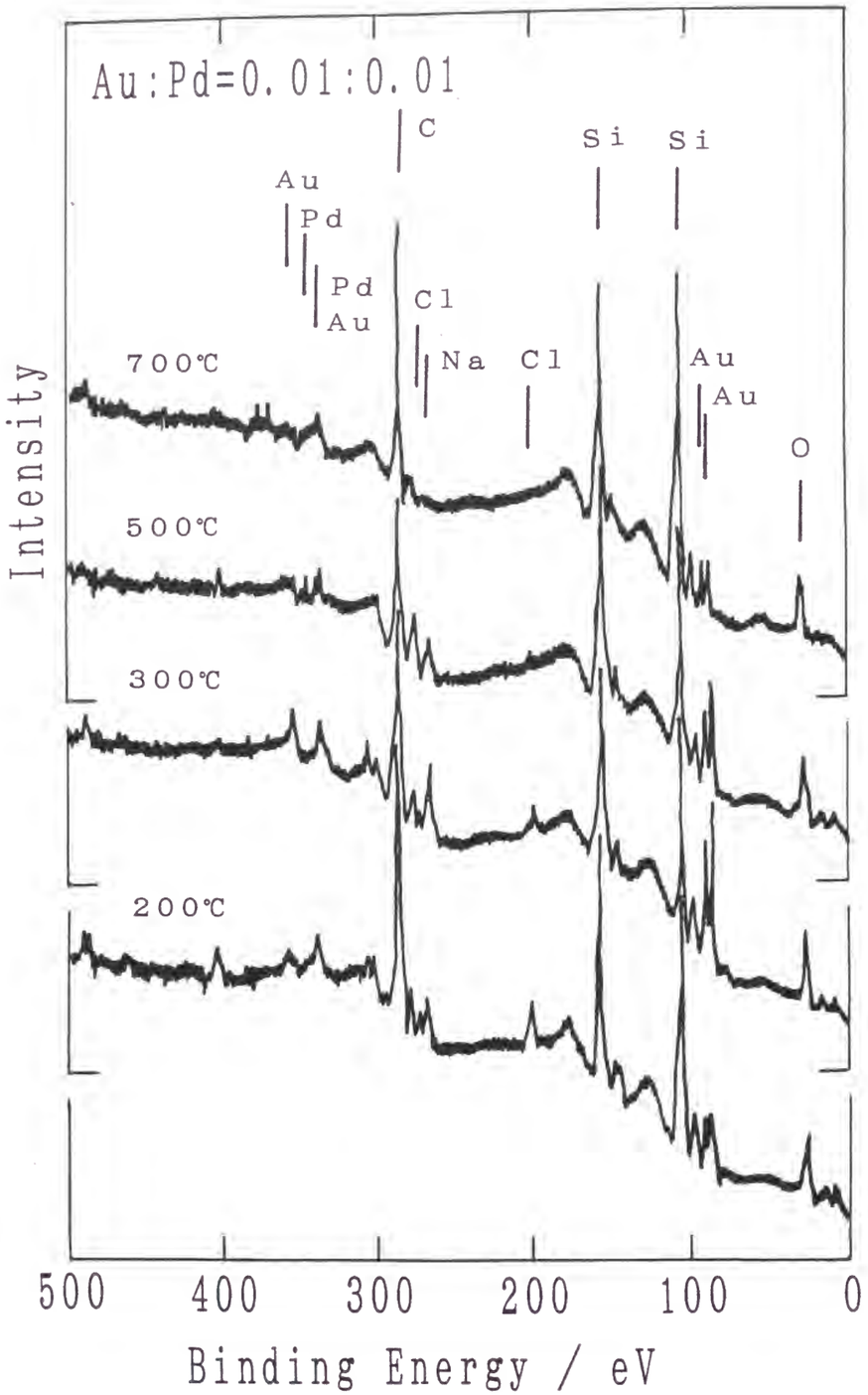

Fig.6(b) Wide range X-ray photoelectron spectra of Au-Pd co-doped films heat-treated at a temperature from 200° to 700° C.

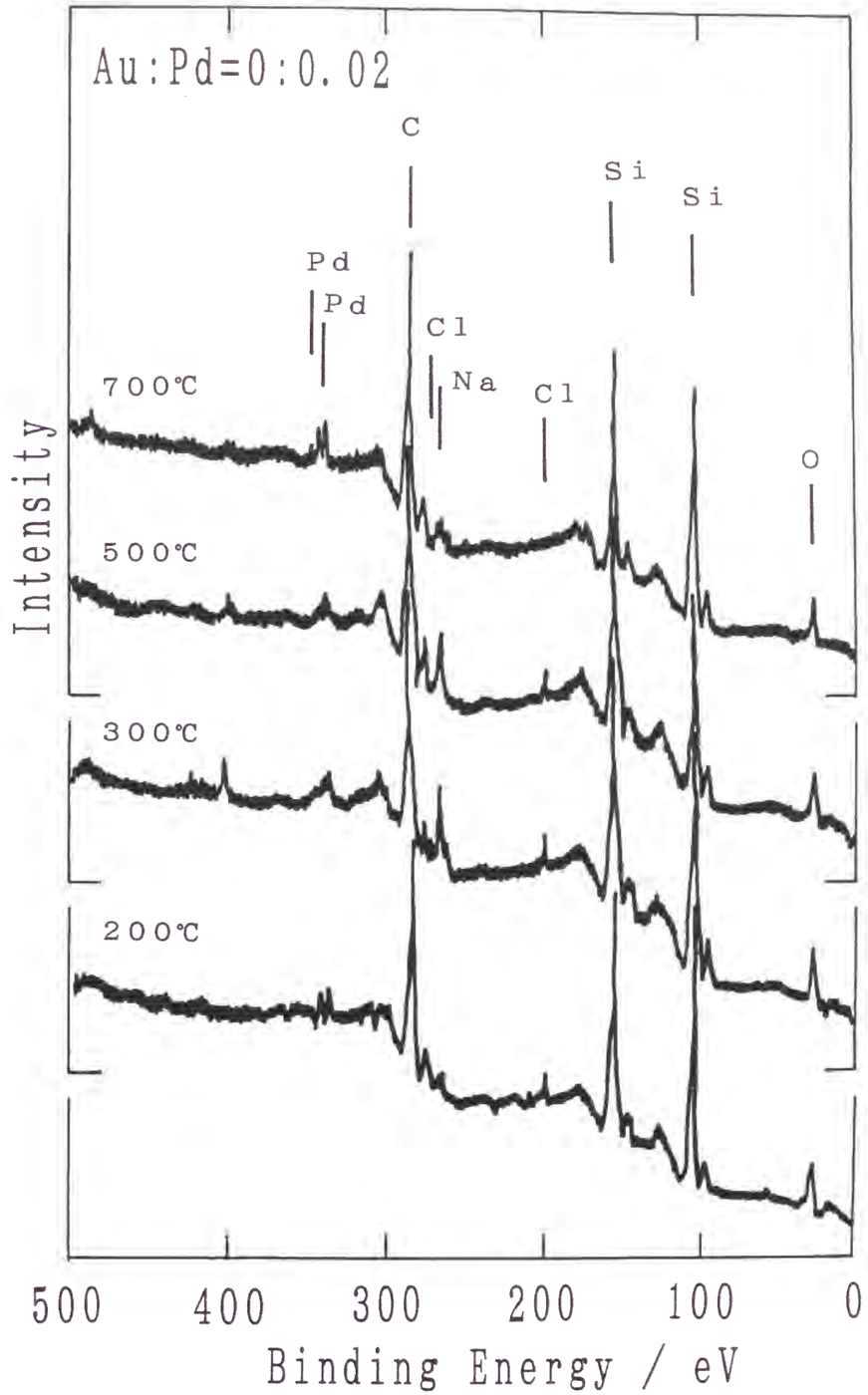

Fig.6(c) Wide range X-ray photoelectron spectra of Pd-doped films heat-treated at a temperature from 200° to 700° C.

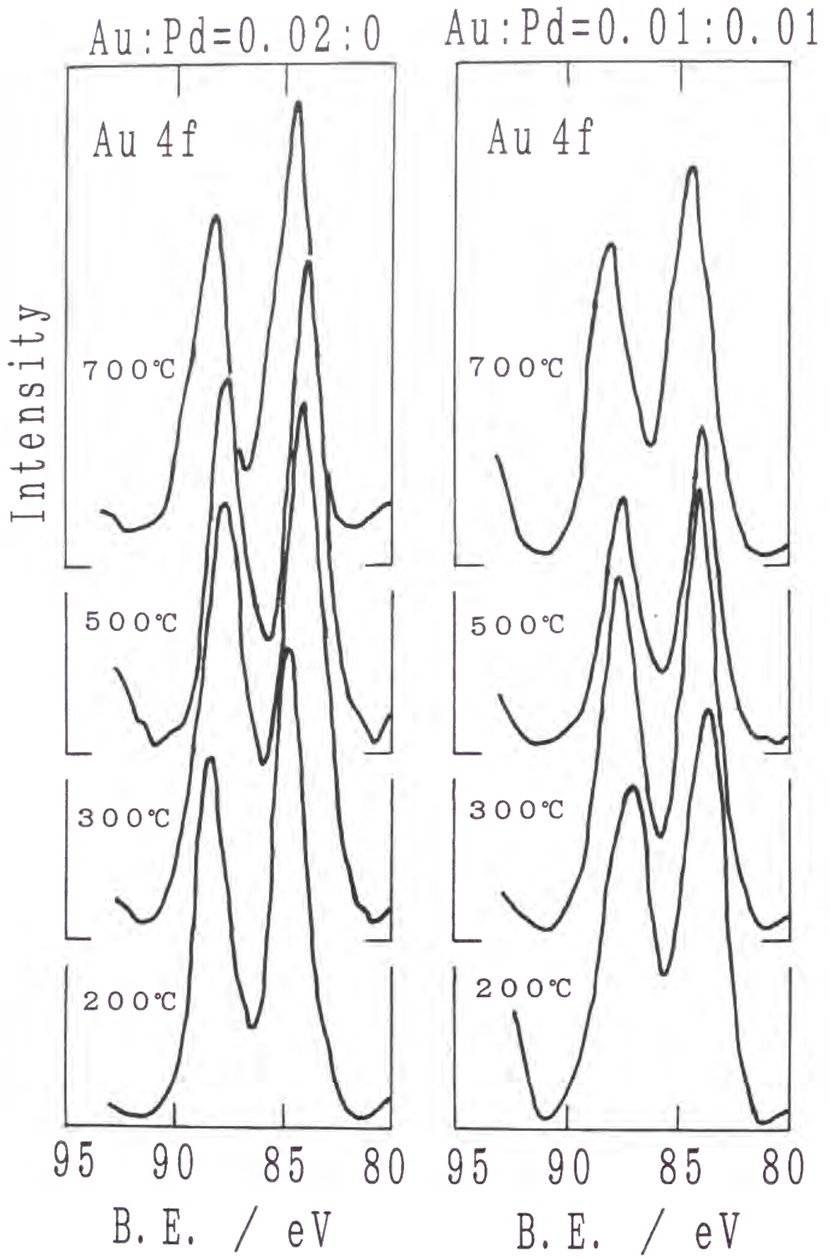

Fig.7(a) Au-4f X-ray photoelectron spectra of Au-doped and Au-Pd co-doped films heat-treated at a temperature from 200° to 700°C.

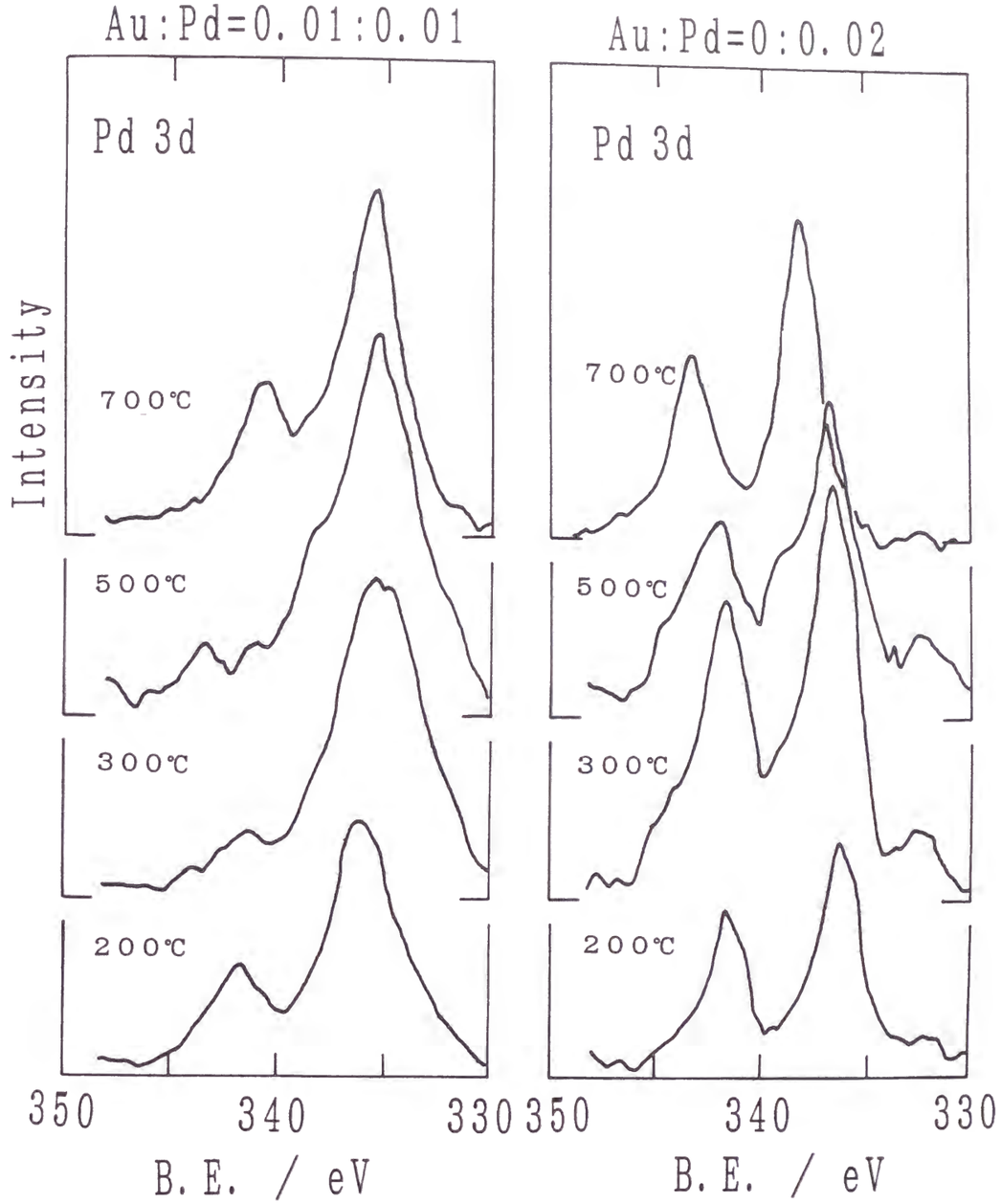

Fig.7(b) Pd-3d (b) X-ray photoelectron spectra of Au-Pd co-doped and Pd-doped films heat treated at a temperature from 200° to 700°C.

observed around 88-89 eV and $4f_{7/2}$ around 84-85 eV. No obvious difference is observed in the Au spectra and its temperature dependence between the Au-doped and Au-Pd co-doped films. In the Pd-3d energy region, the Pd-$3d_{3/2}$ peak is observed around 342 eV and the Pd-$3d_{5/2}$ peak around 336 eV. The latter is overlapped with the Au-$4d_{5/2}$ peak.

In the Pd-doped films, the BE peak of Pd-$3d_{3/2}$ shows a slight shift to the high BE side without changing the peak height when the heat treatment temperature is increased. At 500° C, a shoulder appears on the high BE side of Pd-$3d_{5/2}$ peak. In the 700° C-treated film, the shoulder grows up, or Pd-$3d_{5/2}$ peak shifts to the higher BE side, accompanying the shift of Pd-$3d_{3/2}$ to high BE side. In contrast with this, the Au-Pd co-doped film exhibits a more complicated change wit heat treatment temperature. The $3d_{3/2}$ peak observed at 341.5 eV in the 200° C-treated Au-Pd film becomes small and broad when the heat treatment temperature is raised to 300° C, and at 400° C, the peak seems to split into two weak peaks around 341 and 343 eV. When the heat-treatment temperature is further increased to 700° C, the peak around 340.5 eV becomes strong.

All of the peak positions of Au-$4f_{7/2}$ and Pd-$3d_{3/2}$ spectra were summarized in Fig. 8. The peak positions of some compounds in literature [5] are also shown in the figure.

4.Discussion

In the Au-doped silica films, the binding energy of Au-$4f_{7/2}$ and XRD pattern indicate that gold atoms exist as a metallic form even when the heat treatment temperature is as low as 200° C. It should be noticed that in the film heat-treated at 200° C, the optical absorption peak at 225 nm which is due to $AuCl_4^-$ ion is observed along with the plasmon peak around 560 nm,

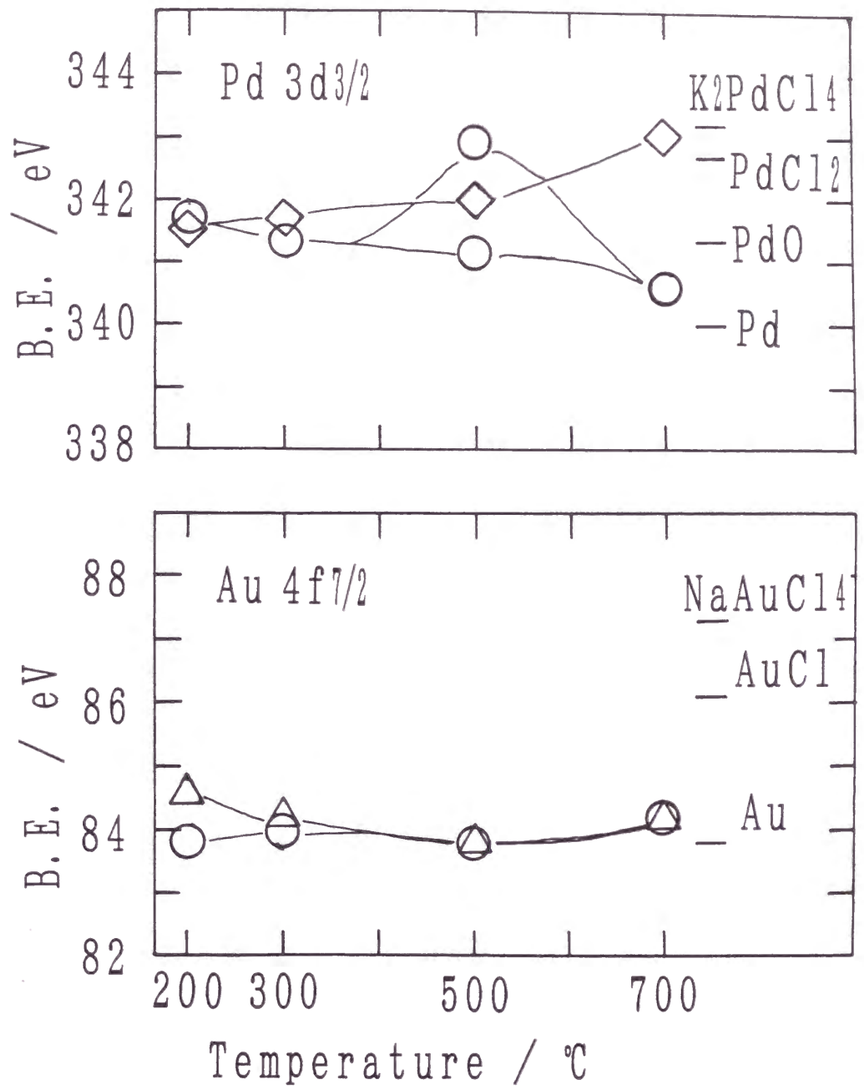

Fig.8 Changes of the Au-$4f_{7/2}$ and Pd-$3d_{3/2}$ XPS peak positions of the films with the heat-treatment temperature. Triangle:Au-doped film, circle:Au-Pd co-doped film, diamond:Pd-doped film.

indicating that a certain amount of gold still remains as $AuCl_4^-$ ions at this heat treatment temperature. However, XPS study indicates that the ratio of $AuCl_4^-$ to the total amount of gold is not so large. The crystal size of Au formed on the decomposition of $AuCl_4^-$ ions is calculated using the Scherrer's equation,

$$R = \frac{0.45\ \lambda}{\beta_{1/2}\cos\theta}$$

where R is the crystal radius, λ is the wavelength of the X-ray, $\beta_{1/2}$ is the full width at half maximum of the diffraction peak in radian and θ is the diffraction angle. The calculated values are shown in Fig. 9 as a function of heat-treatment temperature. The crystal size of Au observed in the films does not depend on heat-treatment temperature and is about 100 Å except for the one heat-treated at 200° C. Kozuka and Sakka [4] proposed that the TEOS-derived Au-doped silica gel film is composed of the stacking of hydrated silica microspheres and Au microcrystals formed by the decomposition of $AuCl_4^-$ ions in the voids between silica microspheres. From this point of view, the invariance of Au microcrystal size with heat-treatment temperature should come from the invariance of void size in the film which can be determined by the size of the primary particles of hydrated silica spheres. A large crystal size observed at the heat treatment temperature of 200° C can be explained as follows. The degree of polymerization by condensation of silanol groups must be small and the silica microspheres formed at such a low temperature is still flexible enough for Au microcrystals to grow up by deforming the silica gel microspheres. In the case of heat-treatment at higher temperatures, the films are heated so rapidly to a desired temperature that the time duration at which films are flexible is too short for the growth of Au microcrystals.

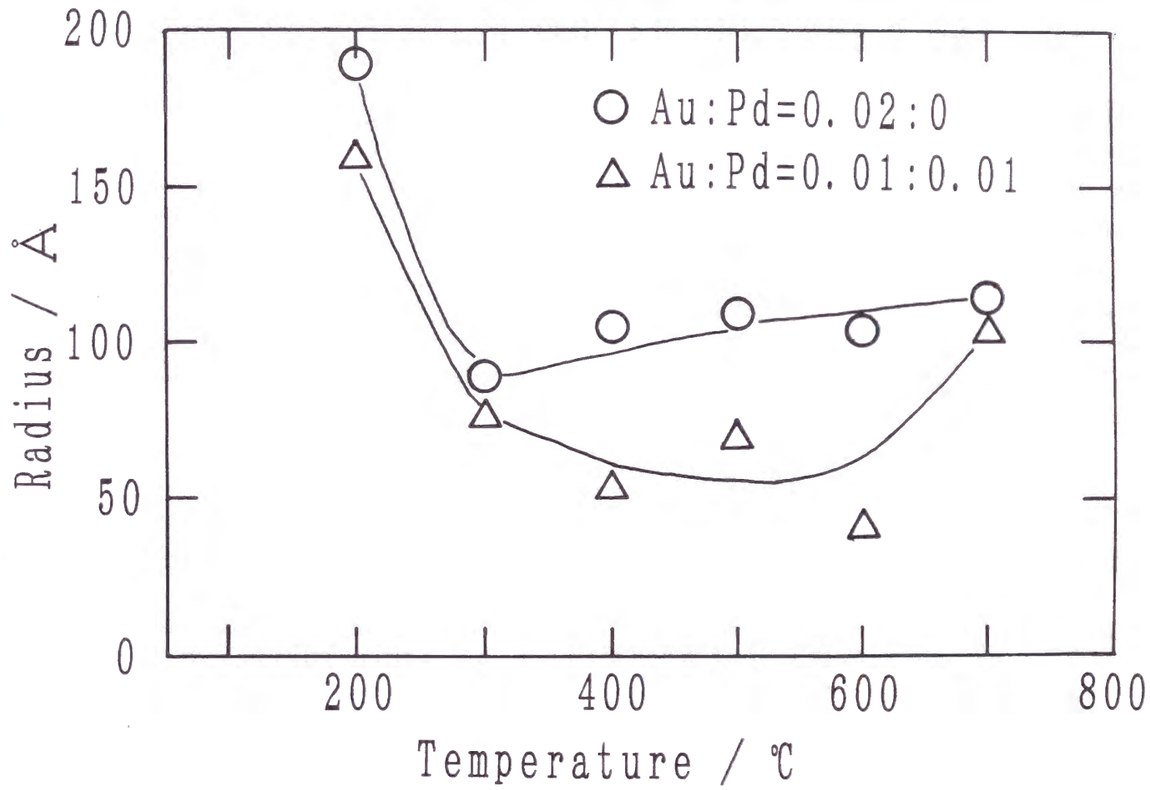

Fig.9 Average microcrystal radius in Au-doped and Au-Pd co-doped films deduced from the width of X-ray diffraction peak as a function of the heat treatment temperature.

On the other hand, the X-ray diffraction data of the Pd-containing film did not reveal the formation of metal microcrystals. Chlorine was found to remain in the film up to 600° C from the wide range XPS spectra. This suggests that palladium remains as $PdCl_4^{2-}$ and/or $PdCl_2$ up to this temperature. At 700° C, chlorine was removed from the film but Pd microcrystal was not formed. The Pd-$3d_{3/2}$ spectra indicate that palladium does not exist as a metallic form or, if any, the fraction of metallic form is very small even at 700° C. The optical absorption also indicates that the films prepared at 700° C was very much different from those heated below 600° C. Therefore, as pointed out by Zao et al.[6] for the Pd-doped TiO_2 film prepared by sol-gel method, palladium should exist mostly as an oxide form in the 700° C-treated film. The differences in chlorine removal and palladium oxide formation temperature between the present study and that reported by Zao et al. should be due to the compositional difference in coating solution and thus the stability of chloride form of palladium in the film. These results indicate that, unlike gold, palladium is not so stable in a metallic state but tends to take a cation form.

In the Au-Pd co-doped films, the radius of metal microcrystals decreases with increasing heat-treatment temperature up to 600° C as shown in Fig. 9. A plasmon peak was observed in the optical absorption spectra in this temperature range. The broadening of the plasmon peak with increasing heat-treatment temperature also indicates the decrease of microcrystal size. These results and the dependence of microcrystal size on the gold to palladium ratio shown in Fig. 10 indicate that palladium or related compounds inhibits the crystal growth. It should be noted that the chlorine content decreases with an increase in heat-treatment temperature but a certain amount remains up to 600° C in the Pd-doped films. By the heat treatment

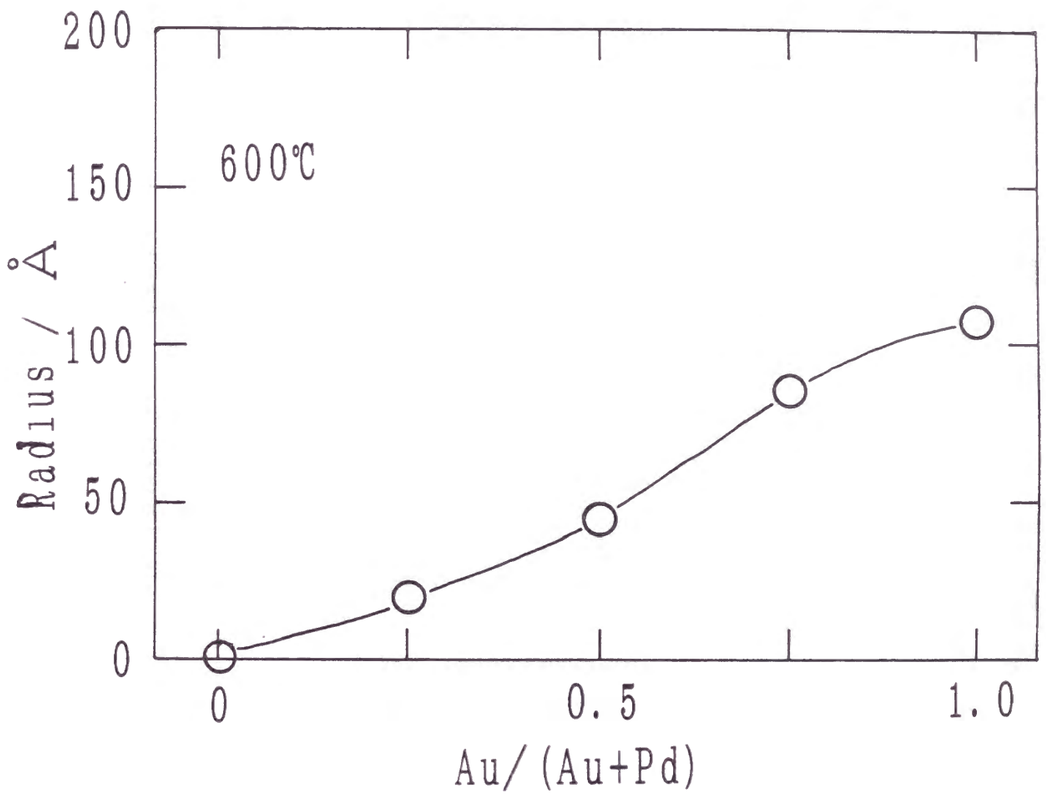

Fig.10 Dependence of the Au/(Au+Pd) ration in coating solution on the average radius of microcrystals formed by heat treatment at 600° C.

at 700° C chlorine was completely removed from the film, and the crystal radius and optical absorption spectra changed from those observed below 600° C. Furthermore, the broadening of the Pd-$3d_{3/2}$ peak of XPS spectra observed in the 300° and 500° C-treated films suggests that palladium exists in more than two types of chemical states in these films. Eventually, considering the stability of Pd-Cl bonds in the Pd-doped films, the change of microcrystals with heat-treatment temperature may be explained by a model schematically illustrated in Figure 11. At a low temperature as 200° C, palladium exists as such a stable form as $PdCl_4^{2-}$ and has no interaction with Au microcrystals as shown in Fig. 11(c). In this case, a gold microcrystal grows large as if palladium does not exist in the film and has a similar structure to that in the Au-doped film. When the heat-treatment temperature is somewhat raised, $PdCl_4^{2-}$ anions should be partially decomposed, and the resultant $PdCl_x$ compounds should react with Au microcrystals by metallic bonding. As the result, Au microcrystals would be covered with chlorines attaching to palladium and terminal chlorines would prevent the further growth of microcrystals. The increase of heat-treatment temperature may enhance the partial decomposition of $PdCl_4^{2-}$ ions, so that the termination effect to decrease the size becomes evident. This mechanism is illustrated in Fig. 11(b).

When the heat-treatment temperature is raised to 700° C in the Au-Pd co-doped glass, chlorines were removed from the film and simultaneously the crystal size became large. Furthermore, XPS of Pd-$3d_{3/2}$ peak position and the optical absorption peak around 290 nm which is assumed to be due to palladium oxide show that palladium becomes metallic in the 700° C-treated Au-Pd co-doped film. Consequently, it is reasonable to assume that palladium is reduced to the metallic state and gold-palladium alloy microcrystals

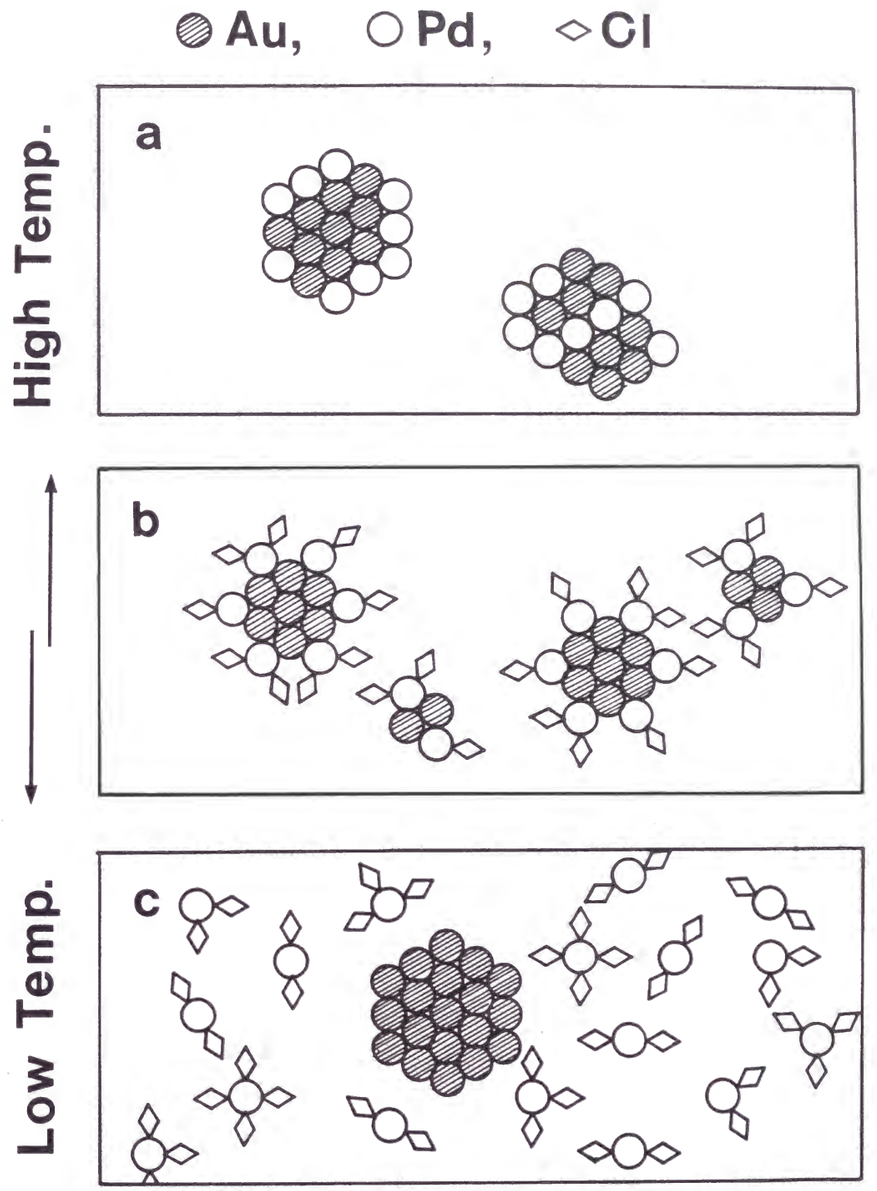

Fig.11 Schematic diagram of the microcrystal formation in Au-Pd co-doped films heat treated at (a) high temperature above 700° C, (b) middle temperatures ranging from 300° to 600° C, and low temperature of about 200° C.

free from terminal chlorine are formed at this heat-treatment temperature as shown in Fig. 11(a). The difference in chemical state of Pd between the Pd-doped and Au-Pd co-doped films heat-treated at 700° C is explainable by assuming that the existence of Au microcrystals stabilizes the reduced form of palladium through the Au-Pd bond formation, i.e., alloying.

In contrast to the Au-doped film, the optical absorption spectra of Au-Pd co-doped film heat-treated at 700° C shows a broad absorption which increases with decreasing wavelength. This is the same as that of the Au-Pd alloy colloid formed in an aqueous solution [2], in which only a broad absorption increasing with decreasing wavelength was observed at Au:Pd=2:3, though the plasmon peak was also observed when Au:Pd=3:2 in ref.[2].

The electronic band structures of Au metal and Au-Pd alloy are much different with each other in their bulk crystals [7]. The plasmon peak shown in Au microcrystals is due to the cooperative motion of free electrons in the 6s electronic band where the electronic structure of a zero-valent Au atom is written as $[Xe]5d^{10}6s^{1}$, and also in bulk crystal, the electronic band from the 5d atomic orbital is completely filled and that from the 6s is half-filled in the bulk crystal. In this case, s band electrons can be treated as a free Fermi gas. On the other hand, a palladium atom takes its electronic structure as $[Kr]4d^{8}5s^{2}$, and in the bulk crystal, both s band and d band are only filled partially. In this case, the band occupancy can be represented as $4d^{10-p}$ and $6s^{p}$ with p=0.55 - 0.60, i.e., the d orbital is not filled completely by electrons in this case. Alloying of Pd with Au fill partially the 4d orbital of palladium with electrons coming from the 6s band of gold, and the remaining Au-6s and Pd-5s orbitals form an electronic band in which free electrons partially fill it. In the obtained alloy, the number of

free electron with s-character differs from that of pure gold, and the life-time of free electron is much shorter than that of Au because of electron scattering caused by the random arrangement of Au and Pd and also of the effect of s-d interband interaction.

In the Au-Pd alloy microcrystals, the electronic structure would be the same with that of the bulk alloy. So, the disappearance of plasmon peak in the optical absorption spectra of Au-Pd co-doped film heat-treated at 700° C in which Au-Pd alloy microcrystals should be formed in it would be due to the shortening of the lifetime of free electron, which makes the absorption peak broad and weak. The shift of the plasmon peak position to the longer wave length caused by the decrease of the number of s-type free electron per metal atom also affects this result. The broad absorption, which increases with decreasing wavelength, would be due to the electronic transition related to the unfilled d-type electronic bands.

In the Au-Pd co-doped film heat treated below 600° C, plasmon peak appears in the optical absorption spectra together with an increscent absorption with decreasing wavelength. It should be noted that the peak position of the plasmon peak of these films is the same as that of the Au microcrystal-doped film. This may be explained by the assumption that, because palladium atoms on Au microcrystal are bonded with chlorine atoms, electrons are supplied from chlorine to palladium to make palladium atoms having just one electron in 5s electronic state like gold atoms. Further, it can be also assumed that, because palladium atom exists only on the surface of Au microcrystal but not at the interior of the crystal in this case, the scattering of free electrons by alloying is small. Broadening of the plasmon peak with increasing the heat-treatment temperature should be due to the decrease of crystal radius with temperature.

5.Conclusion

The TEOS-derived silica gel films containing $NaAuCl_4$ and/or Na_2PdCl_4 were prepared by the dip-coationg method with heat-treatment at several temperatures ranging from 200° to 700° C. Au microcrystals were formed in the Au-doped film and the crystal radius is almost constant of about 50 Å when the heat-treatment temperature is higher than 300° C. In the Pd-doped films, palladium seems to exist as a chloride form up to heat-treatment temperature of 600° C, and palladium oxide should be formed by the heat treatment at 700° C. The Au-Pd co-doped films heat-treated at a temperature lower than 600° C show the metal microcrystal-formation, which gives a plasmon peak in optical absorption spectra similar to that of the Au-doped films. The crystal radius decreases with increasing heat-treatment temperature and with Pd/(Au+Pd) ratio. These results suggest the formation of Au microcrystals covered with palladium chloride. The heat treatment of the Au-Pd co-doped film at 700° C should form Au-Pd alloy microcrystals which do not give plasmon peak in optical absorption spectra.

References

[1] R. H. Magruder III, J. E. Wittig and R. A. Zuhr, J. Non-Cryst. Solids, **163**, 162-168 (1993)

[2] G. De, M. Gusso, L. Tapfer, M. Catalano, F. Gonella, G. Mattei, P. Mazzoldi and G. Battaglin, J. Appl. Phys., 80, 6734-6739 (1996)

[3] N. Toshima, M. Harada, Y. Yamazaki and K. Asakura, J. Phys. Chem., **96**, 9927-33 (1992)

[4] H. Kozuka and S. Sakka, Chem. Mater., 5, 222-228 (1993)

[5] "Handbook of X-ray Photoelectron Spectroscopy", ed. by C. D. Wagner, W. M. Riggs, L. E. Davis, J. F. Moulder and G. E. Muilenberg, Perkin-Elmer Corp., 1979

[6] G. Zao, H. Kozuka and S. Sakka, J. Sol-Gel Sci. Tech., **4**, 37-47 (1995)

[7] N. F. Mott and H. Jones, "The Theory of the Properties of Metals and Alloys", Chapters VI & VII, Oxford University Press, Oxford, 1936

Chapter 5

Sol-Gel Synthesis of Au Microcrystal-Doped TiO_2, ZrO_2 and Al_2O_3 Films

1.Introduction

In chapter 1, Au-microcrystals with the average diameter of 8nm were incorporated into SiO_2 dip-coated films by using $NaAuCl_4 \cdot 2H_2O$ and $Si(OC_2H_5)_4$ (TEOS) as the starting materials and HCl as a hydrolysis-catalyst [1,2]. In this case, the maximum amount of Au microcrystals incorporated in the silica film was 0.04 in the molar ratio to SiO_2 (Au/SiO_2). When the Au/Si ratio in the coating solution was increased to more than 0.04, the excess amount of Au was depleted to the surface of SiO_2 coating film during consolidation by heat-treatment.

The use of $HAuCl_4 \cdot 4H_2O$ instead of $NaAuCl_4 \cdot 2H_2O$ as a starting material was unsuccessful in the preparation of Au microcrystal-doped SiO_2 film by a similar method. Some amount of gold was depleted to the SiO_2 film surface even when the amount of gold in the coating solution was as low as 0.01 in Au/SiO_2. In order to overcome this problem, Kozuka and Sakka [3] treated the dip-coated SiO_2 gel film containing $HAuCl_4 \cdot 4H_2O$ by monoethanolamine vapor before heat treatment. By this treatment, they were able to form the Au microcrystal-doped SiO_2 glass film containing 1 vol% Au, which corresponds to Au/SiO_2 = 0.028. Fernàndez-Navarro et al.[4] also used $HAuCl_4 \cdot 4H_2O$ and TEOS to prepare Au microcrystal-doped silica glass in a bulk form. They found that Au microcrystals with an average particle size of 20nm was formed in the glass when the amount of Au was 0.001wt% (this corresponds to 0.0001vol% ,or $Au/SiO_2 = 3.1 \times 10^{-6}$ in molar ratio), but the

particle size became as large as 300nm when the amount of Au was increased to 0.05wt%. This increase of particle size in the bulk glass would correspond to the depletion of Au in the case of glass film, because both of the phenomena indicate that the Au-SiO_2 binary system tends to be separated and Au microcrystals tend to be aggregated each other when the amount of Au is large.

It has not been clarified yet why the use of $NaAuCl_4 \cdot 2H_2O$ enables the formation of Au microcrystals in the silica gel without any sophisticated techniques. In addition, mechanism of the stabilization of Au-doped silica glass film by monoethanolamine treatment in [3] remains unclarified.

Other alkoxides than TEOS have been also used to prepare Au microcrystal-doped oxides through thermal decomposition of gold compounds in the oxide gel. Innocenzi et al.[5] used methyltriethoxysilane (MTES) and $HAuCl_4 \cdot 4H_2O$ as sources of SiO_2 and Au, and successfully obtained the Au microcrystal-doped silica glass film without amine-treatment of the gel. Tohge et al.[6] prepared Au microcrystal-doped silica glass films by the sol-gel method using aminopropyltriethoxysilane and $HAuCl_4 \cdot 4H_2O$ as starting materials. Tseng et al.[7] made Au microcrystal-doped Ormosil by heat treating the organic group-containing silica gel doped with $AuCl_4^-$ ions at a moderate temperature like 200°C [7]. Furthermore, Kozuka et al.[8] found that the use of a titanium alkoxide (titanium isopropoxide) led to the highly Au microcrystal-containing transparent TiO_2 film. In their case, Au microcrystals with an average crystal diameter of 20nm were incorporated by as much as 8vol%.

All these results suggest that the stability of gold microcrystals in the oxide matrix depends on the matrix composition and co-existing chemical spices. However, it is still unclear what determines the stability of Au

microcrystals. So, it is attempted in this chapter to investigate the dependence of the maximum amount of Au microcrystals attainable in the sol-gel derived oxide films on the metal species in starting alkoxides. Alkoxides of titanium, zirconium and aluminum were used as sources for TiO_2, ZrO_2 and Al_2O_3, respectively, and $HAuCl_4 \cdot 4H_2O$ was used as a source of Au. The sol-gel reaction to form coating films were catalyzed with HCl. The maximum amount of Au microcrystals in these oxide films was compared with that in SiO_2 films from TEOS, and discussed from the viewpoint of the electrical charge of the oxide gel surfaces.

2.Experimental

Titanium isopropoxide ($Ti(OC_3H_7^i)_4$; TIP), zirconium n-propoxide ($Zr(OC_3H_7^n)_4$; ZNP) and aluminum sec-butoxide ($Al(OC_4H_9^s$; ASB) were used as the starting alkoxides. At first, one of the alkoxides was diluted with anhydrous ethanol, and then the mixed solution of ethanol, water, HCl and stabilizing agent (acetic acid) were added to form dip-coating solutions, followed by the addition of the prescribed amount of $HAuCl_4 \cdot 4H_2O$. $NaAuCl_4 \cdot 2H_2O$ was not used as a source of Au in the present study because its solubility in the dip-coating solutions was found to be very low.

Dip-coating was performed by dipping a silica glass substrate in the coating solution and pulling it out of the solution with a withdrawal velocity of 0.15 mm/sec. The gel film was dried in air for about 30 sec and immediately put into a furnace preheated to the designed temperatures. Heat-treatment was carried out for 15 min at a temperature ranging from 200° to 600°C. This procedure was repeated for several times so as to obtain a dip-coating film with sufficient thickness for the measurement.

The dip-coating solution for Au:TiO_2 films was prepared using TIP

(Tokyo Kasei Kogyou Co. Ltd.), distilled water, acetic acid, hydrochloric acid, ethanol and chloroauric acid tetrahydrate. The compositions of the dip-coating solutions are listed in Table 1. First, TIP was dissolved in a half of the prescribed amount of ethanol. Then mixture of the other half of ethanol, water, acetic acid and hydrochloric acid was added dropwise very slowly to the former solution under stirring and keeping the temperature at 0° C. After that, the solution was further stirred for 1 hr at room temperature. Then, $HAuCl_4 \cdot 4H_2O$ was dissolved to the solution, which was served for dip-coating. This procedure is schematically illustrated in Fig. 1(A).

In a similar manner, as shown schematically in Fig. 1(B), Au:ZrO_2 films were prepared from ZNP (70% solution in n-propanol, Aldrich Chemical Company Inc.), water, hydrochloric acid, ethanol and chloroauric acid tetrahydrate. The compositions of the dip-coating solutions are listed in Table 1. Although the addition of the aqueous solutions to the alkoxide solution was carried out very slowly, the resultant solution was opaque at first. However, further stirring of it for 1 day at room temperature made the solution transparent and free from precipitations. Then, dip-coating was carried out after it became transparent.

The Au:Al_2O_3 dip-coating films were also prepared from ASB (Wako Chemical Industry Co. Ltd.), water, acetic acid, hydrochloric acid, ethanol and chloroauric acid tetrahydrate according to the flow chart shown in Fig. 1(C). The composition of the dip-coating solutions are listed in Table 1. In this case, acetic acid was added to the solution after the solution of water, ethanol and HCl was mixed with ASB-ethanol solution, and the resultant solution was stirred for 1 day. Then, $HAuCl_4 \cdot 4H_2O$ was dissolved in the alkoxide solution.

The optical absorption spectra of the films were measured from 200 to

Table 1 Composition of dip-coating solutions.

alkoxide	molar ratio to alkoxide					
	H_2O	CH_3COOH	HCl	C_2H_5OH	n-C_3H_7OH	$HAuCl_4 \cdot 4H_2O$
$Ti(OC_3H_7^i)_4$	1.00	2.46	0.24	8.00		0 - 0.32
$Zr(OC_3H_7^n)_4$	1.00		0.10	10.00	2.34	0 - 0.12
$Al(OC_4H_9^s)_3$	3.73	1.80	1.00	10.00		0 - 0.24

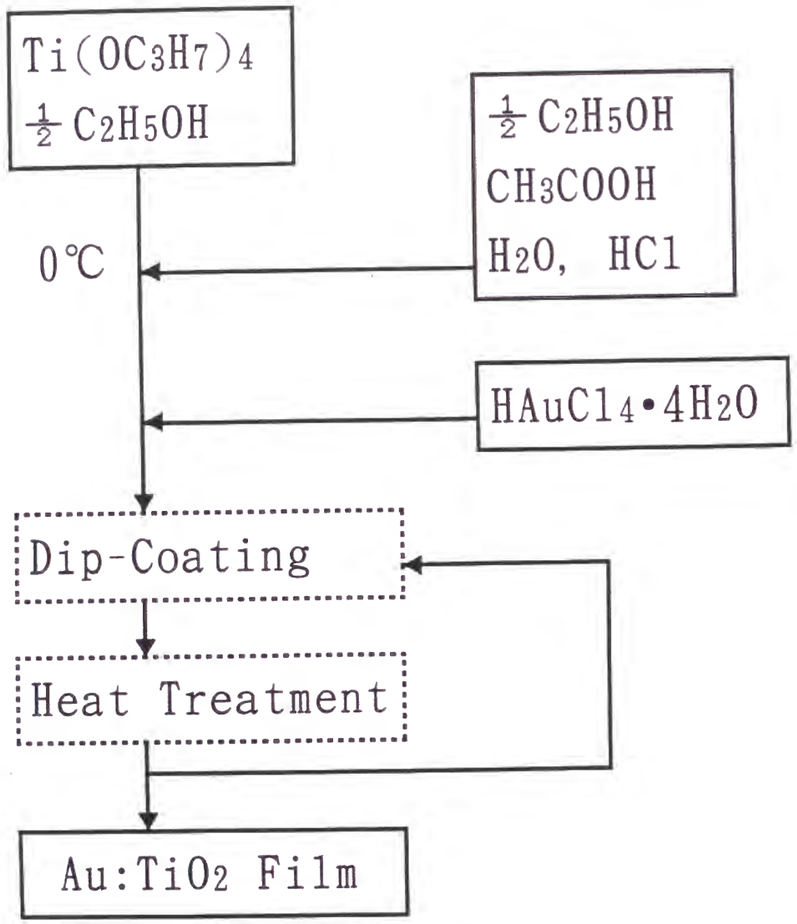

Fig.1(a) Flow charts of the preparation of Au microcrystal-doped Au:TiO_2 film.

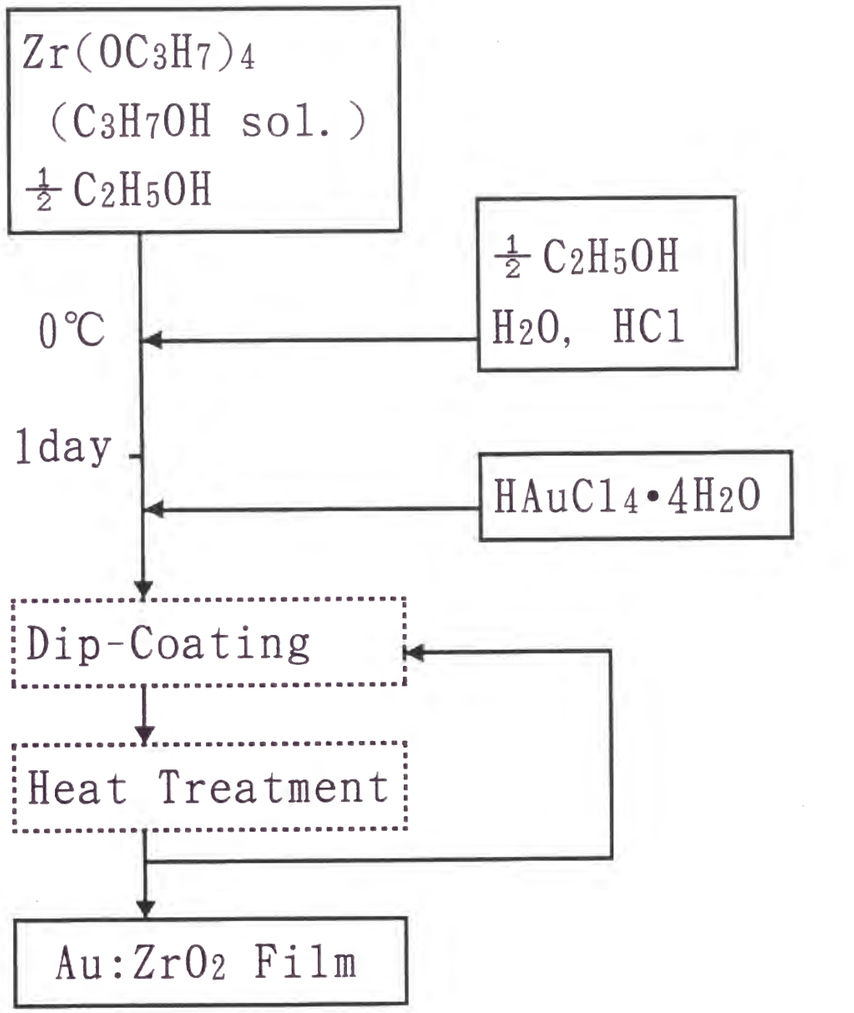

Fig.1(b) Flow charts of the preparation of Au microcrystal-doped Au:ZrO_2 film.

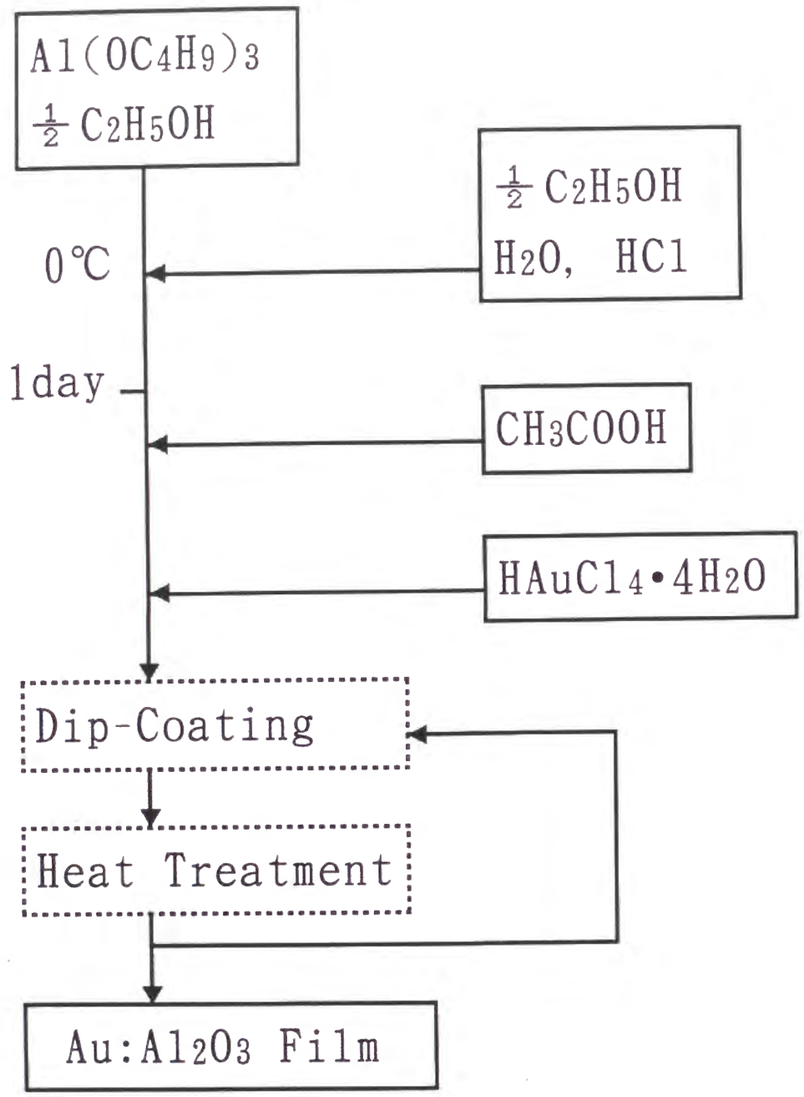

Fig.1(c) Flow charts of the preparation of Au microcrystal-doped $Au:AlO_{1.5}$ film.

1200 nm. When the concentration of $AuCl_4^-$ in the dip-coating solution is not so high, it decomposes to form Au microcrystals in the oxide film when heat treated. On the other hand, when the concentration exceeds a critical value, the heat treatment of gel film causes the depletion of the excess amount of Au microcrystals to the film surface. In such a case, the absorption spectra of the film is known to be changed by wiping the surface [3]. Therefore, the absorption spectra were measured for both of the as-prepared and surface-wiped films. The comparison in spectra of the as-prepared film with the wiped one enables the determination of the maximum amount of Au which is incorporated in the film as microcrystals.

3.Results

Figure 2 shows the optical absorption spectra of the as-prepared and the surface-wiped $Au:TiO_2$ films prepared from the solutions of molar ratio of Au/TiO_2 = 0.16 and 0.20 via heat-treatment at 600° C. The absorption spectra of pure TiO_2 film (Au/TiO_2=0.00) is also shown in the figure. As the heat-treatment temperature as high as 600° C is high enough to remove hydroxyl groups from the starting gel films, these films are considered to be composed mostly of Au microcrystal and TiO_2 matrix. A small and broad increase in absorbance from 500 to 1200nm in the pure TiO_2 film is due to the interference of light by the film which has a high refractive index. This can be also seen in pure ZrO_2 film.

The as-prepared film with the gold amount of Au/TiO_2 = 0.16 has an absorption peak at 710 nm, which should be due to the surface plasmon resonance of Au microcrystals. Wiping the surface of this film scarcely changed the spectra. Accordingly, all the Au microcrystals are considered to be incorporated in the TiO_2 film. On the other hand, wiping the surface of the

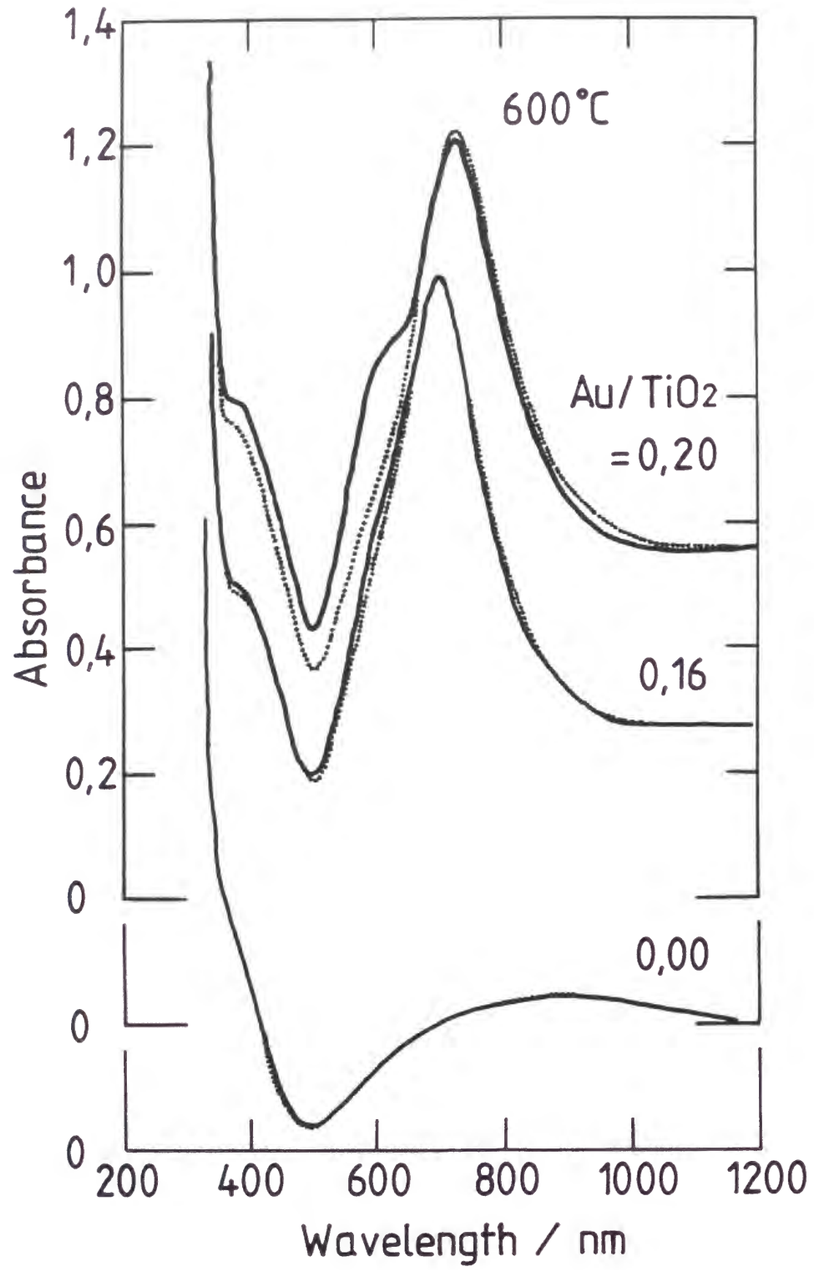

Fig.2 Optical absorption spectra of the 600°C-treated Au:TiO_2 films. Full line : as-prepared film, Dotted line : surface-wiped film.

film having the nominal gold amount of Au/TiO_2 = 0.20 caused the obvious change in absorption spectra. While the as-prepared film with nominal Au/TiO_2 = 0.20 shows an absorption peak at 730 nm with a relatively large shoulder at 600 nm, the surface-wiped film does not show the shoulder any more, with the position of the main peak being not changed. Thus, from the difference in spectra between the non-wiped and the surface-wiped films, it is considered that the maximum amount of Au present as microcrystals in TiO_2 matrix is more than 0.16 but less than 0.20 in the molar ratio to TiO_2. This value is close to 0.178 which was reported by Kozuka et al.[8]. When much larger amount of tetrachloroauric acid was included in the coating solution, e.g. Au/TiO_2 = 0.28, the as-prepared film heat-treated at 600° C showed gold-colored metallic luster, which was lost by surface wiping.

Figure 3 shows the absorption spectra of the surface-wiped films with nominal Au/TiO_2 = 0.16 which were heat-treated at three different temperatures. The 200° C-heated film exhibits an absorption peak due to the surface plasmon resonance at 650 nm with a shoulder at 550 nm. The increase of heat-treatment temperature to 400° C caused the change in absorption peak position to 640 nm. In addition, this heat-treatment made the width of this absorption band narrower and the intensity of this peak higher. A further increase in heat treatment temperature to 600° C brings about the shift of the peak position to 710 nm, with the width of this absorption band being broader.

Figure 4 shows the absorption spectra of the as-prepared and the surface-wiped Au:ZrO_2 films prepared from the solutions of the Au/ZrO_2 molar ratios of 0.00, 0.04, 0.08 and 0.12 via heat-treated at 600°C. These spectra show an absorption peak around 590 nm due to the surface plasmon resonance. The absorption intensity was somewhat decreased by surface-

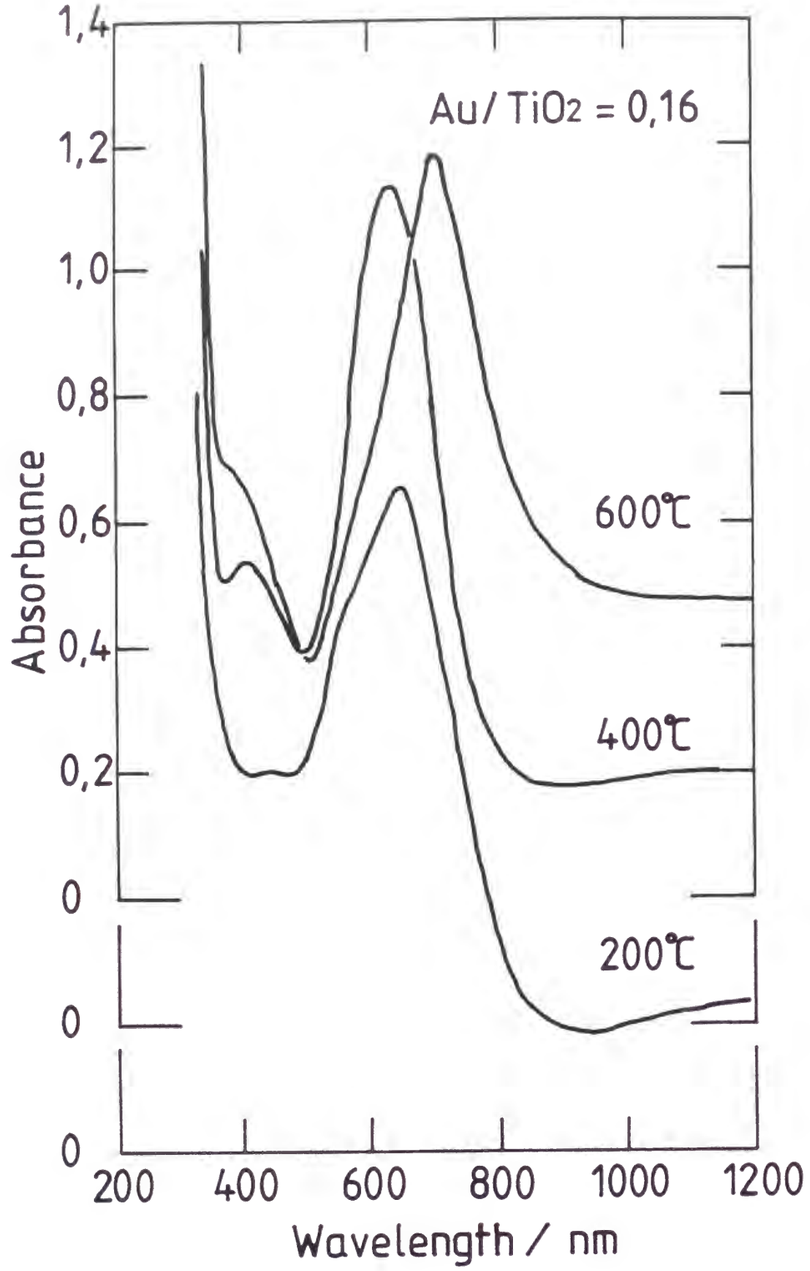

Fig.3 Optical absorption spectra of surface-wiped Au:TiO_2 films heat-treated at 200° , 400° and 600° C. A small and broad increase of absorbance from 500 to 1200nm in pure TiO_2 is due to the interference of light by the film with high refractive index.

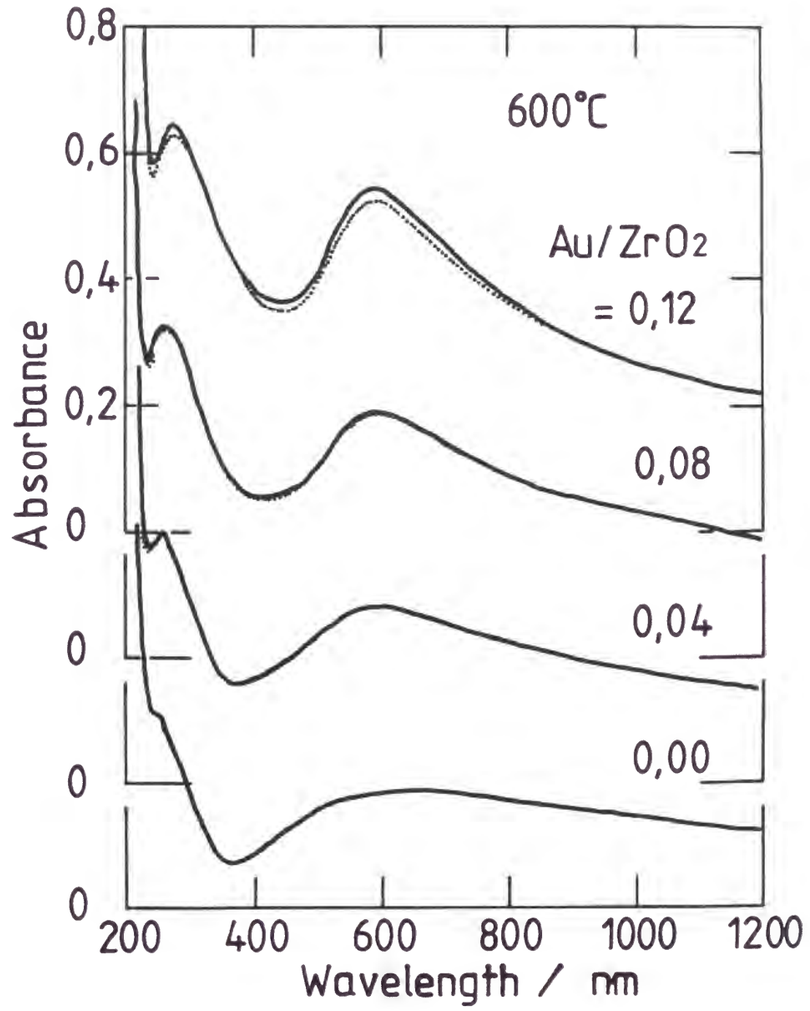

Fig.4 Optical absorption spectra of the 600°C-treated Au:ZrO_2 films. Full line : as-prepared film, Dotted line : surface-wiped film.

wiping for the film with Au/ZrO_2 = 0.12, but was not changed for the films with less Au content. Therefore, the maximum amount of Au in ZrO_2 matrix is considered to be between Au/ZrO_2 = 0.08 and 0.12.

Figure 5 shows the absorption spectra of the wiped films with Au/ZrO_2 = 0.08 heat-treated at 200° , 400° and 600° C. All of these films show a surface plasmon absorption band around 600 nm. The increase of heat-treatment temperature from 200° C to 400° C causes an increase in absorption intensity, and that from 400° C to 600° C brings about broadening of the absorption band and shifting of the peak position to the long wavelength side from 570 nm to 590 nm. These tendencies are similar to those seen in $Au:TiO_2$ films.

Figure 6 shows the absorption spectra of the as-prepared and the surface-wiped $Au:Al_2O_3$ films prepared from the solutions of the $Au/AlO_{1.5}$ molar ratios of 0.00, 0.06, 0.12, 0.18 and 0.24 via heat-treatment at 600° C. In this case, no optical interference is observed in the pure Al_2O_3 film because the refractive index of alumina is similar to that of silica glass substrate. The films with $Au/AlO_{1.5}$ = 0.06 and 0.12 show sharp absorption peak at 570 nm and 600 nm, respectively, which should be due to surface plasmon resonance. No surface-wiping effect is observed in these two films. The film with $Au/AlO_{1.5}$ = 0.18 shows a very broad absorption band which is considered to consist of a major peak around 630 nm and a minor peak around 570 nm. Furthermore, this film has a long wavelength tail. Wiping the film somewhat decreases the absorption around 570 nm but causes no change in absorption at the 630 nm peak and the long wavelength side. When the gold content is increased to $Au/AlO_{1.5}$ = 0.24, the absorption peak at 630 nm becomes strong. This film shows an obvious surface-wiping effect. Wiping the film decreases the absorptions both around 630 nm and around

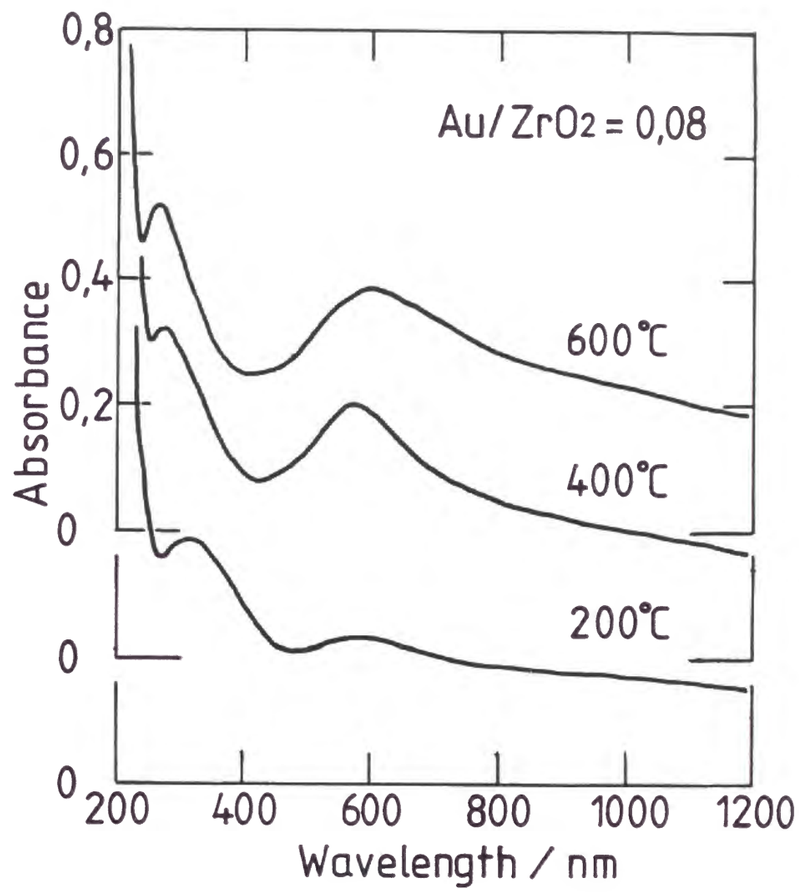

Fig.5 Optical absorption spectra of surface-wiped $Au:ZrO_2$ films heat-treated at 200° , 400° and 600° C. A small and broad increase of absorbance from 350 to 1200nm in pure ZrO_2 film is due to the interference of light by the film which has high refractive index.

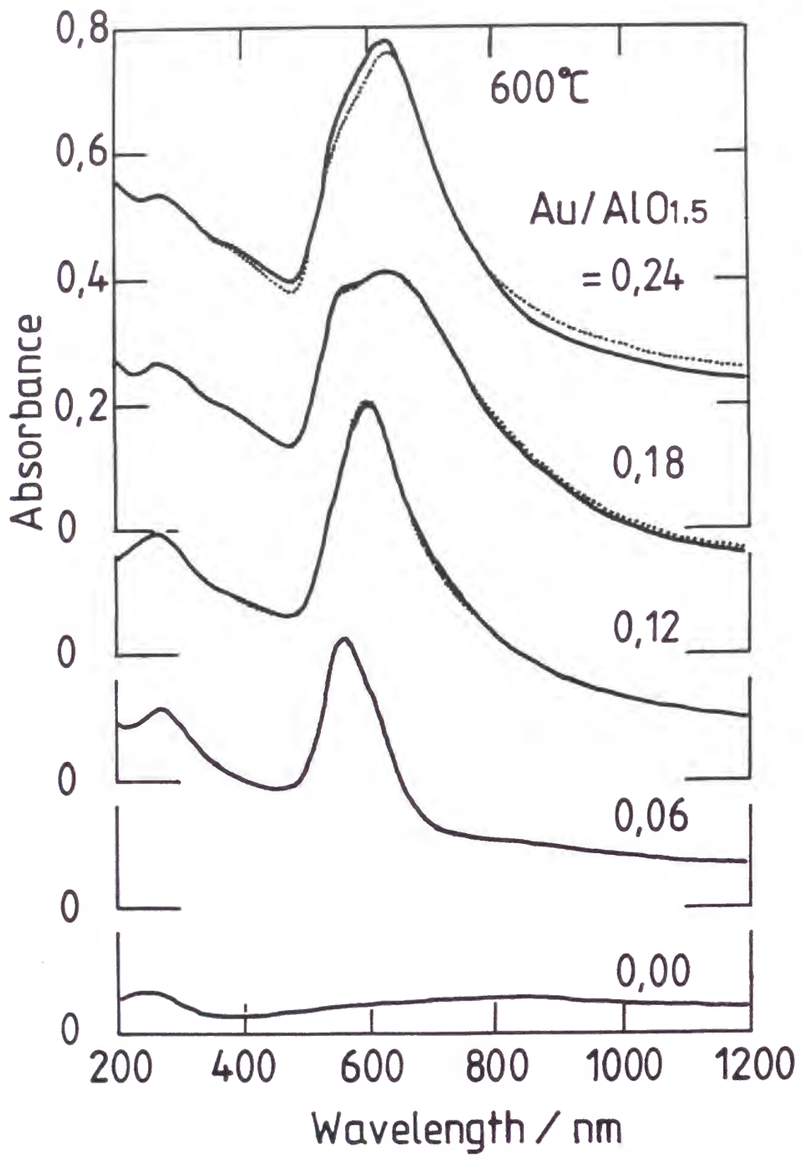

Fig.6 Optical absorption spectra of the 600°C-treated Au:$AlO_{1.5}$ films. Full line : as-prepared film, Dotted line : surface-wiped film.

570 nm. Thus, in the case of Al_2O_3 matrix, the maximum amount of Au microcrystals in the film is between $Au/AlO_{1.5}$ = 0.18 and = 0.24.

Figure 7 shows the absorption spectra of the wiped films with Au/AlO_2 = 0.18 prepared by heat treatment at 200° , 400° and 600° C. The film heat treated at 200° C has no absorption peak in the visible region but has a sharp absorption peak at 320 nm, accompanying a cut off at 260 nm. In the absorption spectra of the 200°C-heated Au:Al_2O_3 films with less Au contents, another sharp absorption peak was observed at 230 nm. These two peaks at 260 and 230 nm are characteristic of $AuCl_4^-$ ions and observable in both $NaAuCl_4$ aqueous solutions and the sol-gel-derived $NaAuCl_4$-doped SiO_2 films heat-treated at 200° C [2]. Therefore, it can be stated that heat treatment at 200° C is not effective in the case of alumina matrix to the decomposition of $AuCl_4^-$ ions to form Au microcrystals. Both 400° C- and 600° C-treated films show an absorption band due to plasmon resonance in the visible region. The 400° C-treated film shows only one relatively narrow peak at 590 nm, while 600°C-treated film shows a broad absorption band consisting of two peaks mentioned above.

The maximum amounts of Au in TiO_2, ZrO_2 and Al_2O_3 films thus determined are summarized in Table 2 together with that in SiO_2 film both in a molar ratio and a volume fraction. As can be seen, the maximum volume fraction as high as 12.6 vol% is attained in a Au:Al_2O_3 film with the molar ratio of $Au/AlO_{1.5}$ = 0.18.

4.Discussion

4.1 Maximum Amount of Au in the Oxide Films

The maximum amount of Au in sol-gel-derived oxide matrix depends on the matrix oxide species used. However, independent from the oxide

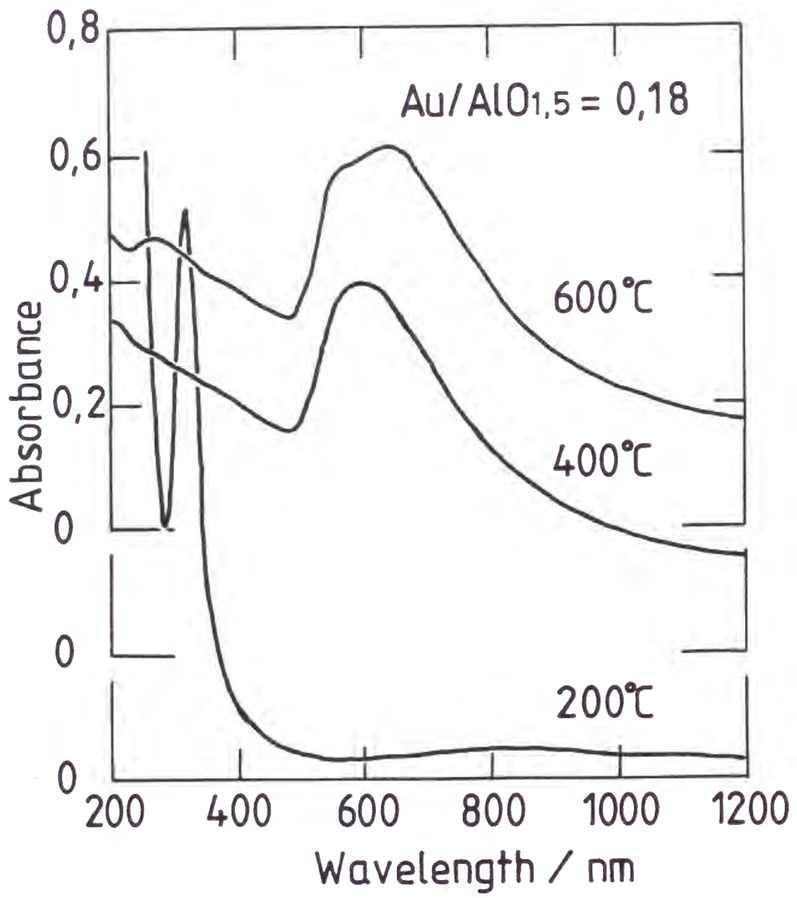

Fig.7 Optical absorption spectra of surface-wiped Au:$AlO_{1.5}$ films heat-treated at 200° , 400° and 600°C.

Table 2 Maximum amount of Au microcrystals which can be incorporated in different oxide matrices by sol-gel method, and the pH point at zero charge (PZC) of the oxides [9].

Oxide	Maximum Amount of Au		PZC
	Au/MO_x Molar Ratio	Vol. %	
TiO_2	0.16	7.9	6.0
TiO_2 (a)	0.178	8.7	
ZrO_2	0.08	3.5	4.0
$AlO_{1.5}$	0.18	12.6	9.2
SiO_2 (b)	0.04	1.5	2.8
SiO_2 (c)	<<0.01	<<0.4	
SiO_2 (d)	0.028	1.0	

(a) Ref.[8],Composition of dip-coating solution was somewhat different from this study.

(b) Ref.[2],$NaAuCl_4 \cdot 2H_2O$ instead of $HAuCl_4 \cdot 4H_2O$ was used as a Au source.

(c) Ref.[3],Conventional sol-gel dip-coating method was adopted.

(d) Ref.[3],Gel film was treated by monoethanolamine vapor before heating.

species, some amount of Au was depleted to the oxide film surface without making very large crystals (as large as 1μm, which give a sharp diffraction peak in XRD pattern and make the film gold colored and metallic lustrous) in the film in any case when the concentration of tetrachloroaurate ions in the starting solution exceeds a critical value. This fact suggests that the $AuCl_4^-$ ions and/or the Au-microcrystals feel a repulsive force from the oxide matrix and/or from the $AuCl_4^-$ ion- and/or Au microcrystal-adsorbed oxide matrix when an excess amount of Au microcrystals are formed in the oxide gel matrix.

In discussing the attractive/repulsive force between oxide matrix and $AuCl_4^-$ ions and/or Au microcrystals, one must remind of the fact that $AuCl_4^-$ ions are charged negative and Au colloids dispersed in an aqueous solution tend to charge negative [10]. This suggests that $AuCl_4^-$ ions and/or Au colloids feel attractive force when the interior surface of gel matrix is charged positive, while they feel repulsive force when the interior surface is charged negative. In the former case, Au microcrystals should be fixed to the interior of oxide gel matrix, and in the latter case microcrystals would be expelled from the gel.

The surface charge of the inner surface of oxide gel can be evaluated from the pH value of the point of zero charge (PZC). When small oxide particles are dispersed in an aqueous solution with pH lower than PZC (acidic side), the particle surface is charged positive. In contrast, when the particles are in a solution with pH higher than PZC (basic side), the surface is charged negative. In a solution with a pH value just at PZC, the oxide surface has no net charge. Thus, it can be said that an oxide having high PZC tends to be charged positive and vice versa. The PZC values for oxides used in the present study and for SiO_2 [9] are listed in Table 2.

It should be noticed that all of the present gel films were prepared under highly acidic conditions, and hence all of the oxides should be charged positive. However, how high they are charged positive depends on the PZC of oxide species. For example, Al_2O_3 should be strongly charged positive while SiO_2 should be much less charged positive.

It is evident from Table 2 that the maximum amount of Au microcrystals in the sol-gel-derived oxide films increases with increasing PZC of oxide, being consistent with the above discussion. The interior surface of oxide gels having high PZC, e.g. Al_2O_3, should be strongly charged positive, and a strong Coulomb's attractive force may act between the oxide matrix and the negatively-charged $AuCl_4^-$ ions and/or Au microcrystals, and the ions and/or the microcrystals are fixed in the oxide film as illustrated in Fig. 8(a). Accordingly, a large amount of Au can be incorporated in the Al_2O_3 film. On the other hand, the inner surface of oxides with low PZC, e.g. SiO_2, should be charged only slightly positive. Then, although a small amount of $AuCl_4^-$ ion and/or Au microcrystal can be adsorbed on the oxide inner surface by Coulomb's attraction, the increase in Au concentration should cause a strong Coulomb's repulsive force between negatively charged $AuCl_4^-$ ions themselves and/or Au microcrystals themselves, and it will surpass the attractive force between the oxide matrix and the $AuCl_4^-$ ions and/or Au microcrystal. As the result, the $AuCl_4^-$ ions and/or the Au microcrystals may become unstable in the oxide film and be expelled to the film surface as is shown in Fig. 8(b). In the case where the oxide interior surface is charged negative, no microcrystal would be able to be incorporated in the oxide film as is schematically illustrated in Fig. 8(c).

In addition to the PZC-effect, the effects of the coexisting chemical species on the maximum amount of Au incorporated in the oxide film is

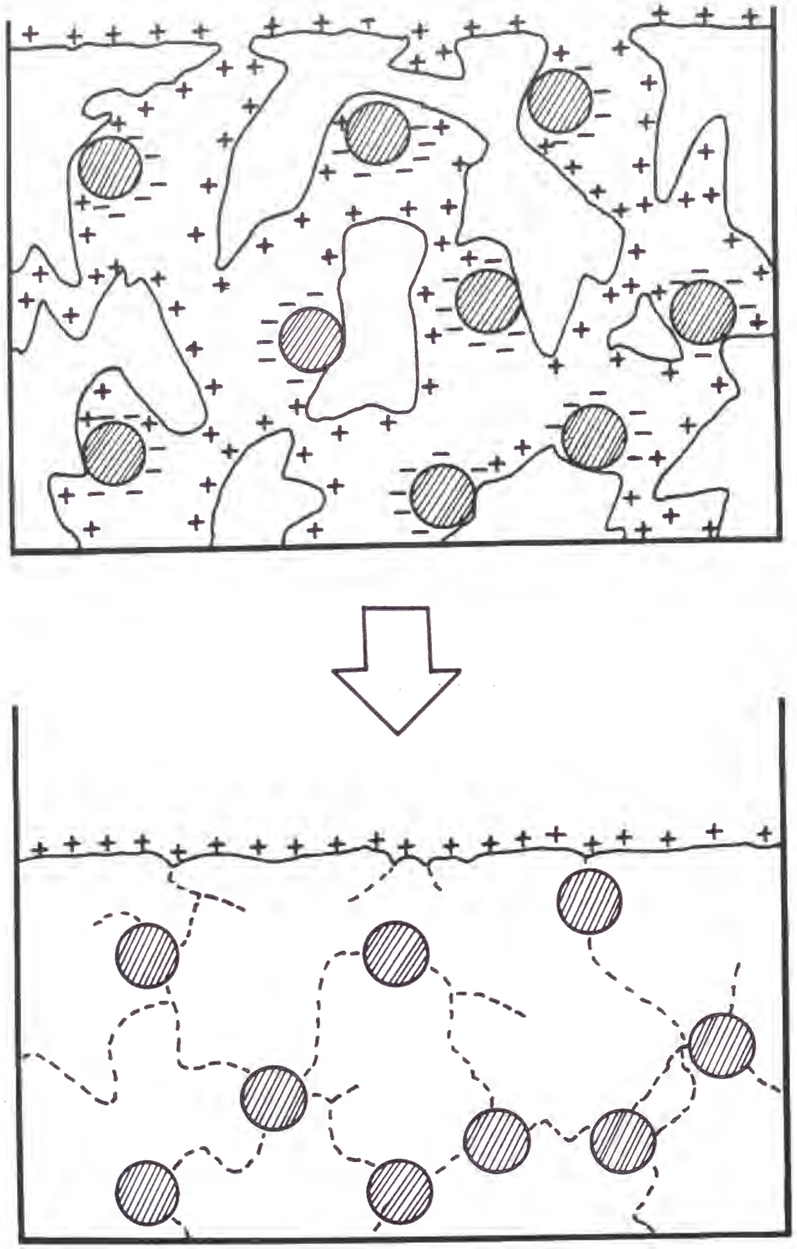

Fig.8(a) Schematic illustrations of the condensation process of Au microcrystal-containing gel films with their inner surface charged positive. Hatched circle represents the $AuCl_4^-$ ions.

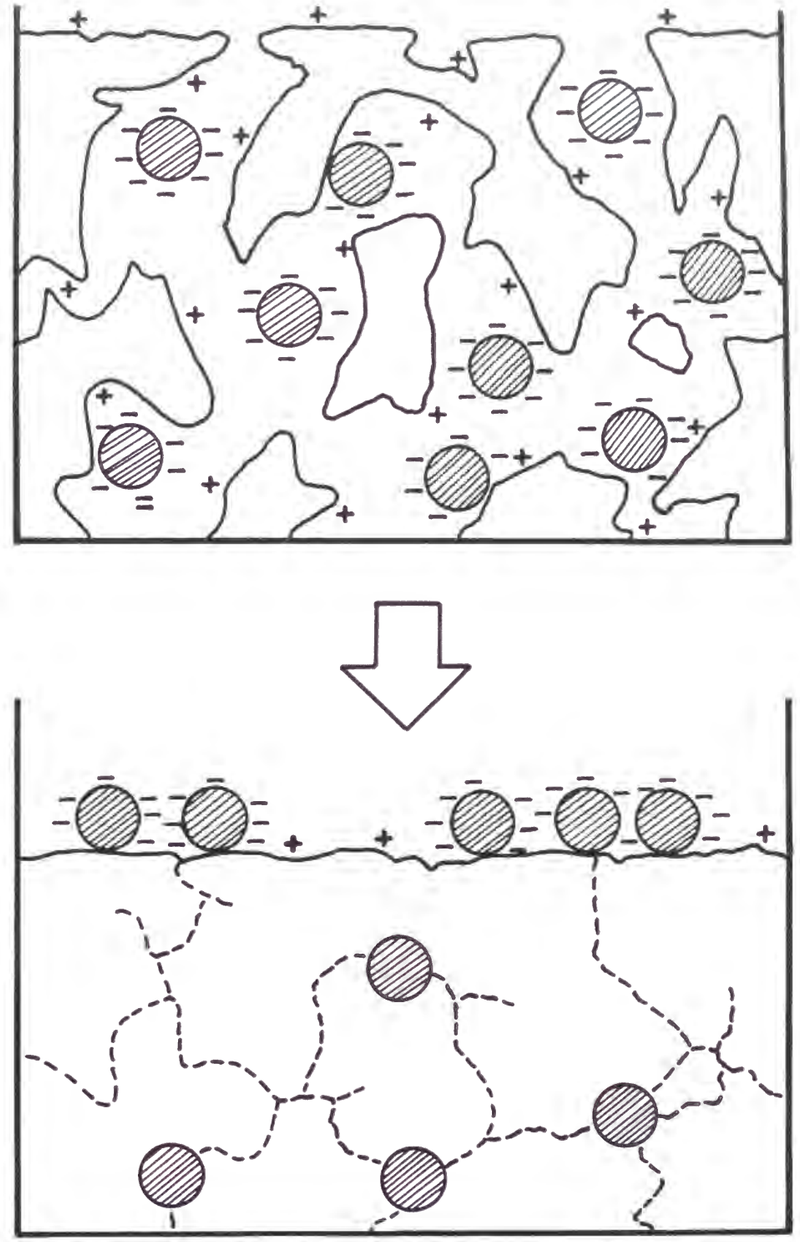

Fig.8(b) Schematic illustrations of the condensation process of Au microcrystal-containing gel films with their inner surface charged slightly positive. Hatched circle represents the $AuCl_4^-$ ions.

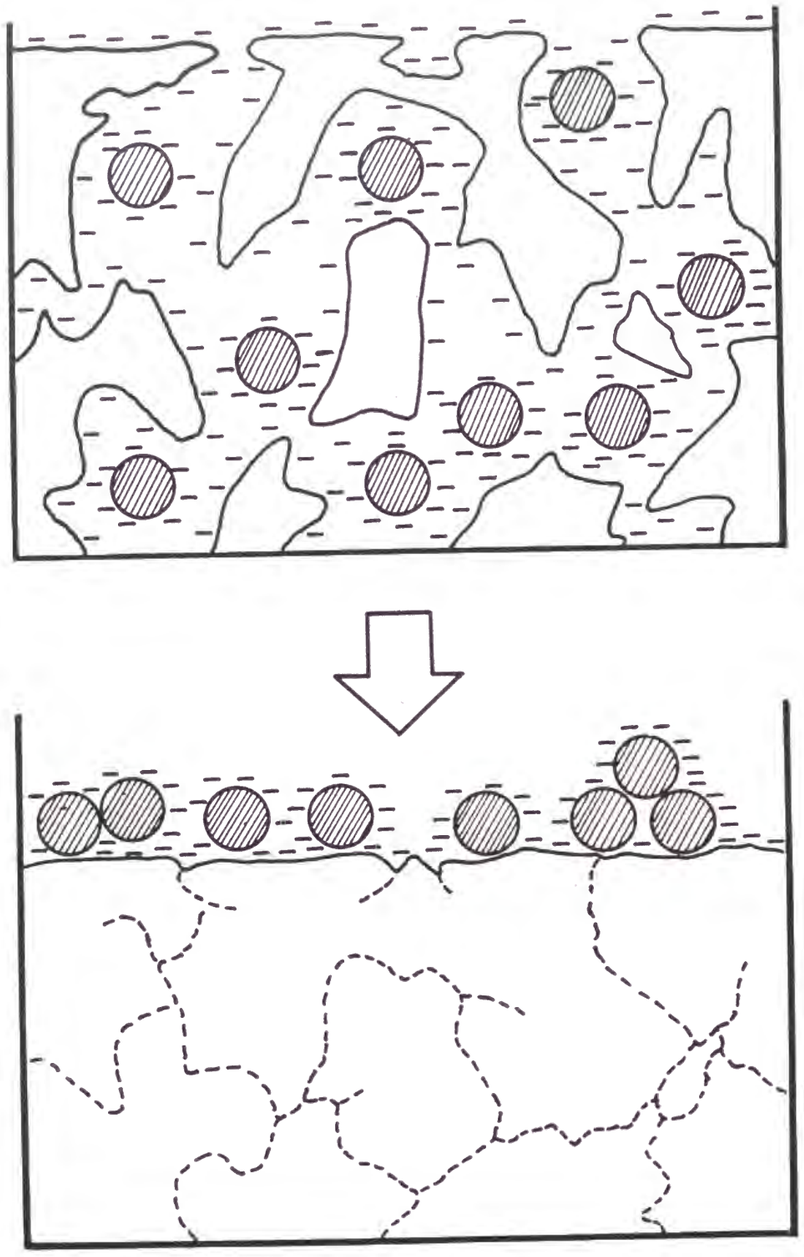

Fig.8(c) Schematic illustrations of the condensation process of Au microcrystal-containing gel films with their inner surface charged negative. Hatched circle represents the $AuCl_4^-$ ions.

known for SiO_2 matrices [2,3]. If $HAuCl_4 \cdot 4H_2O$ was used as a source of Au microcrystals in the sol-gel dip-coationg method under weak acidic conditions, the preparation of Au microcrystal-doped SiO_2 film was not successful. In this case, almost all of Au microcrystals were known to be depleted to the film surface [3]. This should be due to the electrostatic repulsive force between the SiO_2 matrix and the $AuCl_4^-$ ions and/or the Au microcrystals, both of which are charged negative. The heat-treatment of the gel would enhance this repulsion because the dielectric constant of gel decreases as water included in the gel is evaporated. On the other hand, the use of $NaAuCl_4 \cdot 2H_2O$ as a source of Au [2] and the sol-gel synthesis with $HAuCl_4 \cdot 4H_2O$ under a highly acidic condition ([HCl]/[TEOS]=0.1) [3] led to the successful incorporation of Au microcrystals in the SiO_2 films. In these cases, Na^+ ions in the former case and H^+ ions in the latter case should be bonded to $AuCl_4^-$ ions and/or adsorbed on the surface of the Au microcrystals, and also they should be adsorbed on the inner surface of SiO_2 gel, resulting a decrease in Coulomb's repulsive force between the SiO_2 matrix and the $AuCl_4^-$ ions and/or the Au microcrystals. As the result, the Au microcrystal-doped films with Au contents as high as Au/SiO_2 = 0.04 can be successfully prepared.

It is reported that the Au microcrystal-doped SiO_2 films can also be prepared from $HAuCl_4 \cdot 4H_2O$ when the as-coated gel films are treated with monoethanolamine ($NH_2CH_2CH_2OH$) vapor before heat treatment [3]. This effect might be essentially the same as that of Na^+; $[NH_3CH_2CH_2OH]^+$ ions are formed in the gel by the reaction of monoethanolamine with HCl and are adsorbed on the Au particles or the SiO_2 matrix, decreasing the repulsive force similarly to the Na^+ ions.

4.2 Optical Absorption Spectra of the Films

In the case of some oxides, i.e., TiO_2 and Al_2O_3, the shape of the optical absorption spectra depends on the amount of Au. It is known that two factors affect the absorption spectrum of surface plasmon resonance of Au microcrystals embedded in dielectric matrices.

One is the dielectric constant of the matrix. Put ε_m' as the real part of the dielectric constant of metal particle and ε_d as that of the matrix, then the local electric field in the metal particle, E_1, can be represented in relation to the macroscopic applied field, E_0, as $E_1 = \{3\varepsilon_d/(\varepsilon_m'+2\varepsilon_d)\}E_0$ [11]. As the dielectric constants are the function of optical wavelength, λ, this equation indicates that the wavelength of the absorption peak position is determined from the equation $\varepsilon_m'(\lambda)+2\varepsilon_d(\lambda) = 0$. Because the ε_m' of gold takes a negative value in the visible region and becomes more negative with the increase of wavelength, an increase in dielectric constant of the matrix, ε_d, leads to the shift of peak position to the longer wavelength side.

Another factor that affects the absorption spectra is the aggregation of Au microcrystals. The aggregation of microcrystals is known to cause the shift of plasmon absorption peak position to the longer wavelength side, accompanying the appearance of absorption tail at the longer wavelength side [12]. These two factors should affect the complex behavior of absorption spectra in the films of $Au:TiO_2$ and $Au:Al_2O_3$.

The $Au:TiO_2$ film with nominal Au/TiO_2 = 0.20 shows the change of absorption spectra by wiping, that is, the shoulder at 600 nm disappears without changing the shape and intensity of the main peak at 730 nm. As mentioned above, the absorption peak position depends on the dielectric constant of matrix. The optical dielectric constant of TiO_2 (rutile) is in the range from 6.7 to 9.8 in the visible region and is much larger than that of

water (1.8) and air (1.0). So, it should be reasonable to say that the absorption shoulder is due to the Au microcrystals depleted to the film surface, which is partially surrounded by a medium such as water and/or air with lower dielectric constants than TiO_2, which is illustrated in Fig.9. The fact that the film with Au/TiO_2 = 0.16 has no shoulder at the short wavelength side may support the above discussion together with the fact that any change does not occur in the absorption spectra by wiping. The $Au:ZrO_2$ and $Au:Al_2O_3$ films do not show such a behavior, i.e., the appearance of absorption shoulder at the short wavelength side by the depletion of Au and its dissipation by wiping. This should be due to the small difference in dielectric constant between the solid matrices and the environmental medium such as water and/or air. In other words, when the concentration of $AuCl_4^-$ in the dip-coating solution is a little higher than the maximum value in which all of Au microcrystals can be incorporated in the film, wiping out of the depleted Au on the film causes the dissipation of absorption shoulder in the case of TiO_2 matrix, but causes the decrease of main absorption peak in the cases of ZrO_2 and Al_2O_3 matrices.

The $Au:Al_2O_3$ films exhibit a different behavior. By increasing the amount of Au to $Au/AlO_{1.5}$ = 0.18, the absorption band becomes split into two bands around 570 nm and around 630 nm. The former band is also seen in the films with less amount of Au, suggesting that this peak is due to Au microcrystals free from aggregation. The latter peak increases its intensity with the further increase of Au amount. As wiping of this film changes only the absorption intensity and does not change the shape of spectra, most of Au microcrystals related either with 570 nm and 630 nm bands are incorporated in the film but not positioned at the film surface. Therefore, the absorption peak around 630 nm should be due to the aggregated Au

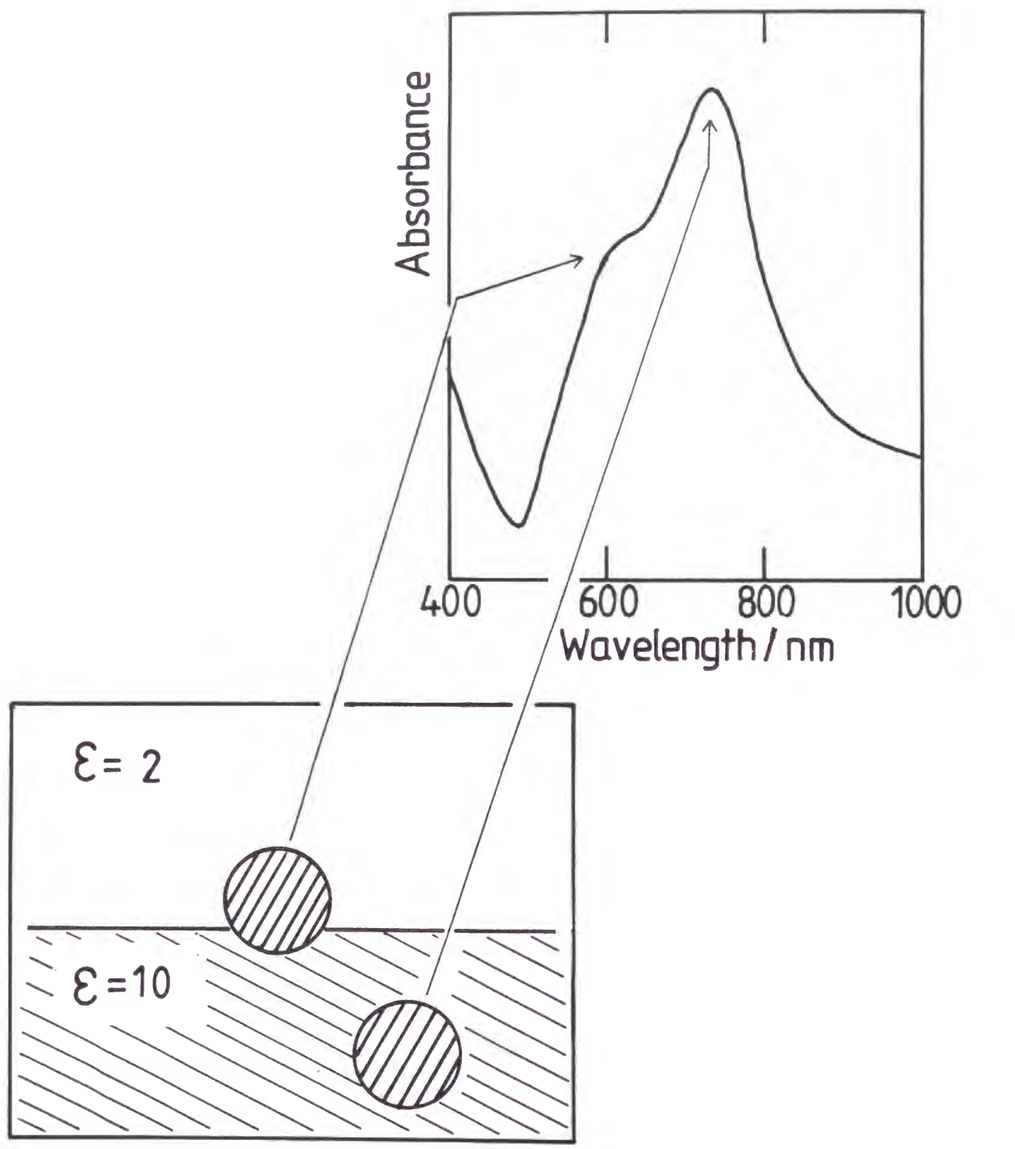

Fig.9 Schematic illustration of the relation between the position of gold microcrystals and the optical absorption spectra in Au/TiO_2 film.

microcrystals in the film. Strong attraction between the Au microcrystal and the Al_2O_3 matrix should be the origin of the aggregation of microcrystals in the film without their depletion.

The heat-treatment temperature of the gel film also affects the absorption spectra. The absorption peak of the $Au:TiO_2$ and the ZrO_2 films shifts to the shorter wavelength side as the heat-treatment temperature is increased from 200° C to 400° C. In addition, the peak widths of the 200° C-treated films are broader than those of the 400° C-treated ones. It is known that by the heat-treatment of alkoxide-derived gel films at 200°C, the hydroxyl group can not be removed completely and the obtained films are porous. Then, $AuCl_4^-$ ions and/or Au microcrystals in the 200° C-treated films should still be able to move in the film. Therefore, the shift to the longer wavelength side and the broadening of the absorption spectra of the 200° C-treated films would be due to the aggregation of microcrystals.

A further increase in heat-treatment temperature to 600° C causes the shift of absorption peak to the longer wavelength side. In addition, appearance of the long wavelength tail is also observed in 600° C-treated films. So, this spectral change seems to be due to the aggregation of the microcrystals. This phenomenon is more obvious in the $Au:Al_2O_3$ films where the absorption spectra indicate that the 400° C-treated film shows no aggregation while the Au particles in the 600° C-treated film are highly aggregated. This phenomenon is explainable by assuming that the decomposition of $AuCl_4^-$ ions to form Au microcrystals occurs much faster than the condensation of hydroxyl groups of the flexible oxide gel, which becomes rigid at 600°C. In this case, mobile Au microcrystals can be aggregated before the completion of densification of the oxide matrix.

The heat-treatment at 200° C gives rise to the formation of Au micro-

crystals in the Au:TiO_2 and Au:ZrO_2 films. On the other hand, in the Au:Al_2O_3 film Au microcrystals are not formed by the heat treatment at 200°C, as well as in the Au:SiO_2 films [1]. Therefore, it can be assumed that TiO_2 and ZrO_2 can act as a catalyst for decomposition of $AuCl_4^-$, but Al_2O_3 and SiO_2 can not do, and the catalytic activity is independent from PZC.

5.Conclusion

Au microcrystal-doped TiO_2, ZrO_2 and Al_2O_3 films are successfully prepared by the sol-gel dip-coating method using tetrachloroauric acid as a starting material of Au. When an excess amount of tetrachloroauric acid was dissolved in the coating solution, some amount of Au microcrystals were depleted to the surface of the Au microcrystal-doped oxide films. The maximum amount of Au that can be incorporated in the oxide film as microcrystals is found to increase with increasing pH point at zero charge (PZC) of the matrix oxide. This should be due to the fact that the $AuCl_4^-$ ions are charged negative and also the Au microcrystals tend to charge negative, and that eventually the oxide gel with high PZC, which has a tendency to charge positive, would fix the ions and/or microcrystals to its interior. The maximum amount of Au microcrystal in the oxide matrix was 12.6 vol%, observed in an Au:Al_2O_3 film.

References

[1] J. Matsuoka, R. Mizutani, H. Nasu and K. Kamiya, J. Ceram. Soc. Jpn., **100**, 599 (1992)

[2] J. Matsuoka, R. Mizutani, S. Kaneko, H. Nasu, K. Kamiya, K. Kadono, T. Sakaguchi and M. Miya, J. Ceram. Soc. Jpn. **101**, 53 (1993)

[3] H. Kozuka and S. Sakka, Chem. Mater 5, 222 (1993)

[4] J. M. Fernández-Navarro and M. Angeles Villegas, Glastech. Ber. 65, 32 (1992)

[5] P. Innocenzi, H. Kozuka and S. Sakka, J. Sol-Gel Sci. Tech. 1, 305 (1994)

[6] N. Tohge, T. Murakami and T. Minami, in Proc. 66th Fall Meeting Chem. Soc. Jpn., (The Ceramic Society of Japan, Tokyo, 1993), p.322 [in Japanese]

[7] J. Y. Tseng, C.-Y. Li, T. Takada, C. Lechner and J. D. Mackenzie, in Proc. SPIE : Sol-Gel Optics II 1758, 612 (1992)

[8] H. Kozuka, G. Zhao and S. Sakka, J. Sol-Gel Sci. Tech. 2, 741 (1994)

[9] A. Kitahara and K. Furusawa, Saisin-Koroido-Kagaku (Latest Colloid Chemistry) (Koudansha, Tokyo, 1990), p.8 [in Japanese]

[10] J. T. Harrison and G. A. H. Elton, J. Chem. Soc. **1959**, 3838

[11] U. Kreibig and M. Vollmer, Optical Properties of Metal Clusters (Springer-Verlag, Berlin, 1995), p.23

[12] S. Hayashi, R. Koga, M. Ohtugi, K. Yamamoto and M. Fujii, Solid State Commun. **76**, 1067 (1990)

Chapter 6

Formation of Au Microcrystal-Doped Oxide Films through Penetration of Tetrachloroaurate Ions in Oxide Gel Films

1. Introduction

In this chapter, a newly developed method for the preparation of gold microcrystal doped oxide films through sol-gel dip coating process is described, in which the gold materials in the process are used effectively. The process consists of three steps. At the first step, oxide gel films are coated on glass substrates by the conventional sol-gel dip-coating process. At the next step, the coated gel films are immersed in $NaAuCl_4 \cdot 2H_2O$ aqueous solution. At the final step, the films are heat-treated to decompose $AuCl_4^-$ ions to form gold microcrystals. The effects of alkoxide species and concentration of $NaAuCl_4 \cdot 2H_2O$ aqueous solution on the availability of this process are investigated. The immersion of gel films into gold colloid aqueous solutions is also examined.

2. Experimental

The oxide gel films of alumina, titania, zirconia and silica were prepared on silica glass substrates by the sol-gel dip-coating process using aluminum sec-butoxide, titanium isopropoxide, zirconium n-propoxide and silicon ethoxide. The composition of dip-coating solutions are listed in Table 1. First, alkoxides of aluminum, titanium, or silicon or propanolic solution of zirconium alkoxide were mixed with a half of the listed amount of ethanol to form alkoxide solutions, and the rest of starting materials were

mixed to form another solutions. Then, the latter solutions were slowly titrated to the former solutions. The solutions thus obtained were served for dip-coating. These procedures are similar to that in chapter 1. Gel films were dip-coated by pulling out a substrate from a dip-coating solution with a withdrawal speed of 0.15 mm/sec, and subsequently dried at 200° C for 10 min to prevent peeling of the gel films. Thickness of all of the films when they were sintered at 600° C was about 0.06 μm measured with a scanning electron microscope.

The dip-coated gel films were immersed in $NaAuCl_4 \cdot 2H_2O$ aqueous solutions at room temperature (around 22° C) for 7 days. The concentrations of $NaAuCl_4$ in the solutions were 0.01, 0.10, and 1.00 wt%. After immersion, the films were washed with distilled water and dried at about 80° C with a hot-air dryer. Subsequently, the films were heat-treated at 600° C for 15 min by inserting them into a preheated electric furnace. This heat-treatment decomposes $AuCl_4^-$ ions to form gold microcrystals together with the dehydration and condensation of oxide gel matrices.

In addition to the above experiments, immersion of gel films in gold colloid aqueous solutions was attempted. A gold colloid solution was prepared by mixing 100 cm^3 of 0.01 wt% $HAuCl_4 \cdot 4H_2O$ aqueous solution with 2.5 cm^3 of 1 wt% sodium citrate aqueous solution under boiling condition. Other procedures of this gold colloid process are the same as those using $NaAuCl_4 \cdot 2H_2O$ aqueous solution.

The optical absorption spectra of the films and gold colloid aqueous solutions were measured from 200 to 1200 nm. The average size of gold microcrystals were estimated from the shape of the plasmon absorption peak in the spectra using a relation [1]

$$r = v_F / \Delta\omega_{1/2} \qquad (1)$$

Table 1 Composition of dip-coating solutions.

alkoxide	molar ratio to alkoxide				
	H_2O	CH_3COOH	HCl	C_2H_5OH	n-C_3H_7OH
$Al(OC_4H_9^s)_3$	3.73	1.80	1.00	10.00	
$Ti(OC_3H_7^i)_4$	1.00	2.46	0.24	8.00	
$Zr(OC_3H_7^n)_4$	1.00		0.25	10.00	2.34
$Si(OC_2H_5)_4$	6.00		0.03	6.00	

where r is the average crystal radius, v_F is the Fermi velocity of electron and is 1.39×10^6 m/s for gold, and $\Delta\omega_{1/2}$ is the full width at half maximum of the plasmon absorption in wavenumber.

3. Results

Figure 1 shows the optical absorption spectra of the heat-treated alumina film immersed in 0.01 wt% $NaAuCl_4 \cdot 2H_2O$ solution, together with the spectra of the gel film before immersion and of the as-immersed gel film. The heat-treated alumina film has an absorption peak around 540 nm together with an increase of absorption in shorter wavelengths. This absorption spectra of the heat-treated film is similar to that of gold microcrystal-doped alumina films prepared from a $HAuCl_4$-contained alkoxide solution by sol-gel process [2,3]. Therefore, the absorption peak is due to the plasmon resonance of gold microcrystals. The color of heat-treated film is wine red, and the average crystal radius of gold in the film calculated from Eq.1 is 1.5± 0.2 nm. The immersed gel film before heat-treatment has a very strong optical absorption in the wavelength range less than 240 nm which should be due to the optical absorption by $AuCl_4^-$ ions [4]. When dip-coating and drying of the gel film was repeated for several times before immersion, the height of the peak at 540 nm of the heat-treated film increased.

Figure 2 shows the absorption spectra of heat-treated titania, zirconia and silica films immersed in 0.01 wt% $NaAuCl_4 \cdot 2H_2O$ solution. The titania film has a strong absorption peak around 620 nm, together with a broad absorption band from 400 to 1000 nm which should be due to the optical interference of light[5]. The titania gel film before heat treatment also has a broad absorption from 400 to 1000 nm due to interference[5], but no absorption peak is observed in the range from 500 to 700 nm in this film. The absorp

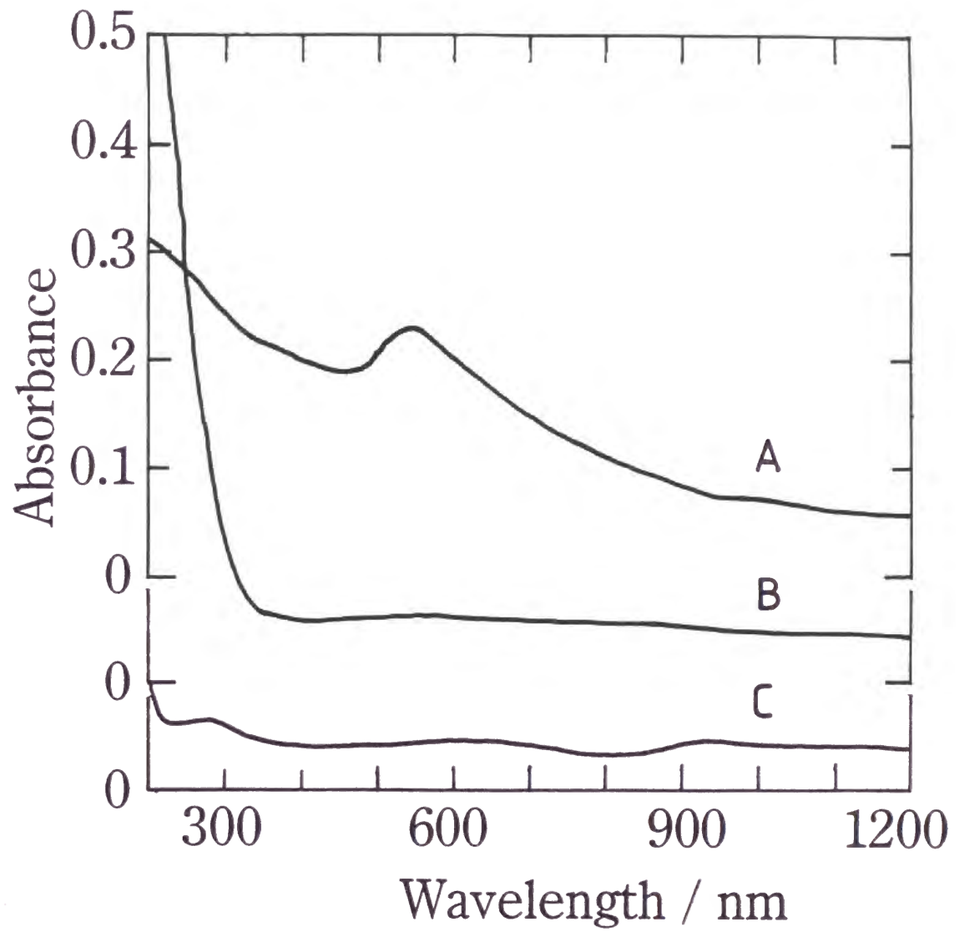

Fig.1 Optical absorption spectra of alumina films. (A) 600° C-heat-treated film after immersion in 0.01 wt% $NaAuCl_4 \cdot 2H_2O$ solution, (B) immersed gel film before heat-treatment, and (C) as dip-coated film before immersion.

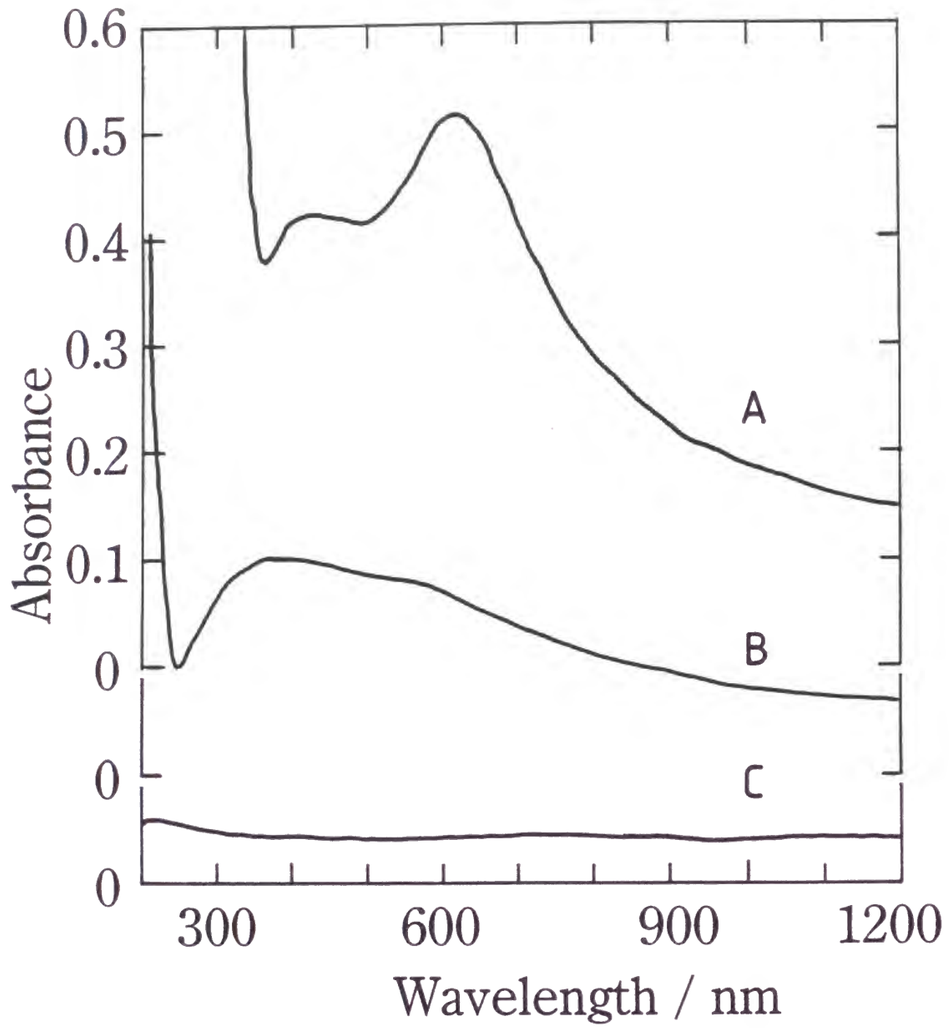

Fig.2 Optical absorption spectra of (A) titania, (B) zirconia and (C) silica films immersed in 0.01 wt% $NaAuCl_4 \cdot 2H_2O$ solution and heat-treated at 600°C.

tion peak at 620 nm may be due to the plasmon resonance of gold microcrystals. The difference in peak position between the alumina and titania films may be due to the difference in dielectric constant of oxide matrix which affects the peak position [6]. The color of heat-treated titania film is blue, and the average crystal radius of gold is 2.0±0.4 nm.

The absorption spectra of zirconia film has a broad absorption band from 250 to 1000 nm due to optical interference, with a small absorption around 590 nm. The position of this hump is equal to that of the plasmon absorption peak of gold microcrystals embedded in the zirconia matrix prepared from $HAuCl_4$-contained zirconium alkoxide solution [2,3]. Therefore, this hump should be due to the plasmon resonance of gold microcrystals. Only a very small amount of microcrystals can be embedded in zirconia matrix by this immersion process. The average crystal radius of gold is 1.7±0.3 nm.

The spectra of silica film has no absorption peak from 200 to 1200 nm. Furthermore, the spectra of immersed silica gel film before heat treatment has no absorption bands due to $AuCl_4^-$ ions. Based on this result, it is assumed that the silica gel film does not adsorb $AuCl_4^-$ ions on its inner surface.

Figure 3 shows the absorption spectra of heat-treated alumina films immersed in 0.01, 0.10 and 1.00 wt% $NaAuCl_4 \cdot 2H_2O$ aqueous solutions. An increase in concentration of $NaAuCl_4 \cdot 2H_2O$ decreases the height of plasmon resonance peak. The average crystal radius prepared using 0.10 wt% solution is 1.8±0.2 nm, which is similar to that prepared using 0.01 wt% solution, i.e., 1.5 ±nm. Similar tendency was also observed in the cases of titania and zirconia films. Gold microcrystal-doped silica films could not be obtained in any $NaAuCl_4 \cdot 2H_2O$ concentration.

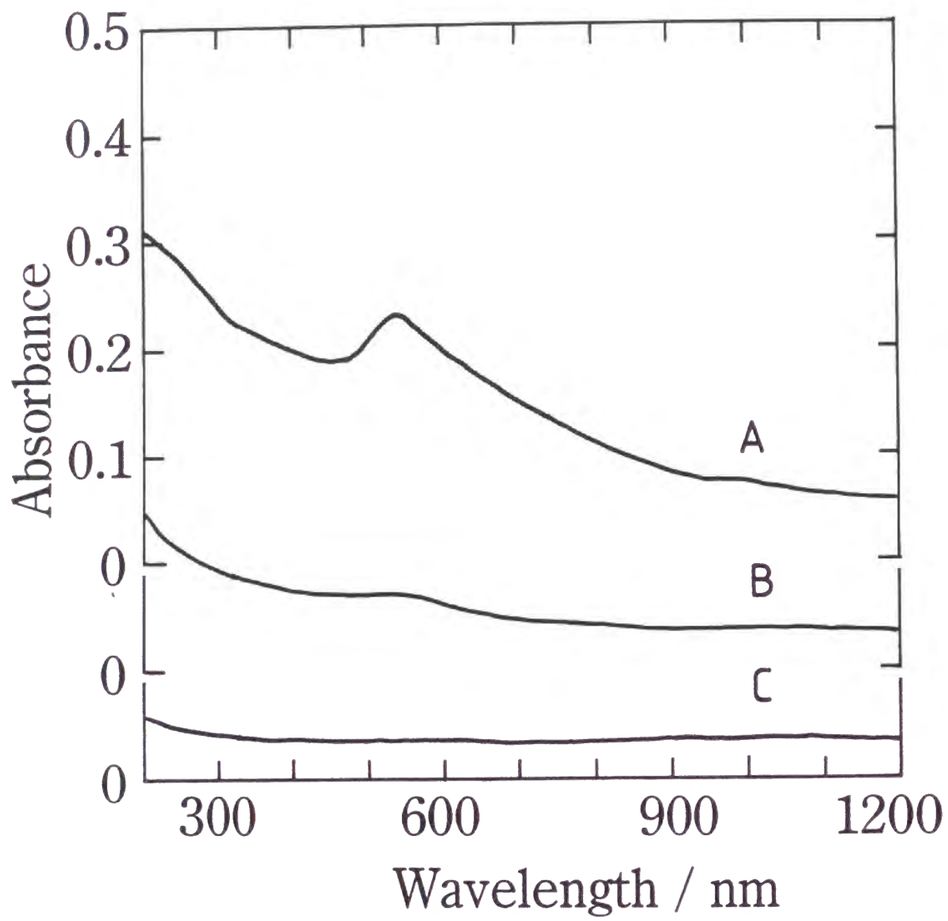

Fig.3 Optical absorption spectra of 600° C-heat-treated alumina films immersed in (A) 0.01, (B) 0.10 and (C) 1.00 wt% $NaAuCl_4 \cdot 2H_2O$ aqueous solutions.

The preparation of gold microcrystal-doped oxide films by immersing the gel films in gold colloid aqueous solutions was also attempted using alumina, titania, zirconia and silica gel films. The average crystal radius of gold colloid particles in the aqueous solution calculated from Eq.1 is 2.2± 0.2 nm in this case. However, the gold microcrystal-doped films were not formed in any case. The absorption spectra of heat-treated films which had been immersed in gold colloid solutions are the same as those of the heat-treated films not immersed.

4. Discussion

The gold microcrystal-doped alumina film can be prepared by immersing the dip-coated gel film into $NaAuCl_4 \cdot 2H_2O$ aqueous solution and heat-treating it. This means that $AuCl_4^-$ ions penetrate into the alumina gel film. From the comparison in absorption spectra and film thickness between this film and the previously reported gold microcrystal-doped alumina film with the gold content of $Au/AlO_{1.5}=0.06$ in molar ratio [3], the gold content of this film should be in the order of $Au/AlO_{1.5}=0.02$ in molar ratio.

The $AuCl_4^-$ ions can also penetrate into the titania gel film, but penetration in the zirconia gel film is less and no penetration in the silica gel film was observed. This difference of penetration ability should be explained by the difference of the point of zero charge (PZC) of these oxide gels [3]. PZC of these oxide gels [7] are listed in Table 2 together with the $AuCl_4^-$ adsorption ability. It is clear that oxide gels with high PZC adsorb $AuCl_4^-$ ions but those with low PZC do not. The surfaces of solids with high PZC tend to be charged positive, whereas those with low PZC tend to be charged negative [7]. Therefore, when gel films with high PZC are immersed in $NaAuCl_4 \cdot 2H_2O$ aqueous solution, $AuCl_4^-$ negative ions should .PA

Table 2 Point of zero charge(PZC) [7] and $AuCl_4^-$ adsorption ability of oxide gels

Oxide	Al_2O_3	TiO_2	ZrO_2	SiO_2
Point of Zero Charge	8.4±1.0	5.8±1.0	4.0±1.0	1.9±0.9
Adsorption Ability	Yes	Yes	Poor	No

penetrate in the gel film and adsorbed on the inner surface of the gel by Coulomb attractive force. On the other hand, when the films with low PZC are immersed in the solution, $AuCl_4^-$ anions should not penetrate into the gel film because of the Coulomb repulsive force. These reactions are schematically illustrated in Fig.4. This effect is the reason why the preparation of gold microcrystal-doped oxide films was succeeded in the cases of alumina and titania but was failed in the cases of zirconia and silica.

An increase in concentration of $NaAuCl_4 \cdot 2H_2O$ aqueous solution causes a decrease in amount of $AuCl_4^-$ ions penetrating the gel films. This phenomenon may be related with the surface charge of oxide gels or with the interaction of gels with $NaAuCl_4 \cdot 2H_2O$ aqueous solution. More study must be required to clarify this phenomenon.

The average radius of gold particles in the alumina, titania and zirconia films calculated from Eq.1 are 20 to 50 % smaller than those in the films prepared using $AuCl_4^-$-contained alkoxide solutions [3]. This smaller size would be due to the fact that gold particles must be formed in previously formed gel micropores and then the particle size should be limited by the pore size in the former case, while the formation of gold particles occurs at the same time with the formation and shrinkage of flexible gels in the latter case.

Gold microcrystal-doped oxide films were not formed by immersing the gel films into the gold colloid solution though the colloid particles tend to charge negative [8] and then expected to adsorb on the oxide gel surface with high PZC. This should be explained by the assumption that the diameter of the colloid particles, 4.4±0.4 nm in average, would be larger than the size of micropores in gel films which is smaller than 2.0 nm in acid-catalyzed oxide without drying control chemical additives [9,10].

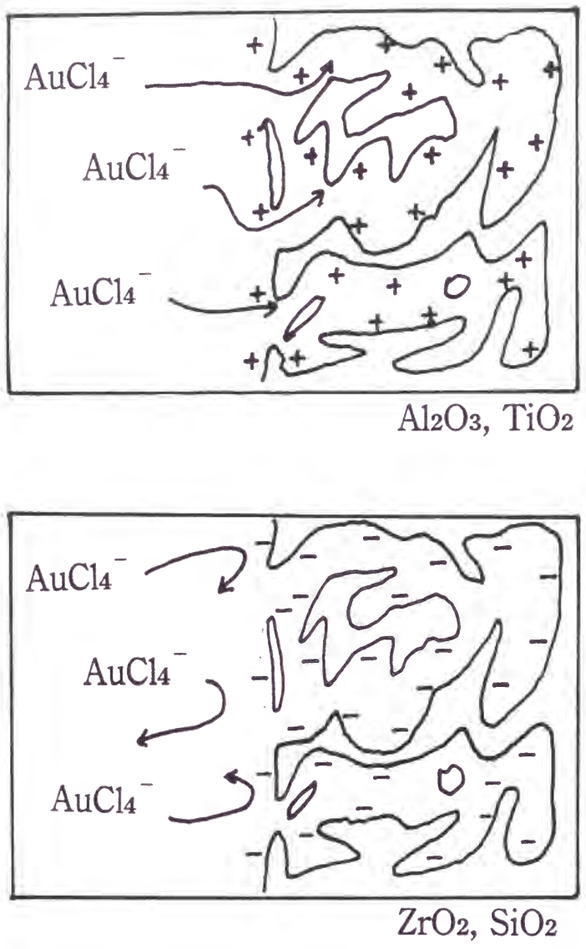

Fig.4 Schematic illustration of the reaction of $AuCl_4^-$ ions with high PZC (Al_2O_3, TiO_2) and low PZC (ZrO_2, SiO_2) oxide films.

5.Conclusion

Gold microcrystal-doped alumina and titania films can be prepared by immersing the dip-coated oxide gel films in $NaAuCl_4 \cdot H_2O$ aqueous solution and heat-treating them. On the other hand, this method is not effective in the cases of zirconia or silica gel films. This difference is explained by the point of zero charge, and then the surface charge in aqueous solutions, of these gels. Increase of the concentration of $NaAuCl_4 \cdot 2H_2O$ aqueous solution decreases the amount of gold microcrystals in the films. Gold microcrystal-doped oxide films can not be prepared by immersing the gel films in gold colloid aqueous solutions.

References

[1] G.W. Arnold, J. Appl. Phys. **46** (1975) 4466

[2] J. Matsuoka, H. Nasu and K. Kamiya, Proc. 17th Internat. Cong. Glass **4** (1995) 252

[3] J. Matsuoka, H. Yoshida, H. Nasu and K. Kamiya, J. Sol-Gel Sci. Tech. **9** (1997) 145

[4] J. Matsuoka, R. Mizutani, H. Nasu and K. Kamiya, J. Ceram. Soc. Jpn. **100** (1992) 599

[5] K. Kamiya and T. Yoko, Hyoumen (Surface), **24** (1986) 131 [in Japanese]

[6] U. Kreibig and M. Vollmer, Optical Properties of Metal Clusters (Springer-Verlag, Berlin, 1995), p.23

[7] A. Kitahara and K. Furusawa, Saisin-Koroido-Kagaku (Latest Colloid Chemistry) (Koudansha, Tokyo, 1990), p.8 [in Japanese], and references cited therein.

[8] J.T. Harrison and G.A.H. Elton, J. Chem. Soc. **1959** (1959) 3838

[9] C.J. Brinker and G.W. Scherer, Sol-Gel Science (Academic Press, San Diego, 1990) pp.518-532

[10] J.C. Debsikdar, J. Non-Cryst. Solids **86** (1986) 231

Summary

In the present thesis, the preparation and property of photonic nano-composite materials were investigated. The materials investigated were the sol-gel derived Au or Au-Pd-alloy microcrystal-doped films of SiO_2, TiO_2, ZrO_2 and Al_2O_3 transparent films. The results obtained are summarized as follows:

In Chapter 1, Au microcrystal-doped silica glass films were prepared by the sol-gel method with dip-coating using $NaAuCl_4 \cdot 2H_2O$ and tetraethyl orthosilicate (TEOS) as starting materials. The glass film with an Au/Si atomic ratio of 0.01 was successfully prepared. Microcrystals with a radius of about 7 Å and of about 30 Å coexisted in the glass film. The subsequent heat treatment of the films above 700° C changed the absorption spectra. The atomic ratio of Au/Si was able to be increased to 0.04, highest amount ever achieved in pure silica glass.

In Chapter 2, in order to clarify the effect of coexisting ions on the maximum amount of gold microcrystals which can be incorporated in silica glass film, Au microcrystal-doped silica glass films were prepared by the sol-gel process from $HAuCl_4$ and TEOS with the existence of nitrates of sodium, calcium, and lanthanum. The maximum amount of gold microcrystals which can be incorporated in the films was found to be increased by the addition of these nitrates. This effect was explained by a decrease in Coulomb's repulsive force between silica gel surface and $AuCl_4^-$ ions by the adsorption of cations on gel surfaces.

In Chapter 3, third order nonlinear optical susceptibility of sol-gel-derived Au microcrystal-doped SiO_2 glass films with the

composition of $Au:SiO_2$ = 0.01:1 and = 0.04:1 in molar ratio was measured by the degenerate four wave mixing method. The measurement was carried out using a frequency-doubled Nd:YAG laser with the pulse width of both nanosecond and picosecond orders, and the susceptibility values obtained at these two pulse widths were compared with each other. The picosecond-measured nonlinear optical susceptibility of the samples were 0.10 to 0.64 x 10^{-8} esu, which ranged between 20 and 40% of the nanosecond-measured susceptibility. The films containing larger size microcrystals had higher susceptibility than those of the smaller one in both the nanosecond and picosecond measurements. The aggregation of microcrystals in the films increased both the nanosecond and picosecond susceptibility. The nonlinear susceptibility of Au microcrystals itself in the film, $\chi_m^{(3)}$, was 1.0×10^{-7} esu in the nanosecond measurements and was two times larger than that observed in Au-doped glasses prepared by the melting method.

In Chapter 4, in order to prepare alloy microcrystal-doped silica glass films which would have a potential to use as a nonlinear optical material, the sol-gel dip-coating method using TEOS, $NaAuCl_4 \cdot 2H_2O$, and Na_2PdCl_4 as starting materials was adopted, followed by the heat-treatment of the gel film from 200° to 700° C. The radius of Au microcrystals formed in the Au-doped film was almost constant and was about 50 Å when the heat-treatment temperature was higher than 300° C. In the Pd-doped films, palladium existed as a chloride form up to 600° C. The heat-treatment at 700° C seemed to led to the formation of palladium oxide. In the Au-Pd co-doped films heat-treated at a temperatures lower than 600° C, metal microcrystals were formed, which gave a plasmon peak in the optical absorption spectra similarly to that of the Au-doped film, and the crystal radius was smaller than that in the Au-Doped films and decreased with increasing the heat-treatment temperature. It was considered that Au microcrystals covered with palladium atoms bonded with chlorine or oxygen were formed below 600° C in the co-doped films. Au-Pd alloy microcrystals were formed in the Au-Pd co-doped film by the heat-treatment at 700° C. However, the plasmon peak in the optical absorption spectra was not observed, which should be associated with the difference of the electronic structures of Au and Pd. Au-Pd co-doping was found to be effective to make the crystal size of Au smaller in the heat treatment range below 600° C.

In Chapter 5, Au-microcrystal-doped TiO_2, ZrO_2 and Al_2O_3 films were made by sol-gel dip-coating method using titanium, zirconium and aluminum alkoxides with $HAuCl_4 \cdot 4H_2O$. The influence of the oxide matrix composition on the maximum amount of the Au microcrystals that can be incorporated in the oxide film was examined. Some amount of Au microcrystals were depleted to the surface of Au microcrystal-doped oxide films when an excess amount of $HAuCl_4 \cdot 4H_2O$ was dissolved in the coating solution. The maximum amount of Au that can be incorporated in the oxide film was found to increase with the increasing pH point at zero charge (PZC) of the matrix oxide. This result was explained by the concept that $AuCl_4^-$ ions are charged negative and also Au microcrystals tend to charge negative, so that the oxide gel with high PZC, which has a tendency to charge positive, may fix the ions and/or microcrystals to its interior. The maximum amount of Au microcrystals as high as 12.6 vol% was attained in an $Au:Al_2O_3$ film.

In Chapter 6, transparent oxide films containing gold microcrys-

tals for nonlinear optics were prepared by a new sol-gel process, in which dip-coated gel films prepared from metal alkoxide solutions were immersed in $NaAuCl_4 \cdot 2H_2O$ aqueous solution and subsequently heat-treated. By this process, $AuCl_4^-$ ions was able to be incorporated in the alumina and titania gel films, and thus gold microcrystals could be formed in the films. On the other hand, $AuCl_4^-$ ions were poorly incorporated in the zirconia gel and not incorporated in the silica gel. This difference was explained by the point of zero charge of these gels. An increase in concentration of $NaAuCl_4 \cdot 2H_2O$ aqueous solution was not effective in increasing the amount of gold incorporated in the gels.

List of Publications

[1] "Preparation of Au-Doped Silica Glass by Sol-Gel Method"
J. Ceram. Soc. Japan, **100**, 599-601 (1992)
(Chapter 1)

[2] "Sol-Gel Processing and Optical Nonlinearity of Gold Colloid-Doped Silica Glass"
J. Ceram. Soc. Japan, **101**, 53-58 (1993)
(Chapters 1 and 3)

[3] "Sol-Gel Processing and Optical Nonlinearity of Au Microcrystal-Doped Oxide Thin Films"
Proce. XVII Internat. Cong. Glass, **4**, 252-57 (1995)
(Chapters 1, 3, 5 and 6)

[4] "Preparation of Gold Microcrystal-Doped TiO_2, ZrO_2 and Al_2O_3 Films through Sol-Gel Process"
J. Sol-Gel Sci. Tech., **9**, 145-55 (1997)
(Chapter 5)

[5] "Preparation of gold microcrystal-Doped Oxide Optical Coatings through Adsorption of Tetrachloroaurate Ions on Gel Films"
J. Non-Cryst. Solids, **218**, 151-55 (1997)
(Chapter 6)

[6] "Effect of Coexisting Ions on the Sol-Gel Synthesis of Gold Microcrystal-Doped SiO_2 Films"
submitted to J. Non-Cryst. Solids
(Chapter 2)

[7] "Picosecond Nonlinear Optical Response of Au Microcrystal-Doped SiO_2 Glass Films Prepared by Sol-Gel Method"
submitted to Jpn. J. Appl. Phys.
(Chapter 3)

[8] "Preparation of Au-Pd Co-Doped Silica Glass Films by Sol-Gel Method"
to be submitted to J. Ceram. Soc. Japan
(Chapter 4)

Other publications related to microcrystal-doped photonic glasses

[1] "Optical Non-Linear Property of Au Colloid-Doped Glass and the Laser Irradiation Stability"
J. Mater. Sci.: Mater. Electron., **4**, 59-61 (1993)

[2] "Effect of Cadmium to Sulfur Ratio on the Photoluminescence of CdS-Doped Glasses"
J. Appl. Phys., **75**, 2251-56 (1994)

[3] "Observation of Electroluminescence from CdSe-Microcrystal-Embedded Indium Tin Oxide Film"

Jpn. J. Appl. Phys., **35**, 3928-29 (1996)

[4] "Quantum Size CdS Particles in a Phosphate Glass Matrix"
Ceramic Transactions, **28**, 493 (1992)

[5] "Effect of Preparation Condition on the Properties of CdSe Microcrystal-Doped SiO_2 Glass Thin Films Prepared by RF-Sputtering"
Jpn. J. Appl. Phys., **31**, 2206 (1992)

[6] "Microstructure and Optical Properties of CdSe Microcrystal-Doped SiO_2 Glass Thin Films Prepared by RF-Sputtering"
J. Ceram. Soc. Japan, **101**, 548 (1993) [in Japanese]

[7] "Preparation and Optical Properties of Semiconductor Microcrystals-Doped SiO_2 Glass Thin Films by RF-Sputtering"
J. Non-Cryst. Solids, **178**, 148 (1994)

[8] "Preparation and Magnetooptical Properties of $Cd_{1-x}Mn_xTe$ Microcrystal-Doped SiO_2 Glass Thin Films"
Jpn. J. Appl. Phys., **34**, L440 (1995)

[9] "Preparation of PbS Microcrystal-Doped SiO_2 Glass Thin Films by RF-Sputtering"
J. Non-Cryst. Solids, **183**, 290 (1995)

Acknowledgements

The studies in this thesis has been carried out partially at Department of Engineering in Mie University, and partially at School of Engineering in The University of Shiga Prefecture.

The author wishes to express his sincere gratitude to Professor Naohiro Soga of Kyoto University for his continuous interest, guidance and encouragement. He is also indebted to Prof. Tadashi Kokubo and Toshinobu Yoko of Kyoto University for their helpful discussions and comments.

The author is greatly indebted to Prof. Kanichi Kamiya of Mie University for his continuous interest, informative discussions, helpful advises and encouragement. He also wishes to thank Prof. Hiroyuki Nasu of Mie University for his continuous interest, informative discussions and encouragement.

The author wishes to thank Dr. Kohei Kadono of Osaka National Research Institute for the measurement of optical nonlinearity and for informative discussions. The profitable suggestions and informative discussions from Prof. Hiromitsu Kozuka of Kyoto University, from Prof. Kazuki Nakanishi of Kyoto University, and from Dr. Kohei Fukumi of Osaka National Research Institute are also gratefully acknowledged. Continuous encouragement given by Prof. Teiichi Hanada of Kyoto University and by Prof. Kazuyuki Hirao of Kyoto University are also acknowledged.

Finally, the author thanks Mrs. Michiko Matsuoka, his wife, and Toshiko Matsuoka, his mother, for their support and encouragement.

Jun Matsuoka